The study of ikaite ($CaCO_3 \cdot 6H_2O$) formation and its impact on biogeochemical processes in artificial sea ice brine

Dissertation

zur Erlangung des akademischen Grades eines

Doktors der Naturwissenschaften

– Dr. rer. nat –

am Fachbereich 2 (Biologie/Chemie)

der Universität Bremen

Yubin Hu

Oktober 2013

Gutachter

Prof. Dr. Dieter A. Wolf-Gladrow

PD Dr. Sabine Kasten

Luck is what happens when preparation meets opportunity.

---- Seneca

Declaration

I hereby declare that I myself have performed the work described in this dissertation. All external resources are appropriately stated.

---------- ----------

Date & Location Signature

Thanks to…

Prof. Dr. Dieter Wolf-Gladrow and Dr. Gernot Nehrke

for your supervision and guidance. Thank you for creating a wonderful working atmosphere that inspires my creativity and giving the academic freedom that allows me to think independently.

Dr. Gerhard Dieckmann

for bringing me into this fantastic sea ice research. I am grateful for your help in correcting my manuscripts and this dissertation.

Dr. Christoph Völker

for introducing me to AWI and support for my master thesis which laid the foundations for my PhD study.

Dr. Mariëtte Wolthers

for many insightful discussions and suggestions on calcium carbonate crystallization and your time in reading and correcting my manuscripts.

PD Dr. Sabine Kasten and Prof. Dr. Kai Bischof

For being part of the promotion committee.

AXA research fund

for providing the financial support for my PhD study.

Biogeosciences group

for the open and friendly working environment. I have always enjoyed being part of this group. I really appreciate the help from people in this group. Special thanks go to the technical staff and all the loving people.

POLMAR graduate school

for the organization of many valuable lectures. Special thanks to Dr. Claudia Sprengel, Dr. Claudia Hanfland and Dörte Rosenbaum for your work and help.

My friends

for your support and true friendship. You make my life joyful and meaningful.

My family

for the support and always being there with me. I would not have made it this far without you. I want to thank my sister for bringing me two adorable nephews. I am deeply grateful to my parents for the unconditional love and care.

Abstract

Calcium carbonate precipitation in polar sea ice has been proposed as one of the driving forces for the carbon pump in sea ice covered regions. After decades of controversial discussion on whether calcium carbonate can be precipitated in sea ice, the mineral ikaite ($CaCO_3 \cdot 6H_2O$) was for the first time discovered in Antarctic sea ice (Dieckmann et al., 2008) and later also found in Arctic sea ice (Dieckmann et al., 2010). However, the mechanism of ikaite precipitation in sea ice is not well known, as is the effect of ikaite precipitation on biogeochemical processes in sea ice.

The aim of this thesis was to study, under simulated sea ice brine conditions, whether ikaite is the only phase of calcium carbonate formed in sea ice and to determine the effect of pH, salinity, temperature and phosphate concentrations on the precipitation of ikaite, as well as the effect of ikaite precipitation on biogeochemical processes in sea ice.

In the first part of this thesis, I investigate the pathway of ikaite formation in solution and the effect of pH as well as phosphate (PO_4) on polymorphism of calcium carbonate in general. It can be shown that the formation of ikaite does not necessarily follow a precursor amorphous calcium carbonate (ACC) pathway and ikaite can be precipitated directly from solution. pH and PO_4 can act as a switch for different calcium carbonate polymorphs. At near freezing temperatures, high pH as well as the presence of PO_4 favours ikaite formation in fresh water, while low pH and the absence of PO_4 are in favor of vaterite formation.

In the second part of this thesis, I study the effect of different parameters in sea ice brine (pH, salinity, temperature and phosphate concentrations) on ikaite formation as well as the effect of ikaite precipitation on PO_4 removal in artificial sea ice brine. The results show that ikaite is very likely the only polymorph precipitated in natural sea ice. Phosphate is not crucial for ikaite formation in sea ice. The change in pH and salinity has a large impact on ikaite precipitation in sea ice, while the change in temperature and phosphate concentrations has little effect. PO_4 can be coprecipitated with ikaite.

pH as well as the initial PO_4 concentrations greatly affects the PO_4 removal by ikaite precipitation, while the change in salinity ($S > 0$) and temperature shows no effect on the coprecipitation of PO_4 with ikaite. These findings may shed some light on the observed variability of PO_4 concentrations in natural sea ice.

Zusammenfassung

Die Fällung von Kalziumkarbonat in den eisbedeckten polaren Meeren wird als wichtiger Antrieb der Kohlenstoffpumpe in diesen Gebieten betrachtet. Nach Jahrzenten der Diskussion bezüglich des Vorkommens von Kalziumkarbonat im Meereis wurde schließlich die Fällung von Ikait ($CaCO_3 \cdot 6H_2O$) im Meereis der Antarktis und Arktis nachgewiesen (Dieckmann et al., 2008, 2010). Der Verlauf der Fällung ist jedoch bis heute noch nicht vollständig entschlüsselt, wie auch die Rolle der Fällung in biogeochemischen Prozessen im Eis.

Ziel dieser Untersuchungen war es, in künstlichem Meerwasser festzustellen, ob Ikait das einzige Kalziumkarbonatpolymorph ist, das im Meereis ausfällt, und welche Rolle pH, Salzgehalt, Temperatur und Phosphatkonzentrationen bei der Fällung spielen. Außerdem sollte die Bedeutung der Ikaitfällung für biogeochemische Prozesse untersucht werden.

Im ersten Teil dieser Arbeit untersuche ich den Ablauf der Ikaitfällung in einer Lösung und den Effekt von pH und Phosphat (PO_4) auf den Polymorphismus von Kalziumkarbonat im Allgemeinen. Es wurde nachgewiesen, dass die Bildung von Ikait nicht notwendigerweise amorphes Calciumcarbonat (ACC) als Vorläufer benötigt und Ikait direkt aus der Lösung ausgefällt werden kann. pH und PO_4 fungieren als Auslöser für die verschiedenen Kalziumkarbonat Polymorphe. Bei Temperaturen nahe dem Gefrierpunkt begünstigt ein hoher pH-Wert sowie die Anwesenheit von PO_4 die Ikait Bildung im Süßwasser, während ein niedriger pH-Wert und das Fehlen von PO_4 die Vateritbildung begünstigt.

Im zweiten Teil dieser Arbeit untersuche ich den Einfluss verschiedener Parameter in der Sole des Meereises (pH, Salzgehalt, Temperatur und Phosphatonzentrationen) auf Ikaitbildung sowie die Wirkung der Ikaitfällung auf die PO_4-Fällung in künstlicher Meereissole. Die Ergebnisse zeigen, dass Ikait sehr wahrscheinlich als das einzige Polymorph in natürlichem Meereis ausgefällt wird. Phosphat ist nicht entscheidend für die Bildung von Ikait im Meereis. Die Veränderungen des pH-Wertes und des Salzgehaltes haben einen großen Einfluss auf die Ikaitfällung im Meereis, während

Veränderungen der Temperatur und der Phosphatkonzentration wenig Wirkung zeigen. Eine Mitfällung von PO_4 mit der Ikaitfällung findet statt. pH sowie die anfänglichen PO_4 Konzentrationen haben einen großen Einfluss auf die Entfernung von PO_4 durch die Ikaitfällung, während die Änderung des Salzgehaltes ($S > 0$) sowie die Temperatur keinen Einfluss auf die gemeinsame Fällung von PO_4 mit Ikait aufweisen. Diese Ergebnisse könnten etwas Licht auf die beobachtete Variabilität der PO_4 Konzentrationen in natürlichem Meereis werfen.

Table of Contents

Chapter 1

Introduction

1.1 Sea ice

Sea ice is a thin, fragile and dynamic solid layer formed when seawater freezes. At its maximum extent, Sea ice covers more than 7% of the Earth's surface, or about 12% of the world's oceans (Weeks, 2010). The presence of sea ice influences the temperature and circulation patterns of both the atmosphere and ocean. It also reduces the amount of solar radiation absorbed at the ocean's surface due to its high albedo (Washington and Parkinson, 1986). While acting to some extent as a barrier and slowing down exchange processes between ocean and atmosphere it is also a source of organic matter, nutrients and gases released to both atmosphere and the ocean (Loose et al., 2011), resulting from a variety of biogeochemical processes mainly associated with a rich microbial community within the ice (Thomas and Dieckmann, 2010).

1.1.1 Sea ice formation

The freezing point of seawater at salinity 34 is -1.86^{o}C. When sea ice forms, dissolved salts are quantitatively expelled from the ice crystal matrix since major ions cannot be incorporated into the ice crystal lattice (Eicken, 2003). Due to gravity drainage, a large portion of the expelled dissolved salts is rejected into the underlying seawater column (Notz and Worster, 2009). However, a certain amount of seawater remains, trapped in the sea ice matrix, forming the so-called brine retained in pockets and channels throughout the sea ice. As temperature decreases, the trapped brine freezes accordingly, resulting in the residual brine becoming more saline. The relationship between brine salinity (S_b) and temperature (T above -23^{o}C) can be approximated by

$$S_b = (1 - 54.11/T)^{-1} * 1000$$

with T in ^{o}C (Eicken, 2003).

The microstructure of sea ice is greatly modified by the interaction of physical, biological and chemical processes, which forms an extremely heterogeneous semi solid matrix (Thomas and Dieckmann, 2010). As shown in Fig. 1.1, depending on the formation conditions (e.g. air temperature, wind and ocean currents), sea ice comprises different textures (Eicken, 2003).

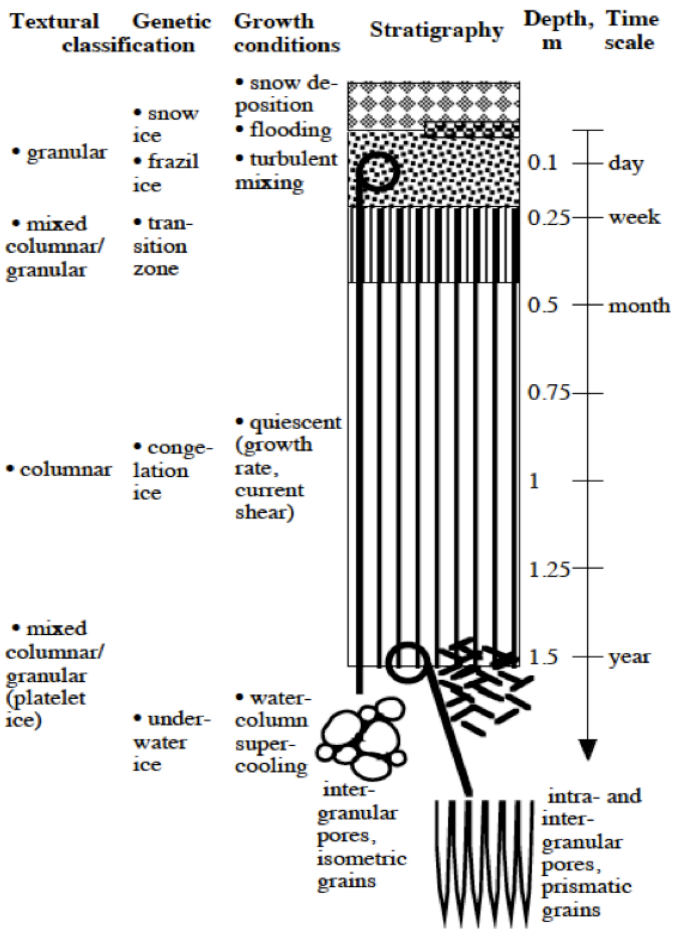

Fig. 1.1 Schematic summarizing the main ice textures, growth conditions and time scales for first-year sea ice (Eicken, 2003).

1.1.2 Sea ice phase diagram

Different from lake ice, sea ice consists of pure ice, brine, precipitated salts (below certain temperature levels) and gas bubbles. As the brine temperature decreases, eutectic points of the various salts are reached and the salts start to precipitate preferentially at different temperatures (Fig. 1.2) (Assur, 1958). The first mineral to precipitate is ikaite, which is predicted to precipitate just below the freezing point of seawater. As the temperature further decreases, the ice mass fraction increases steadily, while the mass fraction of brine can drop bellow 6% at –40^{o}C. Nevertheless, even at the lowest temperatures, a small but non-negligible liquid fraction remains (Eicken, 2003).

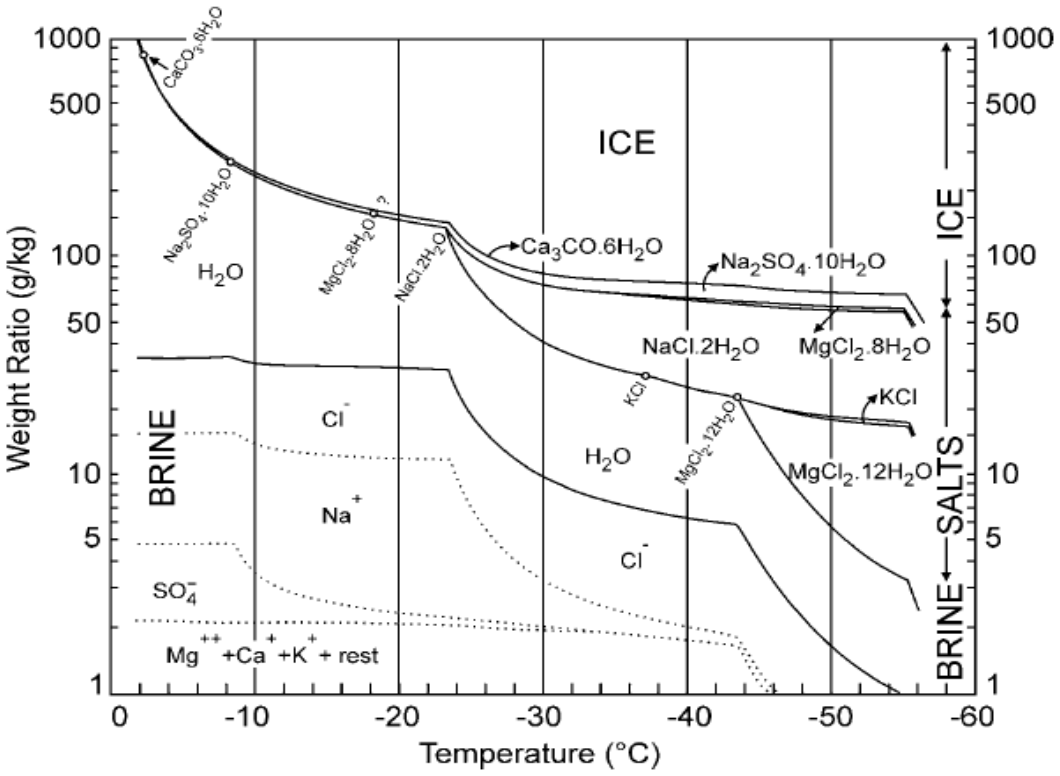

Fig. 1.2 Phase diagram of sea ice. The difference curves indicate the mass fraction of solid ice (top), salts (middle) and liquid brine (bottom) present in a closed volume of standard seawater at different temperatures (Assur, 1958).

1.1.3 Biogeochemical processes in sea ice

During the last decades, major efforts have been undertaken to study the biogeochemical processes within sea ice (Delille et al., 2007; Gleitz et al., 1995; Papadimitriou et al., 2012; Rysgaard et al., 2007). Nevertheless, the existing evidence regarding controls on the biogeochemical processes in sea ice is still sparse (Papadimitriou et al., 2007; Thomas and Dieckmann, 2010).

As illustrated in Fig. 1.3, starting with a decrease in brine temperature, the brine salinity increases accordingly, affecting the chemical environment in brine with regard to the CO_2 system (dissolved inorganic carbon (DIC), total alkalinity (TA), pCO_2 and pH) as well as elevated major nutrient concentrations (nitrate, silicic acid and phosphate). The photosynthetic activity in sea ice leads to depletion of the major nutrients, while driving the accumulation of O_2 and increasing brine pH (Gleitz et al., 1996; Günther et al., 1999). The brine pH can rise up to ~10 (Gleitz et al., 1995; Papadimitriou et al., 2007). This extreme chemical environment leads to the

precipitation of ikaite, which has recently been discovered both in Antarctic and Arctic pack ice (Dieckmann et al., 2008, 2010). The precipitation of ikaite in turn alters the chemical environments in sea ice. Among which, the CO_2 cycle is of pivotal interest, since the formation/dissolution of ikaite is considered to play an important role in the sea ice carbon cycle (Geilfus et al., 2012; Rysgaard et al., 2007).

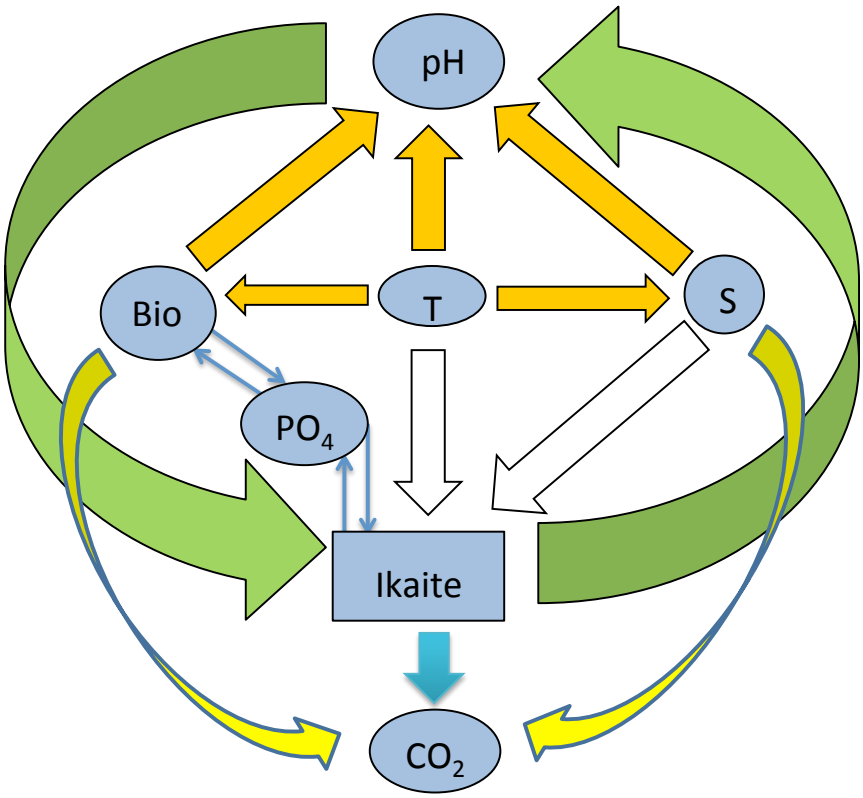

Fig. 1.3 Scheme of biogeochemical processes in sea ice. The change in temperature (T) is the driving force for other parameters (e.g. salinity (S), biological activity (Bio) and pH) in sea ice. The precipitation of ikaite in sea ice is affected by these parameters and in turn affects the chemical environment (e.g. pH, CO_2) as well as phosphate (PO_4) concentrations in sea ice.

1.2 Calcium carbonate

Calcium carbonate is an important mineral in nature. The precipitation of calcium carbonate (biominerals and geological deposits) can bind a large amount of CO_2 and affect the seawater chemistry. Calcium carbonate is also an ideal mineral for nucleation and crystal growth study, since it has several polymorphs and the morphology of each form varies with the precipitation conditions.

1.2.1 Calcium carbonate polymorphs

Different phases of calcium carbonate are known to exist: amorphous calcium carbonate (ACC), calcium carbonate monohydrate (MCC), calcium carbonate hexahydrate (ikaite) and the three anhydrous polymorphs: vaterite, aragonite, and calcite. The solubility products (*K*) are given in Table 1.1.

Table 1.1 Solubility constants of different calcium carbonate polymorphs (modified after Nehrke (2007)).

Polymorph	p*K* at 0^{o}C	Log (*K*) (T in ^{o}K and t in ^{o}C)	Ref.
ACC	6.20	-6.1987 – 0.005336 t – 0.0001096 t^2	a
MCC	7.05	-7.05 – 0.000159 t^2	b
Ikaite	7.20	0.15981 – 2011.1/T	c
Vaterite	7.74	-172.1295 – 0.077993 T + 3074.688/T + 71.595 log T	d
Aragonite	8.22	-171.9773 – 0.077993 T + 2903.293/T + 71.595 log T	d
Calcite	8.38	-171.9065 – 0.077993 T + 2839.319/T + 71.595 log T	d

a: Brečević and Nielsen (1989), b: Kralj and Brečević (1995), c: Bischoff et al. (1993a), d: Plummer and Busenberg (1982).

The formation of different phases of calcium carbonate might be explained by Ostwald step rule (Ostwald, 1897), which states that in general it is not the most stable but the least stable polymorph that crystallizes first. The empirical observation shows that crystallization from a solution preferentially starts from the thermodynamically less stable phase followed by the thermodynamic stable phase, indicating that the less stable phase may be kinetically favored (as illustrated in Fig. 1.4 pathway A).

Nevertheless, the most stable phase can also be precipitated directly from solution without going through all the precursors (as illustrated in Fig. 1.4 pathway B).

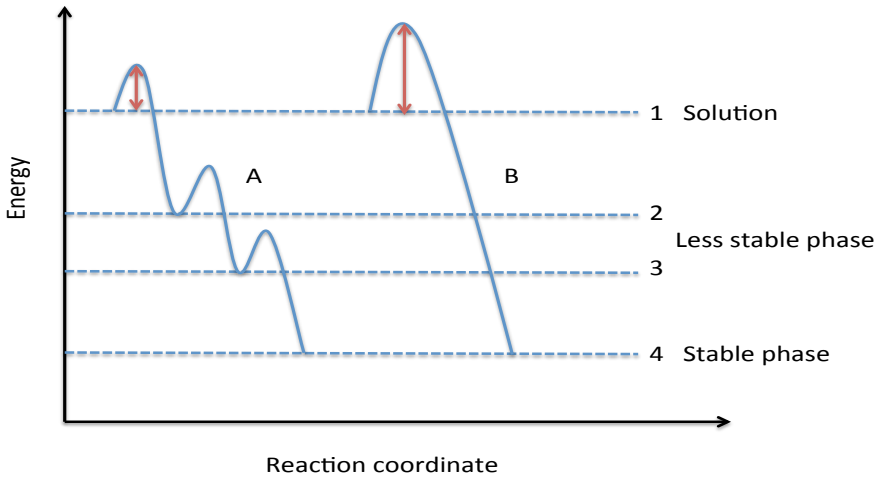

Fig. 1.4 Illustration of the Ostwald step rule. The transformation through pathway A is kinetically more favored than the direct formation through pathway B (modified after Nehrke (2007)).

Recently, it was postulated that stable prenucleation clusters exist and that ACC is the first precipitated phase of calcium carbonate after nucleation (Gebauer et al., 2008). It was further proposed that different forms of ACC exist (e.g. ACC I, ACC II, …), which correspond to particular crystalline calcium carbonate after its transformation, as illustrated in Fig. 1.5 (Gebauer et al., 2008).

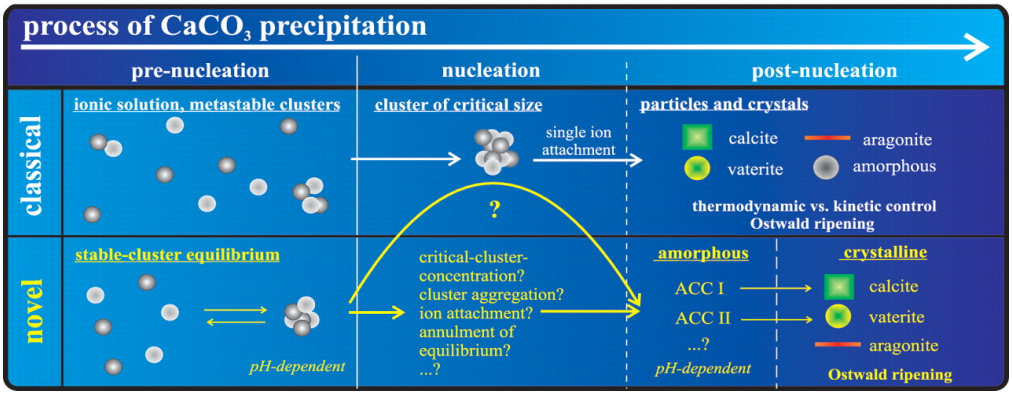

Fig. 1.5 Schema of the classical and novel view on precipitation (not to scale). Prenucleation-stage calcium carbonate clusters provide an early precursor species of different ACC phases giving rise to an alternative crystallization-reaction channel (from Gebauer et al. (2008)).

1.2.2 Ikaite

Synthetic $CaCO_3 \cdot 6H_2O$ was already known from laboratory studies in the nineteenth century (Pelouze, 1865). It was first found in nature at the bottom of the Ika Fjord in Greenland (Pauly, 1963), and named *ikaite* after the location of its discovery. This mineral was subsequently found in deep-sea sediments (Jansen et al., 1987; Suess et al., 1982), Mono Lake, California, USA (Bischoff et al., 1993b; Council and Bennett, 1993) and cold spring water at Shiowakka, Hokkaido, Japan (Ito, 1996). Recently, it was discovered in polar sea ice in both the Antarctic and Arctic (Dieckmann et al., 2008; Dieckmann et al., 2010). The natural occurrences of ikaite are characterized by low temperatures (below 4°C), high pH, high alkalinity, elevated concentrations of phosphate and organic matter (Buchardt et al., 1997; Rickaby et al., 2006).

Ikaite ($CaCO_3 \cdot 6H_2O$) is a metastable mineral of calcium carbonate. It is only stable at low temperatures and/or high pressure (Marland, 1975). The crystal structure of ikaite is monoclinic, containing discrete $CaCO_3$ ion pairs, each surrounded by an envelope of 18 water molecules. The Ca^{2+} is bound more closely to the six water molecules than to the CO_3^{2-} ion (Fig. 1.6) (Dickens and Brown, 1970). The density of ikaite (1.8 g cm^{-3}) is much lower than that of calcite (2.71 g cm^{-3}). In contrast to other calcium carbonate phases, the solubility of ikaite increases with temperature (Bischoff et al., 1993a).

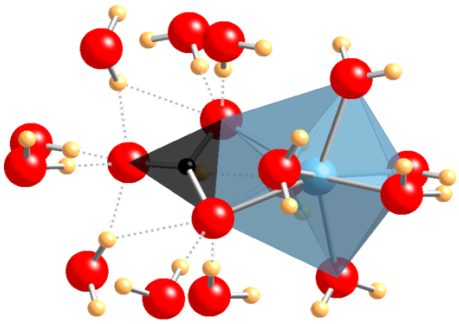

Fig. 1.6 Part of the crystal structure of ikaite. Ca (blue) is in dodecahedral coordination with O atoms (red) of the carbonate (black planar) and water molecules, while hydrogen bonds (dotted) between H-atoms (yellow) of the water molecules to the O-atoms of the carbonate ion exist (From Wikipedia after Dickens and Brown (1970); Swainson and Hammond (2003)).

At a temperature above 0°C, normal seawater is supersaturated with both calcite and aragonite, but largely undersaturated with respect to ikaite (Fig. 1.7). The precipitation of ikaite from seawater thus requires an excess concentration of Ca^{2+} and/or CO_3^{2-}. This might partly explain the rare occurrences of ikaite in nature.

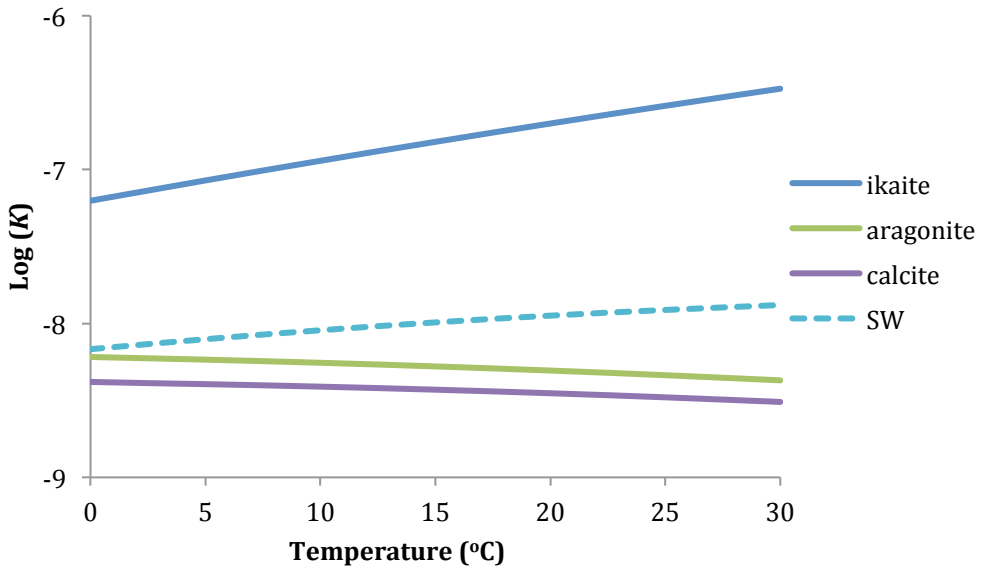

Fig. 1.7 Common logarithm of the solubility product constants, log (*K*), versus temperature for ikaite (Bischoff et al., 1993a), aragonite and calcite (Plummer and Busenberg, 1982). The dotted line representates the ion activity product of calcium carbonate in artifical seawater (salinity 35, pH 8.1, Ca 10 mM and DIC 2mM) calculated from Visual-Minteq in the temperature range from 0 to 30°C.

The occurences of ikaite in nature are of great importance. It has been reported that ikaite can be used to trace the evolution of oceanic $\delta^{18}O$ (Rickaby et al., 2006), and thus act as a record of late Holocene climate (Lu et al., 2012). It is commonly believed that ikaite is the precursor of the calcite pseudomorphs (Bischoff et al., 1993a; Council and Bennett, 1993; McLachlan et al., 2001). The calcite pseudomorphs (Glendonite) after ikaite decomposition are considered to be a valuable indicator of cold paleoenvironments (De Lurio and Frakes, 1999; Selleck et al., 2007; Suess et al., 1982). Furthermore, precipitation of calcium carbonate (ikaite) in sea ice is considered fundamental in catalyzing chemical processes (Sander et al., 2006; Sander and Morin, 2009), as well as important for the CO_2 flux in polar sea ice covered regions (Geilfus et al., 2012; Rysgaard et al., 2007).

1.3 Objective and outline of the thesis

Ikaite is one of the hydrated forms of calcium carbonate. Due to the rare occurrences in nature as well as being a metastable form, studies of ikaite compared to other forms of calcium carbonate are sparse. The recent discovery of ikaite in polar sea ice (Dieckmann et al., 2008, 2010) has received new attention among polar scientists, since its formation and dissolution are considered to be important for carbon cycle in sea ice covered regions. However, the conditions in sea ice brine leading to ikaite precipitation as well as the effect of ikaite precipitation on the biogeochemical processes in sea ice brine are poorly understood. Since the natural sea ice brine system is too complex and inaccessible to identify the parameters leading to ikaite precipitation directly in the field, it is necessary to investigate the parameters separately under controlled laboratory conditions. The objective of this thesis was to set up lab experiments so as to study ikaite formation under optimal experimental conditions, resembling as close as possible natural sea ice conditions. Aim was to understand ikaite formation in general and to study the effect of different parameters on ikaite formation in artificial sea ice brine as well as to determine the effect of ikaite precipitation on phosphate removal under different conditions.

Chapter 2 addresses whether amorphous calcium carbonate is a necessary precursor in the formation of ikaite. The precipitation of ikaite from solutions covering a wide range of saturation levels with respect to ikaite is discussed.

Chapter 3 deals with how a change in solution pH as well as the presence of phosphate plays a role in calcium carbonate polymorphism at near freezing temperatures. The mechanism of pH and phosphate in controlling the calcium carbonate polymorphs is discussed.

Chapter 4 addresses the effect of different parameters (pH, salinity, temperature and phosphate concentrations) on ikaite formation, in order to investigate whether ikaite is the only phase of calcium carbonate formed in sea ice and to qualify the effect of different parameters on the precipitation of ikaite.

Chapter 5 deals with the coprecipitation of phosphate with ikaite under different experimental conditions. The effect of pH, salinity, temperature and initial phosphate concentrations on phosphate removal by ikaite precipitation is presented.

Chapter 2

Is amorphous calcium carbonate a necessary precursor for ikaite formation?

Abstract

It has recently been proposed that amorphous calcium carbonate (ACC) represents the general precursor phase during the formation of crystalline calcium carbonate minerals and that different forms of ACC exist, which are related to the particular crystalline calcium carbonate polymorphs they transform into. In order to investigate if ACC is involved in the formation of the hydrated calcium carbonate polymorph ikaite, we performed calcium carbonate precipitation experiments by titrating $CaCl_2$ and $NaHCO_3$ solutions into a reaction vessel at different titration rates and at near-freezing temperatures. At all conditions tested, ikaite was the only precipitate observed. At slow titration rates, the ion activity product of calcium and carbonate remained below the saturation level of calcium carbonate monohydrate, which is the most soluble crystalline calcium carbonate at near-freezing temperatures. These results indicate that, from a thermodynamic perspective, formation of any ACC precursor is not possible at our experimental conditions. Our results therefore suggest that, ACC is not a necessary precursor for the formation of ikaite.

2.1 Introduction

Five crystalline polymorphs of calcium carbonate are known to exist, namely, calcite, aragonite, vaterite, calcium carbonate hexahydrate (ikaite) and calcium carbonate monohydrate (MCC), listed in order of increasing solubility at near-freezing temperatures. During the formation of anhydrous crystalline polymorphs, amorphous calcium carbonate (ACC) is generally known as a precursor for which the existence of different forms or structures is currently widely discussed (Cartwright et al., 2012; Lam et al., 2007).

Ikaite ($CaCO_3 \cdot 6H_2O$) represents a rare mineral in the natural environment. It is a metastable form of calcium carbonate, normally found in environments characterized by low temperatures (below 4 °C) and/or high pressure (Marland, 1975), high alkalinity and high phosphate concentrations (Buchardt et al., 1997). Unlike other forms of calcium carbonate, the solubility of ikaite increases with temperature (Bischoff et al., 1993a).

The study of ACC has recently attracted much attention (Bots et al., 2012; Rodriguez-Blanco et al., 2011). It has been hypothesized that ACC represents the general precursor phase during the formation of crystalline calcium carbonate phases and that different forms of ACC are related to the particular crystalline calcium carbonate polymorphs they transform into (Gebauer et al., 2008). Other studies (Hetherington et al., 2011; Rodríguez-Ruiz et al., 2014) on the other hand showed that ACC is not a necessary precursor for crystalline calcium carbonate formation. However, due to the fast transformation of ACC into crystalline calcium carbonate polymorphs, it is not always possible to detect the presence of ACC (Bots et al., 2012).

In the study of Gebauer et al. (2008), the existence of different ACC precursors was postulated based on different solubilities determined from precipitation experiments in a titration setup. Their study looked at the formation pathway of anhydrous forms of calcium carbonate. Here we investigate if their findings can be also applied to the precipitation of hydrated polymorphs of calcium carbonate. From the variety of different methods used throughout the literature to investigate the existence of precursor phases we chose precipitation experiments, using solution

chemistry evolution and titration data, that provided us with data directly comparable to the study of Gebauer et al. (2008). To investigate whether ACC is a necessary precursor in the formation of the hydrated calcium carbonate phase ikaite, we performed experiments at near-freezing temperatures and high pH at different titration rates of $CaCl_2$ and $NaHCO_3$ solutions. This approach leads to the precipitation of ikaite from solutions covering a wide range of supersaturation levels with respect to ikaite, including levels below the solubility of MCC, the most soluble of crystalline calcium carbonate phase at near-freezing temperatures. The results show that, at our experimental conditions, the formation of ikaite does not necessarily follow a precursor ACC pathway.

2.2 Experimental procedure

2.2.1 Solution preparation

Stock solutions of $CaCl_2$ and $NaHCO_3$ at concentrations of 0.3 mol/L were prepared by dissolving 2.205 g $CaCl_2 \cdot 2H_2O$ (ACS, Reag. MERCK) and 1.26 g $NaHCO_3$ (ACS, Reag. MERCK) into ultrapure water with a final volume of 50 mL, respectively. Working solution (0.04 mol/L NaOH) was prepared by diluting 8 mL, 1N NaOH (TitriPUR, MERCK) into ultrapure water with a final volume of 200 mL.

2.2.2 Experimental setup

Solutions of 0.3 mol/L $CaCl_2$ and $NaHCO_3$ solutions were titrated into a 200 mL 0.04 mol/L NaOH solution (pH = 13.4) using a peristaltic pump (IPC-N, Ismatec) at titration rates between 3.6 µL/min and 100 µL/min. The working solution in the reactor vessel was continuously stirred at a rate of 400 rpm by means of a Teflon-coated magnetic stirring bar. The working solution pH did not change throughout the experiment. The reactor temperature was kept at 0.5±0.5 °C by a water-bath using double walled water jackets. Duplicate experiments were carried out at 10 min interval.

2.2.3 Onset time determination

The time from the moment when titration started until the moment that the first crystals were observed was recorded as onset time. The appearance of crystals in the

working solution was determined by optical microscopy (Zeiss, Axiovert 200M) at the experimental temperature. Every 5 min, around 2 mL of solution from one experiment was taken in a petri dish and checked carefully under the microscope using an objective with 63X magnification. To more accurately determine the onset time, solutions from the parallel experiment that started 10 min after the first one were checked every 2 min after the onset of crystallization was observed in the first experiment.

2.2.4 Crystal identification

The mineral phase was identified by means of Raman spectroscopy. This method can reliably distinguish between the various polymorphs of calcium carbonate (Nehrke et al., 2012; Tlili et al., 2001). The confocal Raman microscope (WITec®, Ulm, Germany) was equipped with a diode laser (532 nm) and an Olympus® 20X Teflon-coated water submersible objective. For the Raman measurement, around 2 mL of the well-stirred solutions was sampled together with the crystals by means of a pipette and quickly transferred to a glass petri dish, which was kept cold during the measurement using an ice-water bath. This method prevented metastable from of calcium carbonate transforming into a more stable polymorph during the measurement (Geilfus et al., 2013).

2.2.5 Evolution of the ion activity product of calcium and carbonate

The evolution of the ion activity product of calcium and carbonate (IAP) until the onset of crystal precipitation at varied titration rates was calculated using the chemical equilibrium model Visual-Minteq 3.0 (Gustafsson, 2011). The input parameters for each run were the same as those for the experiments, and the models ran as titrations, simulating the experimental titration of $CaCl_2$ and $NaHCO_3$ into the reactor vessel. Activities were calculated using the Davies Equation.

2.3 Results and discussion

Fig. 2.1 shows a typical spectrum obtained using Raman microscope on our precipitates formed. According to the vibrational modes ν_1 (1071 cm^{-1}) and ν_4 (718 cm^{-1}) of CO_3^{2-} obtained in our Raman measurements, ikaite is the only polymorph of calcium carbonate identified at all titration rates. While titration rates

increased from 3.6 to 100 µL/min, the onset time was observed to decrease from 180 to 17 min (Table 2.1). The morphologies of ikaite are similar at all titration rates; with an average size around 20 µm (Fig. 2.2), which are similar to those reported in the study of Bischoff et al. (1993a).

Table 2.1 Precipitate of calcium carbonate and the onset time of precipitation at different titration rates and at constant Ca^{2+}/CO_3^{2-} ratio, pH and temperature.

	Ca^{2+}/CO_3^{2-} = 1:1, pH = 13.4, T = 0.5 °C				
Titration rate (µL/min)	3.6	5	20	50	100
Precipitate	ikaite	ikaite	ikaite	ikaite	ikaite
Onset time (min)	180±5	127±2	53±2	24±1	17±1

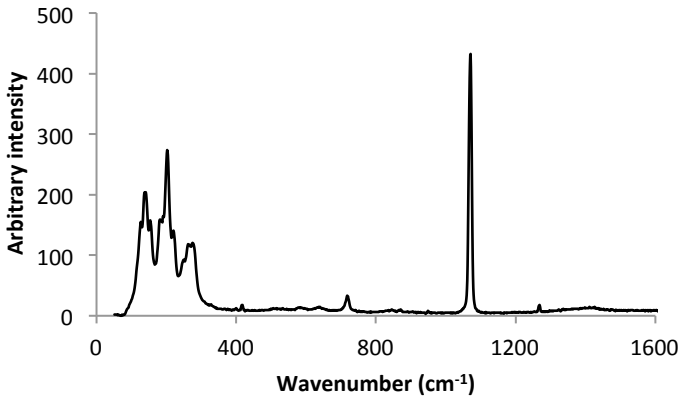

Fig. 2.1 Ikaite Raman spectrum of precipitates obtained at 20 µL/min titration rate, and representative of all spectra obtained for precipitates formed in our experiments.

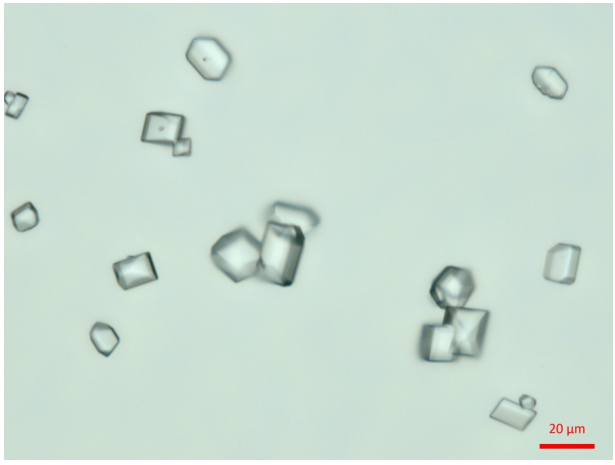

Fig. 2.2 Ikaite morphology observed in a sample at 20 µL/min titration rate, and representative for all precipitates formed in our experiments.

The different rates at which $CaCl_2$ and $NaHCO_3$ solutions were pumped into the reaction vessel resulted in different rates at which the working solutions evolved. Fig. 2.3 illustrates the evolution of log(IAP) relative to solubility products of ACC, MCC and ikaite. The solubility products of ACC, MCC and ikaite at 0.5 °C obtained from Brečević and Nielsen (Brečević and Nielsen, 1989), Kralj and Brečević (Kralj and Brečević, 1995) and Bischoff et al. (Bischoff et al., 1993a) are -6.20, -7.05 and -7.19, respectively. The rate of IAP evolution increases with increasing titration rate. At higher titration rates, the solutions need a shorter time to reach supersaturation with respect to ikaite, explaining the decrease in onset time. And also, at higher titration rates a higher degree of solution supersaturation is reached before ikaite precipitation starts (Fig. 2.3). Nevertheless, even at the highest titration rate, the solution remains undersaturated with respect to ACC, where the solubility product is derived from Brečević and Nielsen (Brečević and Nielsen, 1989). At our lowest titration rates of 5 µL/min and 3.6 µL/min, the solutions are just supersaturated with respect to ikaite while still undersaturated with respect to MCC when ikaite precipitation starts (Fig. 2.3). Thus, even if we assume that various forms of ACC with different solubilities exist, like suggested by some authors (Gebauer et al., 2008; Lam et al., 2007), ACC should still represent the most soluble form of calcium carbonate (Brečević and Nielsen, 1989; Sugiura et al., 2013) and therewith cannot have a solubility lower than the most soluble crystalline calcium carbonate polymorph, which under the experimental conditions of this study is MCC.

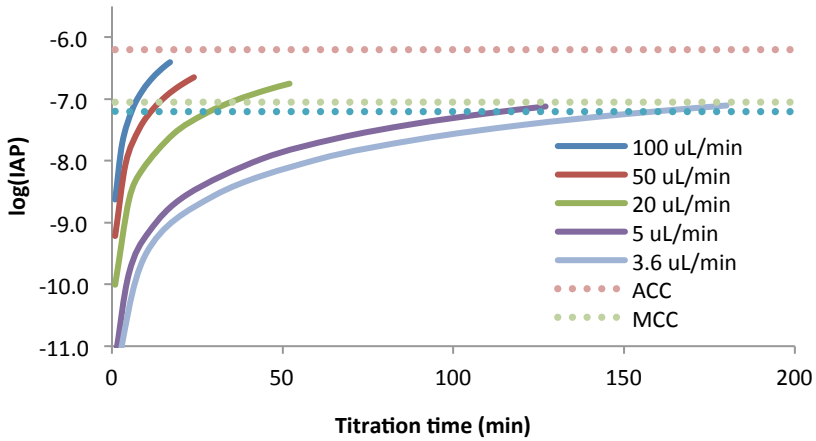

Fig. 2.3 Evolution of the logarithmic ion activity product of calcium and carbonate in solution at varied titration rates, and the solubilities of ACC, MCC and ikaite at 0.5 °C.

Our results therefore indicate that ACC is not necessary as a precursor in the formation of the hydrated calcium carbonate polymorph ikaite, because from a thermodynamic point of view, it is not possible for any form of ACC to precipitate at low titration rates at our experimental conditions. Therefore, the premise of Gebauer et al. (Gebauer et al., 2008) that ACC represents the general precursor phase during the formation of crystalline calcium carbonate phases and that different ACC phases exist as precursors for the different crystalline polymorphs might not hold true when it comes to the formation pathway of the hydrated calcium carbonate, ikaite.

2.4 Conclusions

The formation of calcium carbonate at different titration rates and near-freezing temperatures in high pH solution was studied. Ikaite is the only form of calcium carbonate observed in this study. The evolution of the ion activity product of calcium and carbonate at slow titration rates shows that ikaite formation occurs well below the saturation level of amorphous calcium carbonate, indicating that amorphous calcium carbonate is not a necessary precursor for ikaite formation.

Chapter 3

Effect of pH and phosphate on calcium carbonate polymorph precipitated at near-freezing temperature

Abstract

The effects of pH and phosphate on calcium carbonate polymorphs precipitation in solution were investigated. Experiments were carried out at near-freezing temperature and two different pH conditions (pH = 13.4 and 9.0). At each pH condition, different concentrations of $CaCl_2$ and $NaHCO_3$ were applied to achieve ratios of 1:1 and 10:1 for Ca/CO_3. $CaCl_2$ and $NaHCO_3$ solutions were pumped into different pH solutions with or without phosphate at different pumping rates. Results showed that, at pH = 13.4, only ikaite was formed, independent of phosphate, pumping rate or the ratio of Ca/CO_3. At pH = 9.0, the precipitate was vaterite in the absence of phosphate and ikaite in the presence of phosphate regardless of the ratio of Ca/CO_3. These results indicate that at low temperature, pH and phosphate can act as a switch between ikaite and vaterite polymorphs.

3.1 Introduction

Calcium carbonate ($CaCO_3$) can exist in different phases. Various amorphous forms: amorphous calcium carbonate (ACC) (Cartwright et al., 2012; Lam et al., 2007), two hydrated forms: calcium carbonate monohydrate (MCC) and calcium carbonate hexahydrate (ikaite), and the three anhydrous polymorphs: vaterite, aragonite and calcite.

The formation of different polymorphs of $CaCO_3$ is strongly affected by precipitation conditions. Among them, pH and additives are considered to be two dominating factors controlling polymorphism during calcium carbonate precipitation (Han et al., 2006; Song and Colfen, 2011). Furthermore, the Ca/CO_3 ratio in solution affects the binding strength of Ca to CO_3, which is postulated to play an important role in determining different forms of ACC, which later transform into the particular calcium carbonate polymorphs (Gebauer et al., 2008). However, the change of solution pH is at the same time associated with a change in hydrogen ion concentration (H^+) and the Ca/CO_3 ratio in solution, making it difficult to separate pH and solution stoichiometry effects. The effect of additives on calcium carbonate crystallization has been extensively studied (Song and Colfen, 2011), however, the mechanism by which additives influence precipitation are still not known (Gebauer et al., 2009).

Ikaite is a metastable calcium carbonate phase for which the formation mechanisms are equally poorly understood. In general, ikaite can be found in environments characterized by near zero temperatures, high alkalinity and phosphate (PO_4) concentrations (Bischoff et al., 1993a; Buchardt et al., 1997; Council and Bennett, 1993). But more recently, ikaite has also been observed in sea ice at much lower PO_4 concentrations (Dieckmann et al., 2010; Geilfus et al., 2013). The objective of this study was to investigate how a change in pH as well as the presence of PO_4 plays a role in calcium carbonate polymorphism at near-freezing temperature.

3.2 Experimental procedure

3.2.1 Experiment setup

Experiments were carried out in solution by pumping different concentrations of $CaCl_2$ and $NaHCO_3$ solutions at two different pH_{stat} conditions (pH = 13.4 and 9.0) at

near-freezing temperature. At pH = 13.4, nearly all dissolved inorganic carbon (DIC) is in form of CO_3^{2-}; while at pH = 9.0, nearly 10% of DIC is in form of CO_3^{2-}. At pH = 13.4, two sets of concentrations of $CaCl_2$ and $NaHCO_3$ were applied (0.3 mol L^{-1} : 0.3 mol L^{-1} and 0.3 mol L^{-1} : 0.03 mol L^{-1}) to achieve ratios of 1:1 and 10:1 for Ca/CO_3. At pH = 9.0, 0.3 mol L^{-1} : 0.3 mol L^{-1} and 0.03 mol L^{-1} : 0.3 mol L^{-1} of $CaCl_2$ and $NaHCO_3$ solutions were applied to achieve ratios of 10:1 and 1:1 for Ca/CO_3. The effect of PO_4 (0 versus 10 μmol L^{-1}) was tested under each experimental condition. At pH = 13.4, various pumping rates ranging from 3.6 to 100 μL min^{-1} were also conducted at concentrations of $CaCl_2$ and $NaHCO_3$ 0.3 mol L^{-1} : 0.3 mol L^{-1} and in the absence of PO_4. At pH = 13.4, solution pH did not change throughout the experiment. At pH = 9.0, 0.1M NaOH solution was added by a titration system (TA20 plus, SI Analytics) to keep the solution pH constant. $CaCl_2$ and $NaHCO_3$ solutions were pumped through a high precision peristaltic pump (IPC-N, Ismatec) into 200 g working solution. The working solution was stirred at a constant rate of 400 rpm by means of Teflon-coated magnetic stirring bar. The reactor temperature was kept around 0 ~ 0.5^{o}C using a water-bath and double walled water jackets. Duplicates for each experimental condition were carried out at 10-min interval.

3.2.2 Determination of onset time

Onset time in this study is defined as the time from the moment when pumping starts until the moment that the first crystals are observed. At pH = 13.4, the onset of precipitation was determined by using a microscope (Zeiss, Axiovert 200M). Every 5 min, around 2 mL solutions from one experiment was taken and checked carefully under the microscope using an objective with 63x magnification. When crystals from the first experiment were observed under the microscope, solutions from the other parallel experiment, which started 10 min after the first one, were checked at 2 min interval until crystals were observed.

At pH = 9.0, the onset of precipitation was determined by the titration curve. While calcium carbonate is precipitated from solution, CO_2 is released, which leads to a decrease in solution pH. This rapid change in pH could have been used to determine the onset of precipitation. However, pH in solution was kept constant by the addition of NaOH during the experiment. Therefore, the sudden increase in NaOH volume

(V_{NaOH}) added into the reactor vessel was used to determine onset time (marked with a circle in the Fig. 3.1).

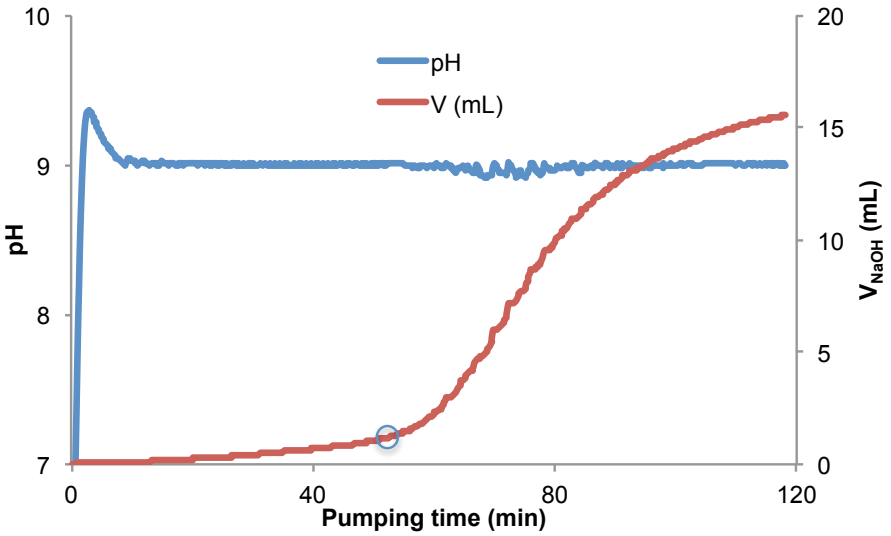

Fig. 3.1 pH curve and volume of NaOH solution added to keep pH constant. The circle indicates the onset of calcium carbonate precipitation.

3.2.3 Crystals identification

The phase identification of the crystals was done by means of Raman microscopy. This method can be used to reliably distinguish between the various polymorphs of calcium carbonate (Nehrke et al., 2012; Tlili et al., 2001). The confocal Raman microscope (WITec®, Ulm, Germany) was equipped with a diode laser (532 nm) and an Olympus® 20x Teflon coated water submersible objective. During the Raman measurement, crystals were maintained in the original solution and placed in a glass Petri dish, which was kept cold using an ice-water bath.

3.2.4 Evolution of the ion activity product of calcium and carbonate

The evolution of the ion activity product of Ca^{2+} and CO_3^{2-} (IAP) in the solution under different experimental conditions was calculated by using the chemical equilibrium model Visual-Minteq 3.0 (Gustafsson, 2011). It was modified by the implementation of the solubility constant of ikaite ($K_{sp,\ ikaite}$), derived from log $K_{sp,\ ikaite}$ = 0.15981 – 2011.1/T (Bischoff et al., 1993a), where T (K) is the absolute temperature. For our experimental conditions log $K_{sp,\ ikaite}$ was -7.20 calculated at 0°C.

3.3 Results

The experiments conducted and the $CaCO_3$ polymorphs precipitated are summarized in Fig. 3.2. At high pH (pH = 13.4), only ikaite was formed, independent of PO_4 or the ratio of Ca/DIC. At low pH (pH = 9.0), the precipitate was predominantly vaterite in the absence of PO_4 and only ikaite in the presence of PO_4 regardless of the ratio of Ca/DIC. At constant pumping rate of 100 µL min^{-1}, the shortest onset time of about 17 min was observed at condition of pH = 13.4 and Ca/DIC = 1:1 regardless of the PO_4. The onset time (~ 44 min) was similar between the conditions of pH = 13.4, Ca/DIC = 10:1 and pH = 9.0, Ca/DIC = 1:1. The longest onset time (~ 100 min) was observed at pH = 9.0 and Ca/DIC = 1:1. No significant difference was found in onset time regardless of the PO_4 (0 versus 10 µmol L^{-1}) under the otherwise same conditions.

The calcium carbonate polymorphs precipitated at different pumping rates at pH = 13.4 and in the absence of PO_4 are shown in Fig. 3.3. At pumping rate from 3.6 to 100 µL min^{-1}, ikaite was the only calcium carbonate phase observed. The corresponding onset time decreased from 180 to 17 min.

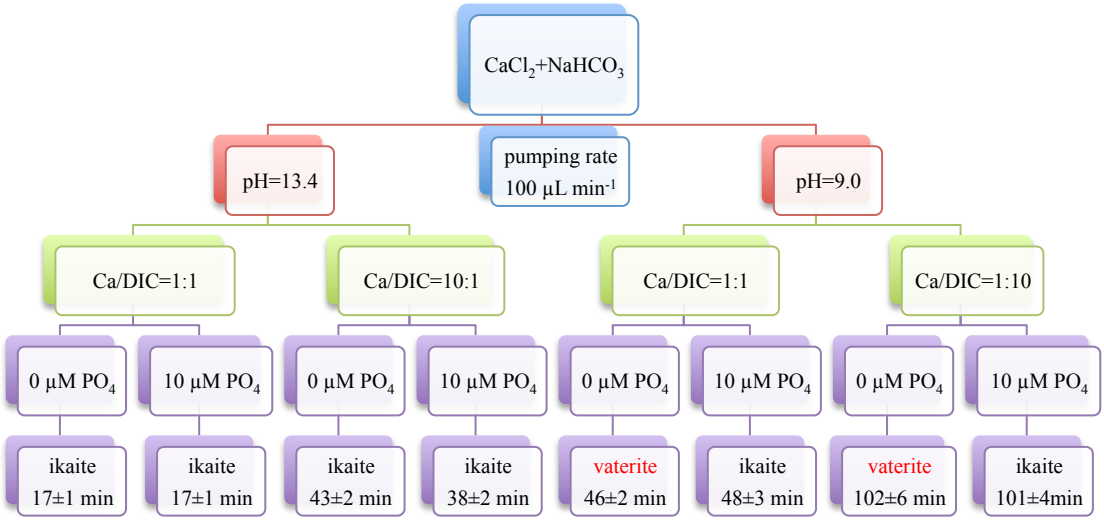

Fig. 3.2 Precipitates of calcium carbonate and onset time at different pH, Ca/DIC ratio and PO_4 concentrations at near-freezing temperature.

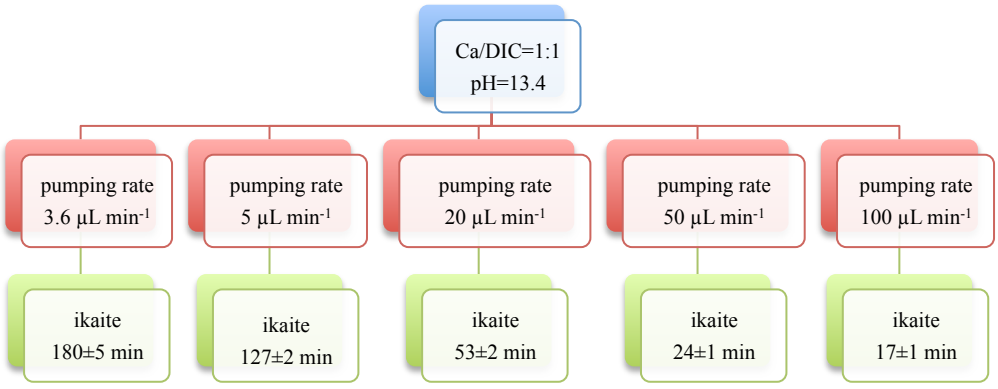

Fig. 3.3 Precipitates of calcium carbonate and onset time at different pumping rates at constant Ca/DIC and pH and in the absence of PO_4 at near-freezing temperature.

3.4 Discussion

3.4.1 Calcium carbonate polymorphs precipitated in the absence of PO_4

The different precipitates of calcium carbonate (ikaite or vaterite) under two pH conditions in the absence of PO_4 might result from the difference in the degree of solution saturation, pH, Ca/CO_3 ratio and potential precipitation time for vaterite $\tau_{p,v}$ (the time span between the moment that the ion activity product of Ca^{2+} and CO_3^{2-} (IAP) passes through the vaterite solubility and the onset of calcium carbonate precipitation). Next, we discuss these effects to determine the controlling factor on the different polymorphs precipitated.

3.4.2 Effect of solution saturation degree

The ion activity product of Ca^{2+} and CO_3^{2-} at the onset of calcium carbonate precipitation is shown in Table 3.1. At the condition of pH = 9.0 and Ca/DIC = 1:1, the log (IAP) is nearly identical to the one at the condition of pH = 13.4 and Ca/DIC = 1:1, but the precipitates are different, namely vaterite at pH = 9.0 and ikaite at pH = 13.4. Similar results are found at the condition of pH = 9.0, Ca/DIC = 10:1 and pH = 13.4, Ca/DIC = 1:10. This suggests that the different precipitates at two pH conditions are not determined by solution saturation degree.

Table 3.1 log (IAP) of calcium and carbonate and precipitates at varied pH and Ca/DIC ratios.

pH	13.4		9.0	
Ca/DIC	1:1	10:1	1:1	1:10
log (IAP)	−6.403	−6.690	−6.408	−6.727
Precipitate	ikaite	ikaite	vaterite	vaterite

3.4.3 Effect of potential precipitation time

The log (IAP) of Ca^{2+} and CO_3^{2-} evolution with time is shown in Fig. 3.4a. Under all conditions, the log (IAP) passes through both vaterite and ikaite solubilities. At pH = 13.4, regardless of the ratio of Ca/DIC, the precipitates are ikaite; at pH = 9.0, the precipitates are vaterite regardless of the ratio of Ca/DIC.

We noticed that $\tau_{p,v}$ is longer at low pH than at high pH at the same Ca/DIC ratio (Fig. 3.4b). Especially at Ca/DIC ratio of 1:10, $\tau_{p,v}$ is up to 81 min. Such a long potential precipitation time might favor the precipitation of the more stable anhydrous form of calcium carbonate, namely, vaterite, which could be an explanation for the precipitation of vaterite at low pH.

Nevertheless, the potential precipitation time effect can be excluded based on another experiment. The evolution of the log (IAP) of Ca^{2+} and CO_3^{2-} with time as well as vaterite potential precipitation time carried out at pH = 13.4 and different pumping rates is shown in Fig. 3.5a and 3.5b. $\tau_{p,v}$ varies from 14 to 100 min, which covers the potential precipitation time apparently sufficient for vaterite formation (Fig. 3.4b). If the long potential precipitation time is the reason for vaterite precipitation, the precipitates at high pH at low pumping rates should be vaterite as well. In fact, no vaterite was observed even at $\tau_{p,v}$ = 100 min. At these pumping rates, ikaite was the only calcium carbonate polymorph precipitated. This evidence excludes the kinetic effect of potential precipitation time for different precipitates.

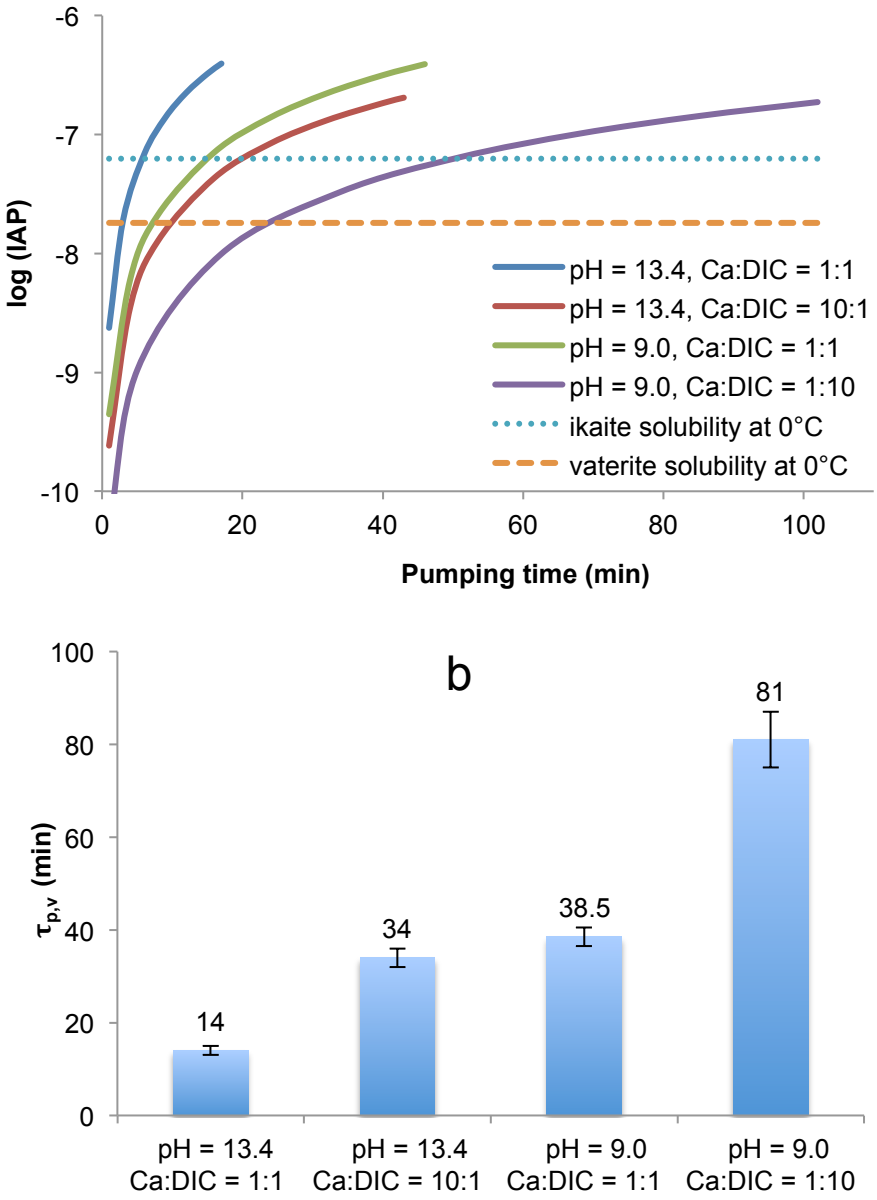

Fig. 3.4 Evolution of the log (IAP) of calcium and carbonate with pumping time until the onset of precipitation (a) and potential precipitation time for vaterite $\tau_{p,v}$ (b) at varied pH and Ca/DIC ratios in the absence of PO_4. The precipitates are ikaite at pH = 13.4 and vaterite at pH = 9.0 regardless of the ratio of Ca:DIC.

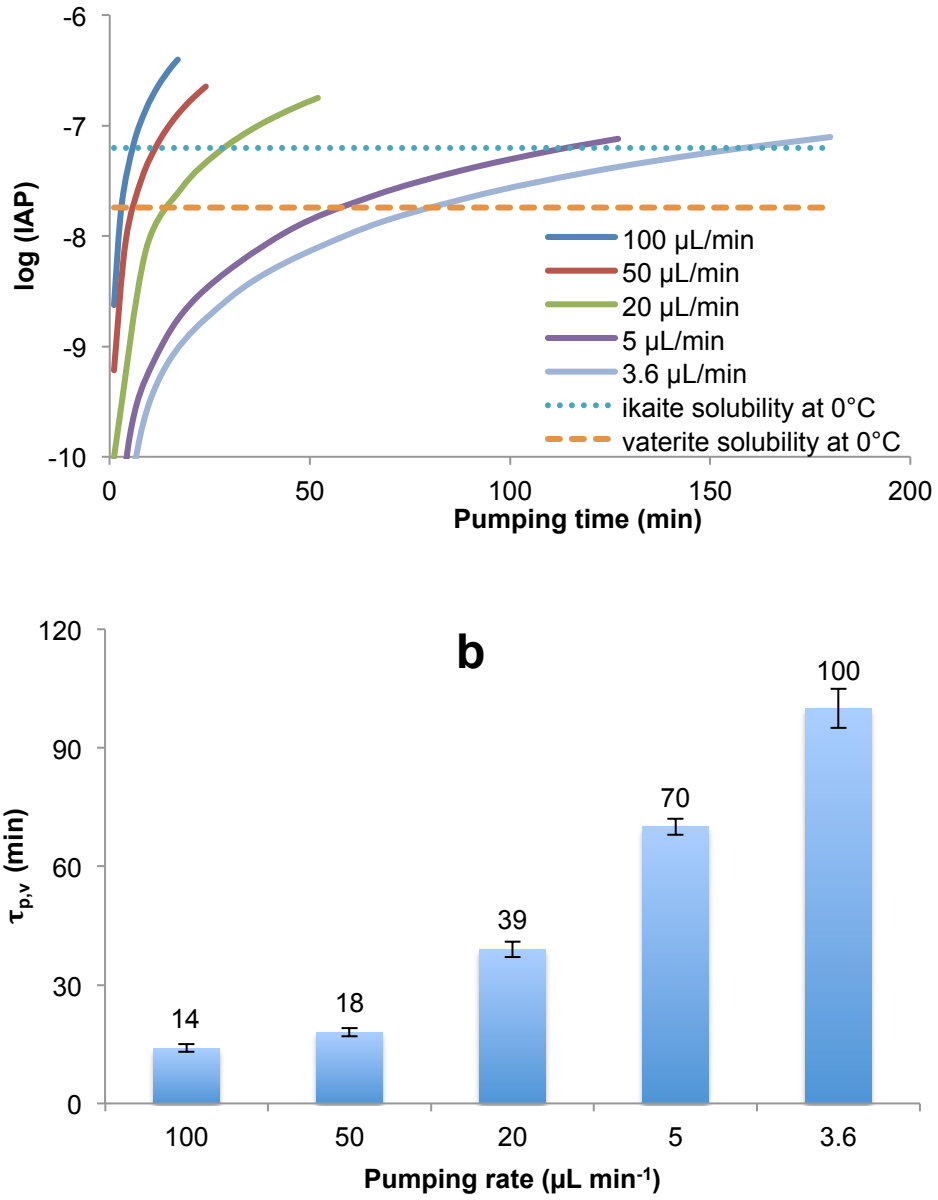

Fig. 3.5 Evolution of the log (IAP) of calcium and carbonate with pumping time until the onset of precipitation (a) and potential precipitation time for vaterite $\tau_{p,v}$ (b) at varied pumping rate under the condition of pH = 13.4, Ca/DIC=1:1 and in the absence of PO_4. Ikaite is the only precipitate under all the pumping rates.

3.4.4 Effect of pH and Ca/CO_3 ratio

Since the effect of solution saturation degree and potential precipitation time are not the reason for the precipitation of different calcium carbonate polymorphs in the absence of PO_4, there are only two variables left: pH and the ratio of Ca/CO_3.

At the same pH but different ratio of Ca/CO_3, the precipitates are the same; at the same ratio of Ca/CO_3 but different pH, the precipitates are different (Table 3.2). This result indicates that the change in pH determines which polymorph is precipitated (ikaite or vaterite) rather than the Ca/CO_3 ratio.

Table 3.2 Ratio of Ca/CO_3 and precipitates at varied pH and Ca/DIC ratios in the absence of PO_4.

pH	13.4		9.0	
Ca/DIC	1:1	10:1	1:1	1:10
Ca/CO_3	1:1	10:1	10:1	1:1
Precipitate	ikaite	ikaite	vaterite	vaterite

3.4.5 Calcium carbonate polymorphs precipitated in the presence of PO_4

At pH = 9.0, different precipitates are observed with or without PO_4 at different ratios of Ca/DIC. The onset time is nearly identical (Table 3.3) at the same Ca/DIC ratio indicating that the degree of solution saturation and $\tau_{p,v}$ are the same regardless of PO_4. So the different precipitates are only caused by the presence or absence of PO_4. This indicates that the addition of PO_4 triggers the formation of ikaite over vaterite.

Table 3.3 Onset time and precipitates at varied pH, Ca/DIC ratios and PO_4 concentrations.

pH	9.0			
Ca/DIC	1:1		1:10	
PO_4 ($\mu mol\ L^{-1}$)	0	10	0	10
Onset time (min)	46±2	49±4	102±6	101±4
Precipitate	vaterite	ikaite	vaterite	ikaite

3.4.6 Mechanisms of the ikaite/vaterite polymorph switch

From the discussion above, it is clear that pH and PO_4 can act as a switch between ikaite and vaterite polymorphs. In the following sub-sections, we look into the mechanisms of pH and PO_4 in controlling the calcium carbonate polymorphs.

3.4.6.1 Mechanism of pH effect

The effect of pH on calcium carbonate polymorphism might be related to the HCO_3^-/CO_3^{2-} distribution in solution. At pH = 13.4, nearly all the dissolved inorganic carbon is in the form of CO_3^{2-}, while at pH = 9.0, HCO_3^- becomes the dominant species with a ratio of HCO_3^-/CO_3^{2-} around 10:1. Now the question is how the change in HCO_3^-/CO_3^{2-} distribution affects the polymorphism of calcium carbonate.

It has long been reported that in calcium carbonate solutions, ion pairs of $CaCO_3^0$ and $CaHCO_3^+$ exist (Greenwald, 1941; Plummer and Busenberg, 1982). According to the calculation results form Visual-Minteq (Gustafsson, 2011), at high pH, $CaCO_3^0$ is the dominant ion pair in solution while at pH = 9.0, $CaHCO_3^+$ becomes a significant ion pair with an activity ratio $\{CaHCO_3^+\}/\{CaCO_3^0\}$ = 0.2 (Fig. 3.6).

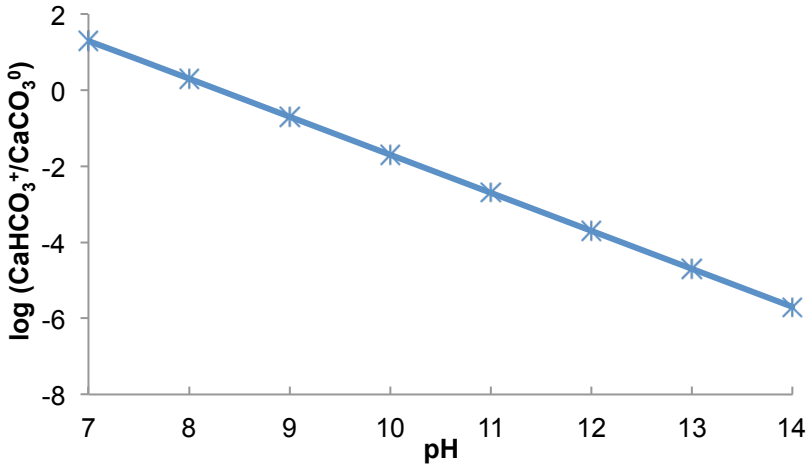

Fig. 3.6 Logarithm of the activity ratio of $CaHCO_3^+$/ $CaCO_3^0$ as a function of pH at 0^oC (Visual-Minteq).

Recent studies revealed that the nucleation of calcium carbonate occurs via stable prenucleation clusters and these calcium carbonate clusters display different structures related to different forms of ACC, which further transform into the particular crystalline polymorphs (Gebauer et al., 2008). According to an atomistic simulation

study (Demichelis et al., 2011), these stable prenucleation clusters might be liquid-like ionic polymers with units of $CaCO_3^0$ and $CaHCO_3^+$, whose structures vary with pH. It was concluded that at low pH, the chain length is limited by competition between CO_3^{2-} and HCO_3^-. The formation of smaller prenucleation clusters at low pH due to the presence of "cluster-terminating" HCO_3^- may, in the present case, drive the ikaite/vaterite polymorph switch; while at high pH, the effect of HCO_3^- becomes unimportant due to the dramatic decrease in HCO_3^- concentration. Our experimental results seem to support the mechanism proposed by Demichelis et al. (2011).

3.4.6.2 Mechanism of PO4 effect

According to a study by Gebauer et al. (2009), the presence of PO_4 can bind calcium ions as well as prenucleation clusters. It was postulated that PO_4 might preferentially adsorb onto clusters with certain structures, which would lead to a change in the local structure of nucleated particles, simplifying the nucleation for particular polymorphs (Gebauer et al., 2009). At the atomic level, where based on first principles molecular dynamics simulations (Di Tommaso and de Leeuw, 2010), it has been suggested that the hydration structure and water dynamics of the first and second hydration shell of calcium can even be influenced by simple anions such as ions of halogen elements. It is plausible to speculate that the presence of PO_4 will play a similar or even more effective role in calcium carbonate crystallization processes. If the presence of PO_4 in solution results in a decreasing dynamics of the solvation shell of Ca^{2+}, dehydration of Ca^{2+} will become slower, which might favor the formation of hydrated calcium carbonate polymorph (Bischoff et al., 1993a), thereby driving $CaCO_3$ precipitation towards the hydrated polymorph, in our case, ikaite at pH = 9.0.

3.5 Conclusions

At near-freezing temperature, precipitation of metastable forms of calcium carbonate in solution is favored (ikaite or vaterite). The pH as well as PO_4 can act as a switch between ikaite and vaterite polymorphs. The effect of pH on different polymorphs of calcium carbonate is related to the distribution of HCO_3^-/CO_3^{2-}, which might affect the structure of prenucleation clusters. The presence of PO_4 may alter the hydration shell of calcium and thus further affect the nucleation processes.

Chapter 4

The study of ikaite formation in artificial sea ice brine

Abstract

Ikaite ($CaCO_3 \cdot 6H_2O$) has only recently been discovered in sea ice, in a study that also provided first direct evidence of $CaCO_3$ precipitation in sea ice. However, little is as yet known about the impact of physico-chemical processes on ikaite precipitation in sea ice. Our study focused on how the changes in pH, salinity, temperature and phosphate (PO_4) concentration affect the precipitation of ikaite. Experiments were set up at pH from 8.5 to 10.0, salinities from 0 to 105 (in both artificial seawater (ASW) and NaCl medium), temperatures from 0 to -4°C and PO_4 concentrations from 0 to 50 μmol kg^{-1}. The results show that in ASW, calcium carbonate was precipitated as ikaite under all conditions. In the NaCl medium, the precipitates were ikaite in the presence of PO_4 and vaterite in the absence of PO_4. The onset time (τ) at which ikaite precipitation started, decreased nonlinearly with increasing pH. In ASW, τ increased with salinity. In the NaCl medium, τ first increased with salinity up to salinity 70 and subsequently decreased with a further increase in salinity; it was longer in ASW than in the NaCl medium under the same salinity. τ did not vary with temperature or PO_4 concentration. These results indicate that ikaite is very probably the only phase of calcium carbonate formed in sea ice. PO_4 is not, as previously postulated, crucial for ikaite formation in sea ice. The change in pH and salinity is the controlling factor for ikaite precipitation in sea ice. Within the ranges investigated in this study, temperature and PO_4 concentration do not have a significant impact on ikaite precipitation.

4.1 Introduction

Ikaite ($CaCO_3 \cdot 6H_2O$) is a metastable phase of calcium carbonate, which normally forms in a cold environment and/or under high pressure (Marland, 1975). It is usually found in environments characterized by low temperatures (below 4°C), high pH, high alkalinity, elevated concentrations of phosphate (PO_4) and organic matter (Buchardt et al., 1997; Rickaby et al., 2006). Although synthetic $CaCO_3 \cdot 6H_2O$ had already been known from laboratory studies in the nineteenth century (Pelouze, 1865), it was first found in nature at the bottom of the Ika Fjord in Greenland (Pauly, 1963) and later in deep-sea sediments (Suess et al., 1982). Recently, Dieckmann et al. (2008, 2010) discovered this mineral in sea ice, which at the same time, was the first direct evidence of $CaCO_3$ precipitation in natural sea ice. The occurrence of $CaCO_3$ is considered to play a significant role in the CO_2 flux of the sea ice system (Geilfus et al., 2012; Rysgaard et al., 2007).

At present it is not clear whether ikaite is the only calcium carbonate phase formed in sea ice (Dieckmann et al., 2010; Rysgaard et al., 2012). Calcium carbonate exists in six phases, namely, amorphous calcium carbonate (ACC), calcium carbonate monohydrate (MCC), calcium carbonate hexahydrate (ikaite) and three anhydrous phases: vaterite, aragonite and calcite. Ikaite is more soluble compared to the three anhydrous phases under normal atmospheric pressure (Bischoff et al., 1993a). The precipitation of ikaite occurs only when the ion activity product (IAP) of Ca^{2+} and CO_3^{2-} in the solution exceeds the solubility product of ikaite ($K_{sp,\ ikaite}$). The activities of Ca^{2+} and CO_3^{2-} can be derived from their concentrations and activity coefficients. The values of the activity coefficient depend on solution ionic strength and temperature. In seawater at salinity 35 and temperature 25°C, for example, the activity coefficients $\gamma_{Ca}^{2+} = 0.203$ and $\gamma_{CO3}^{2-} = 0.039$ (Millero and Pierrot, 1998) are much smaller than 1. In normal seawater at a temperature above 0°C, seawater is undersaturated with respect to ikaite (Bischoff et al., 1993a). The precipitation of ikaite from seawater requires a higher concentration of Ca^{2+} and/or CO_3^{2-}, such as can be achieved in sea ice brine. Given the consideration that brine salinity can easily be over 200 at a corresponding temperature as low as -40°C (Eicken, 2003), this extreme environment would greatly affect the chemical environment in brine with regard to calcium concentrations and dissolved inorganic carbon (DIC). Depending on the

physico-chemical environments as well as biological effect (respiration and photosynthesis), brine pH can vary from less than 8 to up to 10 (Gleitz et al., 1995; Papadimitriou et al., 2007). Due to the inhibiting role of PO_4 in the formation of anhydrous calcium carbonate polymorphs (Burton and Walter, 1990; Reddy, 1977), it is assumed that elevated PO_4 concentrations play a crucial role in ikaite formation (Buchardt et al., 1997; Dieckmann et al., 2010). However, this has never been tested under conditions representative for natural sea ice.

Despite of the apparent significance of calcium carbonate precipitation in sea ice, little is as yet known about the impact of physico-chemical processes on ikaite precipitation in sea ice. Papadimitriou et al. (2013) studied the solubility of ikaite in seawater-derived brines. In their study, the $K_{sp,\ ikaite}$ was measured in temperature-salinity coupled conditions, and based on simple modeling it was concluded that the precipitation of ikaite in sea ice possibly only occurs when brine pCO_2 is reduced. However, as the conditions leading to calcium carbonate precipitation in brine are normally coupled, a variation in sea ice temperature will change the brine salinity and also the chemical environment. It has therefore not been possible to distinguish/identify the dominant process that controls calcium carbonate precipitation under conditions representative for natural sea ice. In this study, we uncoupled the conditions in sea ice brine and each condition (pH, salinity, temperature and PO_4 concentration) was studied independently in the laboratory, in order to investigate whether ikaite was the only phase of calcium carbonate formed in sea ice and to qualify the effect of pH, salinity, temperature and PO_4 concentration on the precipitation of ikaite.

4.2 Methods

4.2.1 Preparation of stock solutions

Artificial seawater (ASW) of different salinities was prepared according to Millero (2006) with slight modifications. Ca^{2+} and HCO_3^- were not initially added in the ASW; the amount of $NaHCO_3$ and $CaCl_2$ was compensated for by adding NaCl. The amount of salt needed at salinity 70 and 105 was two and three times of that at salinity 35 (Table 4.1). Ten kilograms ASW of salinity 70 was prepared as a stock

solution. In addition, 1 kg ASW of salinity 35 as well as salinity 105 was prepared separately. The salinity of the ASW stock solutions was checked with a conductivity meter (WTW cond 330i). Subsamples of 10 mL stock solution of salinity 70 and 105 were diluted to salinity 35 before beginning with measurements; the differences between the theoretical and measured values were within ±0.2. Stock solutions of $CaCl_2$ and $NaHCO_3$ at concentrations of 2.5 mol kg^{-1}(soln) and 0.5 mol kg^{-1}(soln) were prepared by dissolving 183.775 g $CaCl_2 \cdot 2H_2O$ and 21.002 g $NaHCO_3$ into 500 g solutions using de-ionized water and subsequently stored in gas-tight Tedlar bags (SKC). All chemicals were obtained from Merck (EMSURE® ACS, ISO, Reag, Ph Eur) except $SrCl_2$ and H_3BO_3, which were from Carl Roth (p.a., ACS, ISO).

Table 4.1 The compounds of ASW at different salinities.

	Amount of salt (g) needed in 1000g solution		
Salt	S=35	S=70	S=105
NaCl	25.122	50.245	75.368
$MgCl_2 \cdot 6H_2O$	10.738	21.477	32.215
Na_2SO_4	4.010	8.020	12.030
KCl	0.699	1.398	2.097
$SrCl_2 \cdot 6H_2O$	0.024	0.048	0.072
KBr	0.100	0.200	0.300
H_3BO_3	0.025	0.051	0.076
$NaHCO_3$	-	-	-
$CaCl_2 \cdot 2H_2O$	-	-	-

4.2.2 Experimental setup

Four parameters were studied: pH (8.5 to 10.0), salinities (0 to 105) both in ASW and the NaCl medium, temperatures (0 to -4°C), and PO_4 concentrations (0 to 50 µmol kg^{-1}). The standard values were pH 9.0, salinity 70, temperature 0°C, PO_4 concentration 10 µmol kg^{-1} and only one of these quantities was varied at a time. Experiments were also carried out in the NaCl medium at salinities from 0 to 105 in the absence of PO_4 at pH 9 and temperature 0°C.

In order to simulate the concentration processes of Ca^{2+} and DIC during sea ice formation, stock solutions of $CaCl_2$ and $NaHCO_3$ (Ca^{2+}:DIC = 5:1, which is the typical concentration ratio in seawater) were pumped from the Tedlar bags into a Teflon reactor vessel with 250 g working solution using a high precision peristaltic pump (IPC-N, Ismatec) at a constant pumping rate of 20 µL min^{-1} (Fig. 4.1). The

solution was stirred at 400 rpm and the temperature was controlled by water-bath using double walled water jackets. pH electrodes (Metrohm 6.0253.100) were calibrated using NBS buffers 7.000 ± 0.010 and 10.012 ± 0.010 (Radiometer analytical, IUPAC standard). The pH of the solution was kept constant by adding 0.5 mol L^{-1} NaOH which was controlled by a titration system (TA20 plus, SI Analytics). pH and the volume of NaOH added to the solution were recorded every 10 s. Depending on the experimental conditions, the maximum input of $CaCl_2$, $NaHCO_3$ and NaOH into the working solution during the experiments is within a few mL, which did not have a significant effect on solution salinity. Duplicates for each experimental condition were run in parallel.

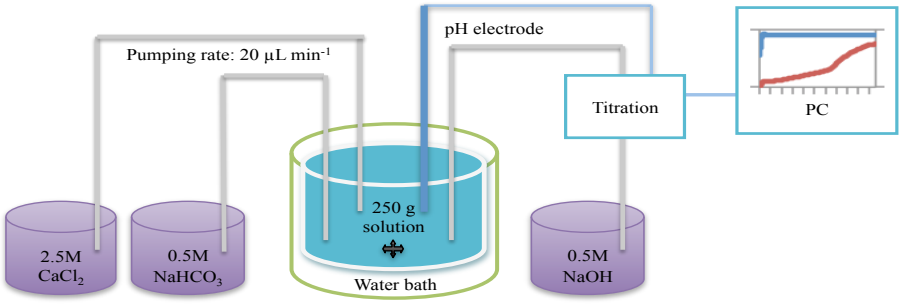

Fig. 4.1 Experimental setup for calcium carbonate precipitation under varied experimental conditions.

4.2.3 Onset time determination

We use the timespan between the start of the titration and the onset of ikaite precipitation, called "onset time (τ)", for the analysis of different experiments. This onset time includes the time for the solution to reach saturation (Ω = 1) with respect to ikaite and the time between reaching the Ω = 1 level and the onset of precipitation (usually at a much higher Ω value). Therefore, τ should be controlled by both thermodynamic and kinetic effects.

While ikaite is precipitated from the solution, CO_2 is released, which leads to a decrease in solution pH. This rapid change in pH could have been used to ascertain the onset of precipitation. However, during the experiment, pH in the solution was kept constant by the addition of NaOH. Therefore, the change in NaOH volume added

into the reactor vessel was used to determine τ as indicated in Fig. 4.2. In order to obtain a higher accuracy, τ was determined from the deviation of NaOH volume change (ΔV) relative to the time interval (Δt = 2 min). The point where the slope ΔV/Δt started to increase was considered as the onset of ikaite precipitation.

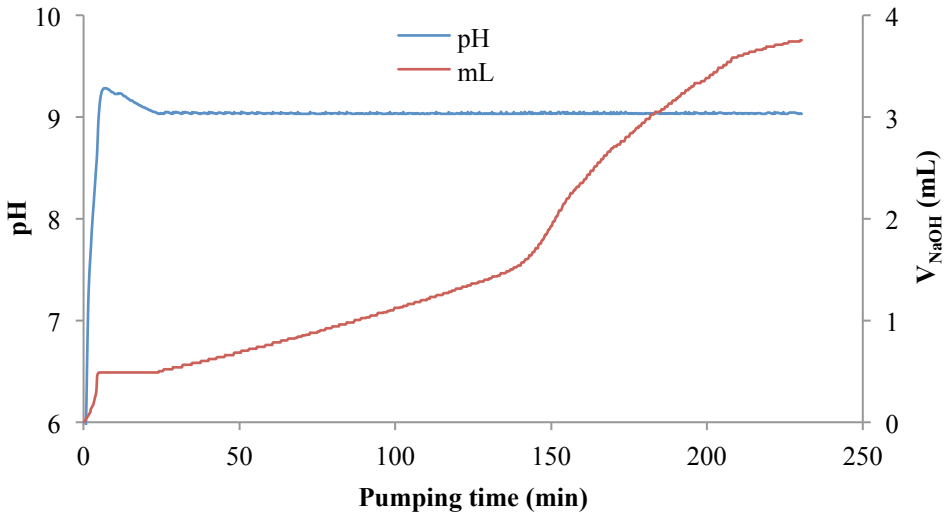

Fig. 4.2 An illustration of a typical NaOH titration profile obtained at pH 9, salinity (ASW) 70, temperature 0°C and phosphate concentration 10 µmol kg^{-1}.

4.2.4 Crystal identification

Immediately after the crystals were precipitated, indicated by the change in the volume of NaOH addition (section 2.3), around 2 mL of the well-stirred solution was sampled together with the crystals by means of a pipette and quickly transferred to a glass petri dish. The morphology of the crystals was characterized using a microscope (Zeiss, Axiovert 200M) with an objective of 63x magnification. The phase identification of the crystals was done by means of Raman microscopy. This method can be used to reliably distinguish between the various polymorphs of calcium carbonate (Nehrke et al., 2012; Tlili et al., 2001). The confocal Raman microscope (WITec®, Ulm, Germany) was equipped with a diode laser (532 nm) and an Olympus® 20x Teflon coated water submersible objective. During the Raman measurements, crystals were maintained in the original solution and placed in a glass petri dish, which was kept cold using an ice-water bath.

4.2.5 Evolution of the ion activity product of calcium and carbonate

The evolution of the IAP of Ca^{2+} and CO_3^{2-} in the solution under different experimental conditions was calculated by using the chemical equilibrium model Visual-Minteq 3.0 (Gustafsson, 2011) modified by the implementation of $K_{sp,\ ikaite}$ according to Bischoff et al. (1993a). The solubility constant of ikaite ($K_{sp,\ ikaite}$) was derived from $\log K_{sp,\ ikaite} = 0.15981 - 2011.1/T$, where $T = {}^{o}K$ (Bischoff et al., 1993a). Since most equilibrium constants (including $K_{sp,\ ikaite}$) at high salinities and low temperatures are not well known, extrapolations of functional relationships had to be used. The input parameters for each run were the same as used in the experiments, and the model was run in the function of "titration", simulating the experimental pumping of $CaCl_2$ and $NaHCO_3$ into the working solution. As in most models, the calculation of ionic activities is not very accurate at high salinities, especially the calculation of CO_3^{2-} activity, the evolution trends under different experimental conditions therefore will be discussed in this study instead of referring to the absolute values.

4.2.6 CO_2 system calculation

The fraction of CO_3^{2-} in DIC (CO_3^{2-} fraction, for short) under all the experimental conditions was calculated from pH and DIC by using CO2SYS (Pierrot et al., 2006). The results of CO2SYS are not reliable for the calculation of the CO_2 system at high salinities because the functional expressions for the equilibrium constants are based on measurements over a limited range of salinities and temperatures. Here, we chose two sets of carbonate equilibrium constants, one from Mehrbach et al. (1973) as refitted by Dickson and Millero (1987) (referred to as constants_a), and the other one from Millero (2010) (referred to as constants_b), to evaluate the sensitivity of the calculated CO_3^{2-} fraction to uncertainties in the magnitude of the equilibrium constants. The remaining parameters were the same: K_{HSO4}^{-} was from Dickson (1990); $[B]_T$ value was from Uppström (1974) and the pH_{NBS} scale was applied. The input parameters for the CO_2 system calculation were consistent with the experimental conditions except that the DIC was fixed at 2000 μmol kg^{-1} for each run, since the change in DIC concentration does not affect the CO_3^{2-} fraction calculation.

4.3 Results

4.3.1 Effect of experimental conditions on the calcium carbonate polymorph precipitated

According to the vibration ν_1 and ν_4 of CO_3^{2-}, two types of Raman spectra were distinguished in this study. After a comparison with the available references (Behrens et al., 1995; Tlili et al., 2001), ikaite was identified by the vibrational modes ν_1 (1071 cm^{-1}) and ν_4 (718 cm^{-1}), and vaterite was identified by the two doublets of the vibration modes ν_1 (1075 cm^{-1}, 1090 cm^{-1}) and ν_4 (742 cm^{-1}, 752 cm^{-1}).

In ASW, according to the Raman measurements (Fig. 4.3a), ikaite is the only calcium carbonate polymorph precipitated at pH ranging from 8.5 to 10.0, salinities from 0 to 105, temperatures from 0 to -4°C and PO_4 concentrations from 0 to 50 μmol kg^{-1}. The morphology of ikaite crystals precipitated from ASW is similar under all the conditions, with an average crystal size of approximately 20 μm (Fig. 4.3b). The morphology resembles that of natural ikaite crystals found in sea ice (Rysgaard et al., 2013), however, crystals in our study are generally smaller.

In the NaCl medium, and the presence of 10 μmol kg^{-1} PO_4, according to the Raman measurements (Fig. 4.3c), ikaite is the only precipitate in the salinity range from 0 to 105. The crystal size is similar to the one observed for the crystals precipitated from ASW. However, the morphology of ikaite crystals differs (Fig. 4.3d). In the absence of PO_4 and the same salinity range, vaterite (see Raman spectrum given in Fig. 4.3e) is the dominant calcium carbonate polymorph precipitated and only few ikaite crystals were observed. The small spherical crystals shown in Fig. 4.3f are vaterite with an average size of ~2 μm (within the same size range as described by Nehrke and Van Cappellen (2006)) whereas the large crystal in the middle of Fig. 4.3f is ikaite.

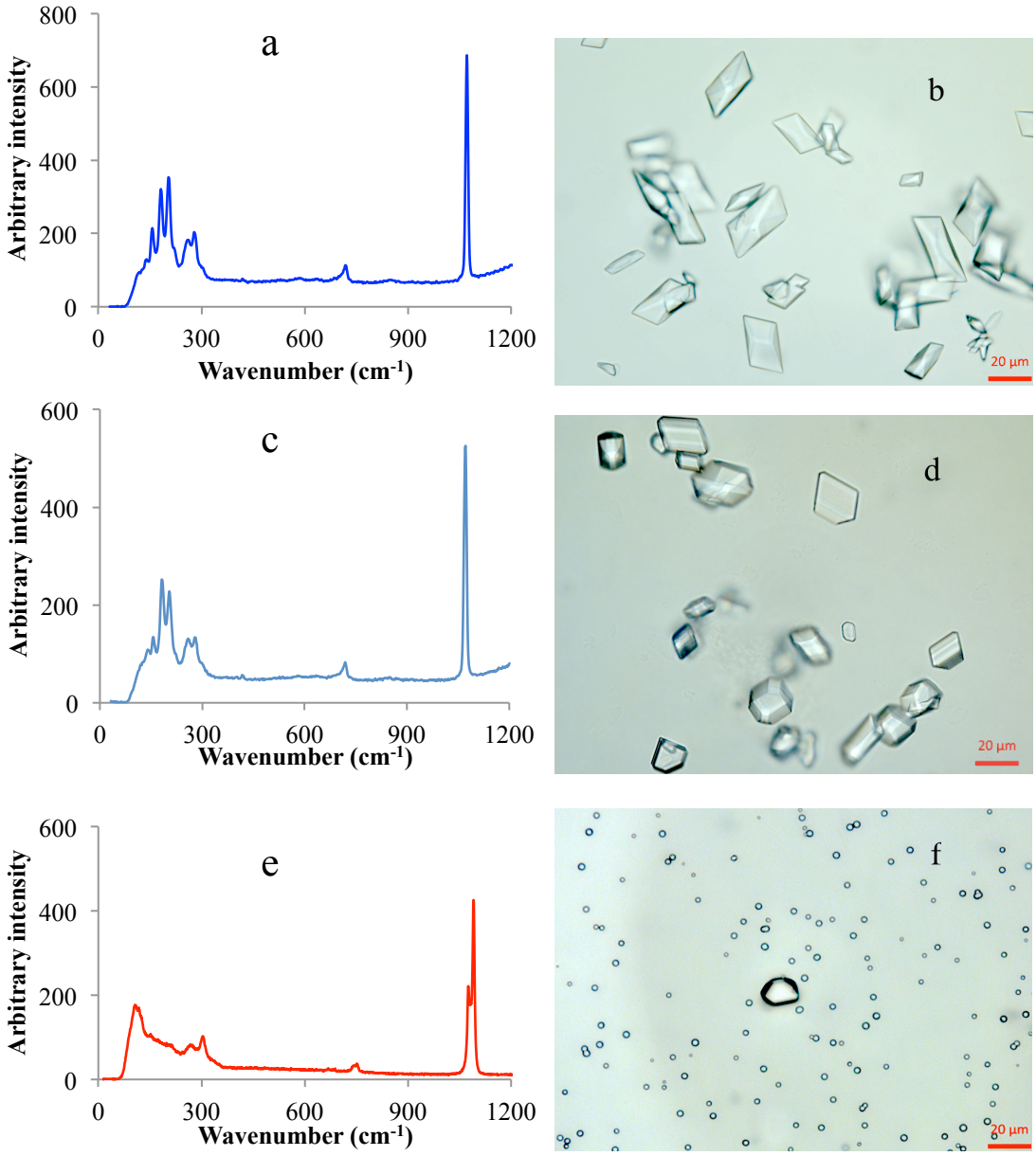

Fig. 4.3 Ikaite Raman spectrum (a) and morphology (b) obtained at the experimental condition pH 9.0, salinity (ASW) 70, temperature 0°C, phosphate concentration 0 µmol kg^{-1}, and representative for all precipitates in the ASW medium. Ikaite Raman spectrum (c) and morphology (d) obtained at the experimental condition pH 9.0, salinity (NaCl medium) 70, temperature 0°C, phosphate concentration 10 µmol kg^{-1}, and representative for all precipitates in the NaCl medium in the presence of PO_4. Vaterite Raman spectrum (e) and morphology (f) obtained at the experimental condition pH 9.0, salinity (NaCl medium) 105, temperature 0°C, phosphate concentration 0 µmol kg^{-1}, and representative for all precipitates in the NaCl medium in the absence of PO_4.

4.3.2 Onset time of ikaite under different experimental conditions

Onset time (τ) under different pH, salinities (both in ASW and NaCl medium), temperatures and PO_4 concentrations is illustrated in Fig. 4.4(a−d) and Table 4.2. At pH from 8.5 to 10.0, τ decreases nonlinearly with increasing pH; it decreases steeply at low pH and then slows down at high pH. At salinities from 0 to 105, in ASW, τ increases with salinity; in the NaCl medium, τ first increases with salinity and above salinity 70, it decreases slightly. τ is longer in ASW than in the NaCl medium under the same salinity conditions. There is no significant difference in τ in the temperature range from 0 to -4°C and in the PO_4 concentration range from 0 to 50 μmol kg^{-1}.

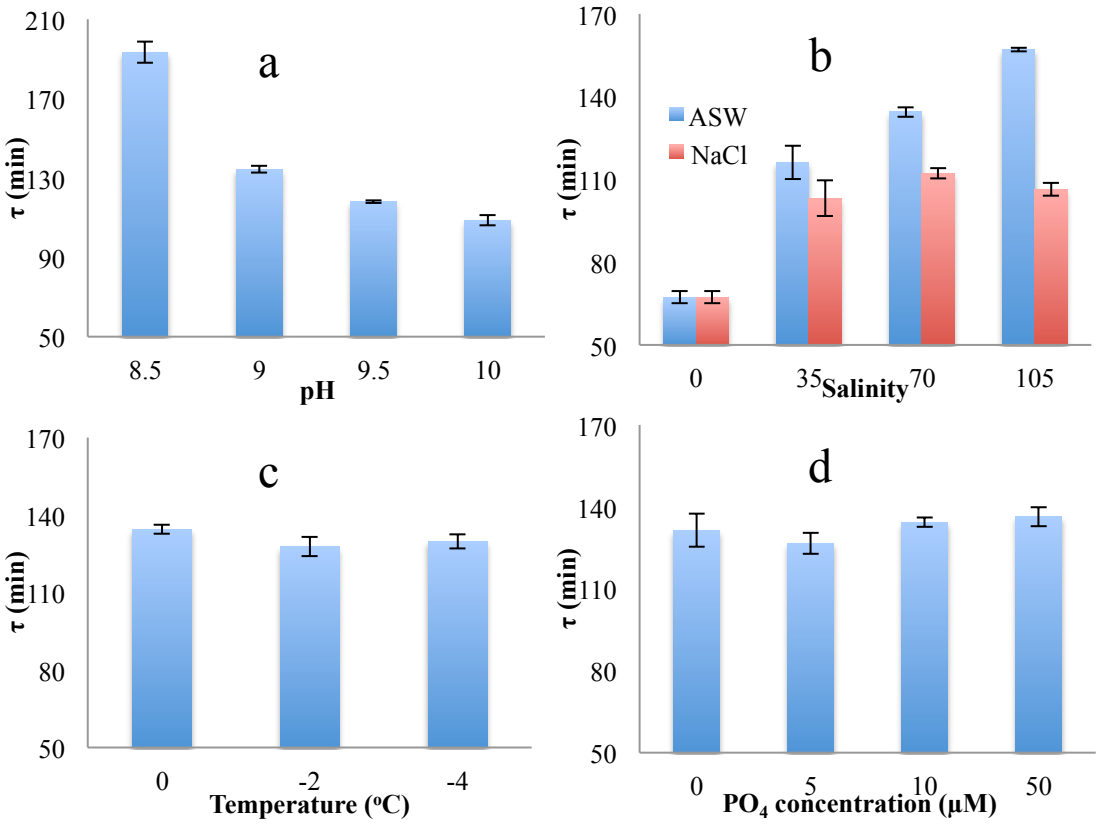

Fig. 4.4 Changes in τ with pH (a), salinity (b), temperature (c) and phosphate concentration (d).

Table 4.2 Pumping time until solution reaching ikaite solubility (t_s), onset time (τ) and the common logarithmic ion activity product of calcium and carbonate (log (IAP)) and solution supersaturation (Ω = IAP/$K_{sp,\ ikaite}$) at the onset of ikaite precipitation under different pH, salinity (ASW and NaCl medium), temperature and phosphate concentration conditions. The standard deviation of τ and log (IAP) is derived from duplicate experiments.

Exp. conditions	**Exp. variations**	**t_s (min)**	**τ (min)**	**log (IAP)**	**Ω**
pH effect: at S (ASW) 70, T 0°C, PO_4 10 µM	8.5	112	193 ± 5.3	-6.73 ± 0.025	3.02
	9.0	72	134 ± 1.8	-6.67 ± 0.011	3.47
	9.5	54	118 ± 0.7	-6.53 ± 0.005	4.68
	10.0	46	109 ± 2.6	-6.48 ± 0.020	5.37
S (AWI) effect: at pH 9.0, T 0°C, PO_4 10 µM	0	28	67 ± 2.2	-6.59 ± 0.021	4.17
	35	62	116 ± 6.1	-6.68 ± 0.051	3.47
	70	72	134 ± 1.8	-6.67 ± 0.011	3.47
	105	78	157 ± 0.6	-6.61 ± 0.003	3.98
S (NaCl) effect: at pH 9.0, T 0°C, PO_4 10 µM	0	28	67 ± 2.2	-6.59 ± 0.021	4.17
	35	58	103 ± 6.5	-6.72 ± 0.049	3.09
	70	65	112 ± 1.8	-6.74 ± 0.014	2.95
	105	70	106 ± 2.4	-6.84 ± 0.019	2.29
T effect: at pH 9.0, S (ASW) 70, PO_4 10 µM	0°C	72	134 ± 1.8	-6.67 ± 0.011	3.47
	-2°C	69	128 ± 3.7	-6.73 ± 0.023	3.39
	-4°C	66	130 ± 2.7	-6.74 ± 0.017	3.72
	-10°C	60	NA	NA	NA
PO_4 effect: at pH 9.0, S (ASW) 70, T 0°C	0 µM	72	131 ± 6.0	-6.69 ± 0.037	3.31
	5 µM	72	127 ± 3.9	-6.71 ± 0.024	3.16
	10 µM	72	134 ± 1.8	-6.67 ± 0.011	3.47
	50 µM	72	136 ± 3.4	-6.66 ± 0.022	3.55

4.3.3 Evolution of the ion activity product of Ca^{2+} and CO_3^{2-}

The evolution of the common logarithmic ion activity product of Ca^{2+} and CO_3^{2-} (log (IAP)) until the onset of ikaite precipitation and the solution supersaturation at the onset of ikaite precipitation ($\Omega = IAP/K_{sp,\ ikaite}$) under different pH, salinities (both in ASW and NaCl medium), temperatures and PO_4 concentrations are illustrated in Fig. 4.5(a~e) and Table 4.2. At pH from 8.5 to 10.0, the rates of log (IAP) evolution are much faster at higher pH but the evolution curves are getting closer with the increase in pH. Ω increases with increasing pH. At salinity from 0 to 105, log (IAP) evolution shows a similar pattern in ASW and NaCl medium: that is at salinity 0, the evolution is much faster than those at salinities equal or larger than 35. And the evolution curves are getting closer with the increase in salinity. The rates in log (IAP) evolution are slower in ASW than those in the NaCl medium under the same salinity conditions. For example, at salinity 70, the time to reach ikaite solubility (t_s) is 72 min in ASW while it is 65 min in the NaCl medium (Table 4.2). Ω is similar in ASW in this studied salinity range; while it decreases with increasing salinity in the NaCl medium. At temperatures from 0 to -4°C, the curves of log (IAP) evolution overlap as do the curves of log (IAP) evolution at PO_4 concentrations from 0 to 50 μmol kg^{-1}. There is no significant difference in Ω in this temperature and PO_4 concentration range.

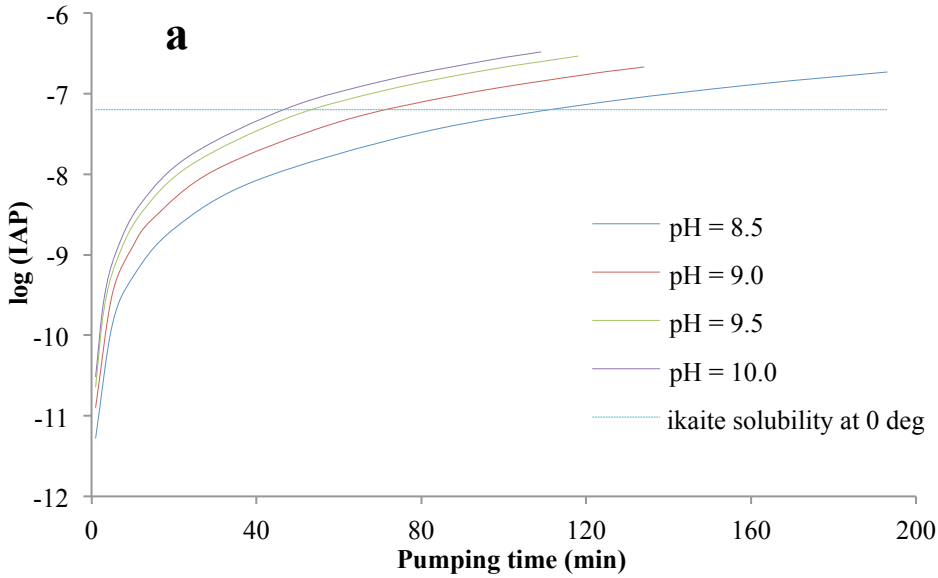
a
log (IAP)
-6
-7
-8
-9
-10
-11
-12
0
40
80
120
160
200
Pumping time (min)
pH = 8.5
pH = 9.0
pH = 9.5
pH = 10.0
ikaite solubility at 0 deg

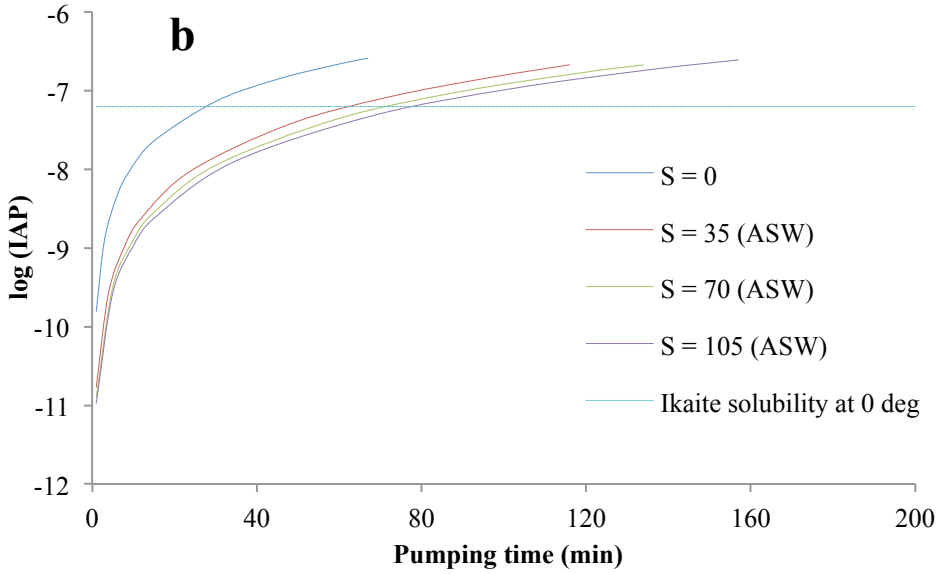
b
log (IAP)
-6
-7
-8
-9
-10
-11
-12
0
40
80
120
160
200
Pumping time (min)
S = 0
S = 35 (ASW)
S = 70 (ASW)
S = 105 (ASW)
Ikaite solubility at 0 deg

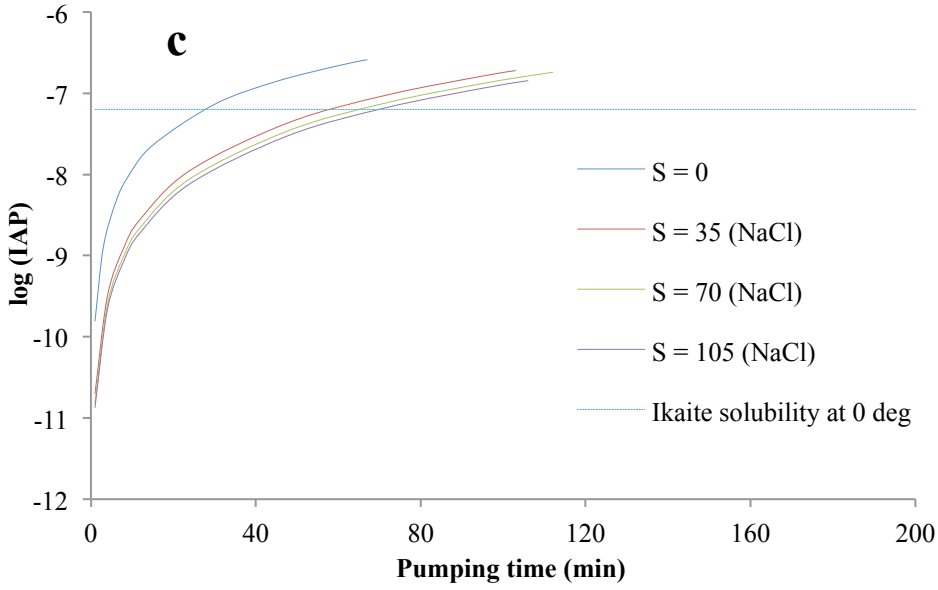
c
log (IAP)
-6
-7
-8
-9
-10
-11
-12
0
40
80
120
160
200
Pumping time (min)
S = 0
S = 35 (NaCl)
S = 70 (NaCl)
S = 105 (NaCl)
Ikaite solubility at 0 deg

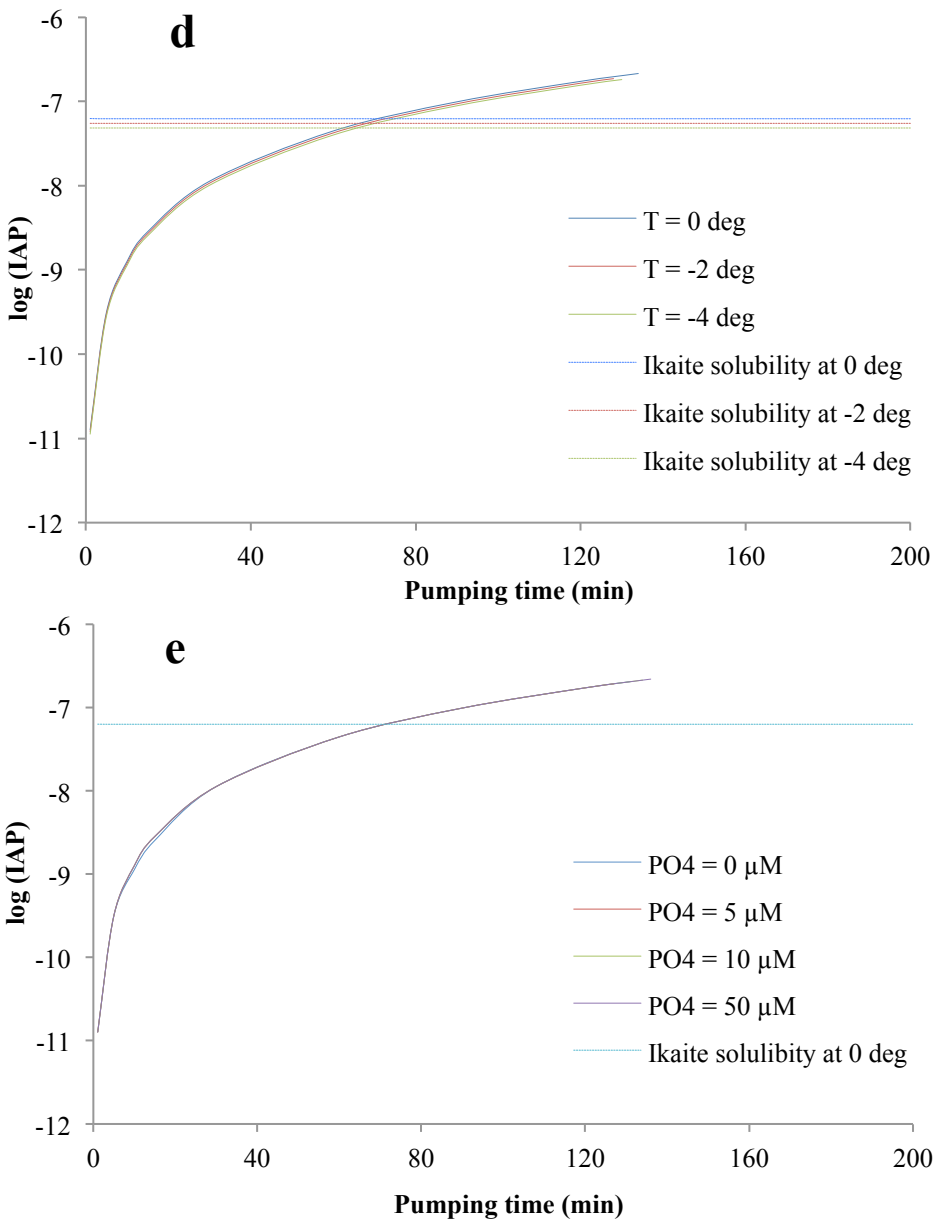

Fig. 4.5 Evolution of log (IAP) at different pH (a), salinities in ASW (b), salinities in the NaCl medium (c), temperatures (d) and phosphate concentrations (e).

4.4 Discussion

4.4.1 Ikaite crystal size

The smaller size of ikaite crystals in our experiments compared to those found in natural sea ice might be due to the much faster precipitation rate under laboratory conditions, which favors calcium carbonate nucleation over further growth of crystals (Vekilov, 2010). In sea ice, the precipitation of ikaite probably goes through a much slower process, allowing the crystals to grow larger. However, the size of natural ikaite in sea ice could also be limited by the dimensions of the brine pockets or brine channels (Dieckmann et al., 2008).

4.4.2 Effect of PO_4 on the polymorph of calcium carbonate precipitated

The different precipitates in the NaCl medium with and without PO_4 indicate that the presence of PO_4 is important for ikaite formation in the NaCl medium. This result is consistent with other studies stating that ikaite is usually found in an elevated PO_4 environment (Buchardt et al., 1997; Council and Bennett, 1993).

The different precipitates in ASW and the NaCl medium in the absence of PO_4 indicate that PO_4 is not crucial for ikaite formation in ASW. It has been reported (Bischoff et al., 1993a; Fernández-Díaz et al., 2010) that Mg^{2+} and SO_4^{2-} ions in seawater could also inhibit the formation of more stable phases of calcium carbonate, and thus could favor ikaite formation. This might explain why ikaite was also found in sea ice even at very low PO_4 concentrations (Dieckmann et al., 2010).

4.4.3 Effect of experimental conditions on ikaite precipitation

According to the evolution curves of log (IAP) under all the experimental conditions, we can conclude that τ is mainly controlled by the rates of log (IAP) evolution and also greatly affected by the kinetic effect, such as inhibitor ions. In the following sub-sections, the effect of experimental conditions on ikaite precipitation will focus on the factors controlling the rates of log (IAP) evolution as well as the kinetic effect.

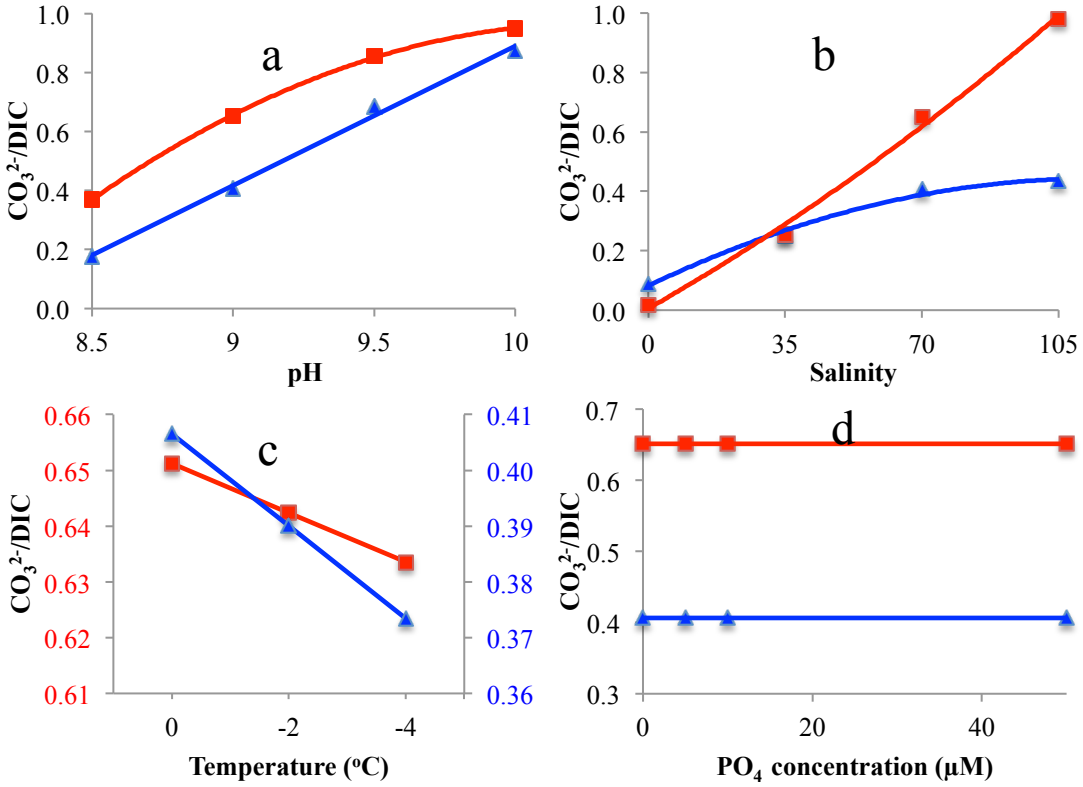

Fig. 4.6 CO_3^{2-} fraction relative to pH (a), salinity (b), temperature (c) and phosphate concentration (d) based on two sets of constants (constants_a, in blue triangle; constants_b, in red square).

4.4.3.1 pH effect

In ASW at a constant salinity of 70 and temperature of 0°C, the activity coefficients of both Ca^{2+} and CO_3^{2-} do not change. Therefore, we only need to focus on the change in CO_3^{2-} concentration with variations of pH. According to the calculation results from CO2SYS, under the same conditions, the results obtained by using constants_a and constants_b show a similar trend (Fig. 4.6a). The increase in pH can greatly increase the CO_3^{2-} fraction in this studied pH range, resulting in a much faster approach to ikaite solubility (Fig. 4.5a). However, the decrease in τ with pH is not linear, which is much faster at low pH than at high pH. This is because the CO_3^{2-} fraction cannot increase infinitely; the increase in the CO_3^{2-} fraction will slow down at high pH and the CO_3^{2-} fraction will approach 1. We can speculate that above a certain pH (depending on the salinity and temperature conditions, since the CO_3^{2-} fraction is also affected by them, as is discussed in section 4.3.2 and 4.3.3), the increase in pH will not have an impact on the CO_3^{2-} fraction, and therefore has no

effect on ikaite precipitation. We notice that Ω in this studied pH range increases from 3.02 to 5.37 with increasing pH (Table 4.2). This indicates that if the evolution of log (IAP) is slow, ikaite could be precipitated at a much lower supersaturation level. This is also confirmed by a second study, which shows that at different pumping rates of Ca^{2+} and DIC, Ω is low at slow pumping rates (Hu et al, submitted).

4.4.3.2 Salinity effect

The different trends in τ in ASW and the NaCl medium indicate that the effect of salinity on ikaite precipitation is not straightforward. First, according to the calculation results from CO2SYS, although there is large uncertainty in predicting the exact CO_3^{2-} fraction change with salinity at high salinities, both the results obtained from two sets of constants show a similar trend (Fig. 4.6b): the CO_3^{2-} fraction increases with salinity (referred to as a positive effect). However, the increase in salinity implies an increase in ionic strength as well and thus a reduction in the activities of both Ca^{2+} and CO_3^{2-} (referred to as a negative effect). This negative effect is much stronger in ASW than in the NaCl medium, since there are ion species like SO_4^{2-} and Mg^{2+} in ASW, which could strongly form ion pairs with Ca^{2+} and CO_3^{2-} (Kester and Pytkowicz, 1969; Pytkowicz and Hawley, 1974), and thus further reduce the activities of Ca^{2+} and CO_3^{2-}. This explains the slower evolution of log (IAP) in ASW than in the NaCl medium under the same salinity conditions.

In ASW or NaCl medium, the rates in log (IAP) evolution are slower at higher salinities but the evolution curves of log (IAP) from salinity 35 to 105 are getting closer (Fig. 4.5b & 4.5c), indicating that the negative effect slightly overweighs the positive one, but that the differences between them become smaller with increasing salinity. However, τ decreases slightly above salinity 70 in NaCl medium. According to a study of calcite crystallization by Bischof (1968), the calcite nucleation rate was found to be proportional to the square root of solution ionic strength. Thus, we speculate that the increase in salinity (ionic strength) might also accelerate ikaite nucleation rate, which explains the decrease in Ω with increasing salinity in the NaCl medium. Nevertheless, the large increase in τ in ASW in the same salinity range requires another explanation. It was shown by other studies (Reddy and Wang, 1980; Zhang and Dawe, 2000) that Mg^{2+} can strongly retard calcium carbonate precipitation. Therefore, we might speculate that the longer τ at higher salinities in

ASW is due to the presence of Mg^{2+}; the inhibiting effect becomes stronger with increasing Mg^{2+} concentration and this effect overweighs the ionic strength catalysis in ASW.

4.4.3.3 Temperature effect

The similar τ at temperatures from 0 to -4°C indicates that the change in temperature does not have a significant impact on ikaite precipitation in this studied temperature range. According to the calculation results from CO2SYS, although the absolute values of the change in the CO_3^{2-} fraction with pH from two sets of constants are quite different, the trend is similar (Fig. 4.6c): the decrease in temperature only slightly reduces the CO_3^{2-} fraction, which explains the overlapping of log (IAP) evolution curves in Fig. 4.5d. On the other hand, log $K_{sp,\ ikaite}$ decreases by 0.11 from temperature 0 to -4°C (Fig. 4.5d), indicating that lower temperatures would favor the precipitation of ikaite. However, no clear trend of temperature effect on ikaite precipitation can be concluded from this narrow studied temperature range.

Unfortunately, based on the relationship between salinity and temperature in sea ice (Feistel, 2008), the freezing temperature of brine is -4.03°C at salinity 70, which limited the range of temperature investigated in this study. Nevertheless, According to the trend in the time required to reach ikaite solubility (t_s) in Table 4.2, we see a steady decrease in t_s with decreasing temperature as low as -10°C as predicted by the model calculations. Thus, from a thermodynamic point of view, we could infer that lower temperatures might have slightly positive influence on ikaite precipitation. However, we cannot exclude the kinetic effect that might arise from lower temperatures and thus the overall effect of temperature on ikaite precipitation at lower temperatures (< -4°C) remains unknown.

4.4.3.4 PO_4 effect

The similar τ at PO_4 concentrations from 0 to 50 μmol kg^{-1} indicates that the change in PO_4 concentration does not have an impact on ikaite precipitation in this studied PO_4 concentration range. According to the calculation results from CO2SYS, although the CO_3^{2-} fraction obtained from two different sets of constants largely differs, both show a similar trend (Fig. 4.6d): the CO_3^{2-} fraction is not affected by PO_4

concentrations. On the other hand, the concentrations of PO_4 investigated in this study even as high as 50 μmol kg^{-1} are much lower compared to the bulk solution indicating that the change in PO_4 concentration has no impact on the solution ionic strength at salinity 70. So the change in PO_4 concentration barely affects the activities of Ca^{2+} and CO_3^{2-}. From a thermodynamic point of view, the change in PO_4 concentration on the solution ionic strength, activities of Ca^{2+} and CO_3^{2-} and thus on IAP evolution is negligible. This explains the overlapping of log (IAP) curves in this studied PO_4 concentration range. However, besides the thermodynamic effect, kinetics due to the inhibiting effect of PO_4 is also considered to play an important role in calcium carbonate precipitation. It was shown in other studies (Morse et al., 2007; Reddy, 1977) that PO_4 could strongly retard the precipitation of calcite and aragonite in the solution. According to our results on Ω (Table 4.2), which shows no difference in the studied PO_4 concentration range, it appears that PO_4 does not have any kinetic effect on ikaite precipitation either, which is consistent with the study of Bischoff et al. (1993a).

4.4.4 Application to natural sea ice scenario

In natural sea ice, temperature is the driving force for the physico-chemical processes in sea ice brine. With the decrease in brine temperature, brine salinity as well as the concentrations of Ca^{2+} and DIC increases correspondingly. However, the change in temperature might not have a significant direct impact on ikaite precipitation. Ikaite precipitation in natural sea ice is mainly controlled by the brine concentration rate, pH and salinity (ionic strength and the concentration of inhibitor ions).

Ikaite precipitation in natural sea ice is mainly found in the upper layer, and the concentration of ikaite decreases with sea ice depth (Dieckmann et al., 2008; Fischer et al., 2013). This might be due to the high concentrations of Ca^{2+} and DIC resulting from high concentration rates of brine solutions in the upper layer of the cold sea ice, even though low pH and high salinities in this layer are not the favored conditions.

Recently, high concentrations of ikaite were found in the both top and bottom of sea ice with a minimum in the middle section of sea ice (Geilfus et al., 2013). The reason for the high ikaite concentrations on the top of sea ice should be the same as in

the first case; the increase in ikaite concentration in the bottom of sea ice is probably caused by the increase in pH due to the photosynthetic activity. Brine pH has been reported to be as high as 10 in sea ice (Gleitz et al., 1995). As a result, although the brine concentration in the bottom of sea ice is low due to the warm sea ice, the dramatic increase in brine pH due to the photosynthetic activity would greatly increase the CO_3^{2-} fraction thus enhancing the likelihood of ikaite precipitation in sea ice, even though the concentrations of Ca^{2+} and DIC are low due to relatively warmer sea ice.

It is important to point out that in our experimental design, the solution pH was kept constant during the course of experiment. However, in natural sea ice, the precipitation of ikaite will lead to a decrease in pH, resulting in a decrease in solution supersaturation. As a consequence, the equilibrium between the solid phase and liquid phase could be established in a short time and thus the precipitation will cease until the equilibrium is broken again by further concentration of brine solution and/or pH change.

4.5 Conclusions

The effect of physico-chemical processes in sea ice on calcium carbonate precipitation was investigated. Ikaite ($CaCO_3 \cdot 6H_2O$) is the only polymorph of calcium carbonate precipitated under all studied experimental conditions in artificial seawater (ASW), suggesting that ikaite is very likely the only polymorph of calcium carbonate formed in natural sea ice as well. PO_4 is crucial for ikaite formation in the NaCl medium. However, it is not important for ikaite formation under ASW conditions. pH is the controlling factor in ikaite precipitation due to its strong impact on CO_3^{2-} concentrations. Ionic strength has two opposite thermodynamic effects on ikaite precipitation, as the change in solution ionic strength affects the CO_3^{2-} concentrations and the activities of Ca^{2+} and CO_3^{2-} in opposite directions. The increase in ionic strength could also kinetically accelerate the ikaite nucleation rate. In ASW, the presence of inhibitor ions could strongly retard ikaite precipitation. The large variations in PO_4 concentrations have no impact on ikaite precipitation, indicating that ikaite precipitation is neither thermodynamically nor kinetically affected by PO_4.

Chapter 5

Coprecipitation of phosphate with ikaite in artificial sea ice brine

Abstract

Ikaite ($CaCO_3 \cdot 6H_2O$) has recently been discovered in sea ice, providing first direct evidence of $CaCO_3$ precipitation in sea ice. However, the impact of ikaite precipitation on phosphate (PO_4) concentration has not been considered so far. Experiments were set up at pH from 8.5 to 10.0, salinities from 0 to 105, temperatures from −4 to 0°C and PO_4 concentrations from 5 to 50 μmol kg^{-1} in artificial sea ice brine so as to understand how ikaite precipitation affects the PO_4 concentration in sea ice under different conditions. Our results show that PO_4 is coprecipitated with ikaite under all experimental conditions. The amount of PO_4 removed by ikaite precipitation increases with increasing pH. The change in salinity ($S \geq 35$) as well as temperature has little impact on PO_4 removal by ikaite precipitation. The initial PO_4 concentration affects the PO_4 coprecipitation. These findings may shed some light on the observed variability of PO_4 concentration in sea ice.

5.1 Introduction

When sea ice forms, a portion of the seawater is trapped in the sea ice matrix, where it becomes concentrated in brine pockets and channels. When the ice temperature further decreases, the brine salinity increases accordingly. As a result, the chemical compounds as well as the dissolved inorganic nutrients (e.g., total dissolved inorganic carbon (C_T), dissolved inorganic phosphate (PO_4)) in the brine are also enriched.

During the formation and melting of sea ice, the nutrients in sea ice brine are expected to behave conservatively as a function of brine salinity (Gleitz et al., 1995). However, it is often found that the salinity-normalized nutrients in sea ice brine are depleted compared to those in surface seawater (Dieckmann et al., 1991; Gleitz and Thomas, 1993), which is generally explained by the biological activity within sea ice (Günther et al., 1999; Papadimitriou et al., 2007). According to the Redfield ratio for inorganic nutrient uptake during photosynthesis, the nutrient uptake follows the ratio C:N:P = 106:16:1 (Redfield et al., 1963). However, quite often there is not clear correlation between the salinity-normalized C_T and the rest of the inorganic nutrients in sea ice (Papadimitriou et al., 2007). Instead, the depletion of PO_4 in sea ice is much stronger than that of C_T (Gleitz et al., 1995; Papadimitriou et al., 2007), which indicates that there might be another mechanism explaining the excess depletion of PO_4 in sea ice.

Ikaite ($CaCO_3 \cdot 6H_2O$) in sea ice was only recently discovered (Dieckmann et al., 2008; 2010) and for a long time PO_4 has been considered to be crucial for ikaite formation (Bischoff et al., 1993a; Buchardt et al., 2001; Council and Bennett, 1993; Selleck et al., 2007). However, recently it was shown that in seawater-based solution, PO_4 is not required for the formation of ikaite (Hu et al., 2014). The effect of ikaite precipitation on PO_4 concentration is studied here because PO_4 is an important nutrient for the biological community in sea ice and the enrichment or depletion of PO_4 in sea ice has a major effect on the biological activity in sea ice.

The removal of PO_4 by calcium carbonate has long been known. PO_4 can be removed by coprecipitation with calcium carbonate as well as through adsorption to suspended calcium carbonate (Kitano et al., 1978). The coprecipitation of PO_4 with

calcium carbonate has been observed in lakes in many studies (Danen-Louwerse et al., 1995; House, 1990; Murphy et al., 1983). The study by Murphy et al. (1983) showed that the PO_4 in the photic zone of a eutrophic lake could be completely removed by calcite precipitation. There is also considerable evidence regarding the adsorption of PO_4 onto calcite, aragonite, vaterite and monohydrocalcite (Millero et al., 2001; Sawada et al., 1992; Yagi and Fukushi, 2011). However, to the best of our knowledge no studies have dealt with the effect of ikaite precipitation on PO_4 removal.

In this study, we investigated how the precipitation of ikaite affects the PO_4 concentration under conditions representative for natural sea ice. Experiments were set up at pH from 8.5 to 10.0, salinities from 0 to 105, temperatures from −4 to 0°C and PO_4 concentrations from 5 to 50 μmol kg^{-1} so as to understand how the change in these parameters affected PO_4 removal during ikaite precipitation in sea ice.

5.2 Methods

5.2.1 Solution preparation

Artificial seawater (ASW) of different salinities was prepared according to Millero (2006) with slight modifications. Ca^{2+} and HCO_3^- were not added initially. The amount of salt missing from not adding $NaHCO_3$ and $CaCl_2$ was compensated for by adding NaCl. Ten kilogram ASW of salinity 70 was prepared as a stock solution. In addition, one kilogram ASW of salinity 35 as well as salinity 105 was prepared separately. Stock solutions of $CaCl_2$ and $NaHCO_3$ at concentrations of 2.5 mol kg^{-1} and 0.5 mol kg^{-1}, respectively, were prepared by dissolving 183.775 g $CaCl_2 \cdot 2H_2O$ and 21.002 g $NaHCO_3$ into 500 g solutions using ultrapure water and subsequently stored in gas-tight Tedlar bags (SKC). All chemicals were obtained from Merck (EMSURE® ACS, ISO, Reag, Ph Eur) except $SrCl_2$ and H_3BO_3, which were from Carl Roth (p.a., ACS, ISO). Different concentrations of PO_4 were prepared from phosphate stock solution (Merck, CertiPUR®) by dilution with ultrapure water.

5.2.2 Experimental setup

Four parameters were varied: pH (8.5 to 10.0), salinity (0 to 105), temperature (−4 to 0°C) and PO_4 concentration (5 to 50 μmol kg^{-1}). The standard values were pH = 9.0,

S = 70, T = 0°C and [PO_4] = 10 μmol kg^{-1}. Only one of these parameters was varied at a time.

Stock solutions of $CaCl_2$ and $NaHCO_3$ (Ca^{2+}:DIC = 5:1, which is the typical concentration ratio in seawater) were pumped from the Tedlar bags into a Teflon reactor vessel with 250 g working solution using a high precision peristaltic pump (IPC-N, Ismatec) at a constant pumping rate of 20 μL min^{-1}. The solution was stirred at 400 rpm and the temperature was controlled by water-bath using double walled water jackets. pH electrodes (Metrohm 6.0253.100) were calibrated using NBS buffers at pH 7.000 ± 0.010 and 10.012 ± 0.010 (Radiometer analytical, IUPAC standard). The pH of the solution was kept constant by adding NaOH (0.5 mol L^{-1}), which was controlled by a titration system (TA20 plus, SI Analytics). The value of pH and the volume of NaOH added to the solution were recorded every 10 s. Depending on the experimental conditions, the input of $CaCl_2$, $NaHCO_3$ and NaOH into the working solution during the experiments is in the range of a few mL, which did not have a significant effect on solution volume. Duplicates for each experimental condition were run in parallel.

5.2.3 Determining the onset of precipitation

When calcium carbonate is precipitated from solution, CO_2 is released, which leads to a large decrease in solution pH. This rapid change in solution pH was compensated by the addition of NaOH. Therefore, the onset of precipitation was determined by the sudden change of NaOH volume (V_{NaOH}) added into the solution, as marked with a circle in Fig. 5.1.

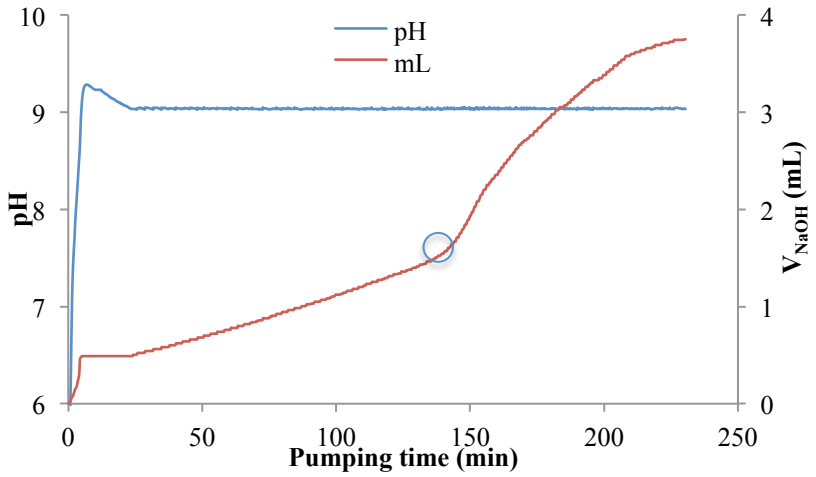

Fig. 5.1 A typical NaOH titration profile obtained at pH = 9.0, S = 70, T = 0°C and $[PO_4]$ = 10 µmol kg^{-1}. The circle indicates the onset of calcium carbonate precipitation

5.2.4 Crystal identification

Immediately after the crystals were precipitated, indicated by a sudden increase in the volume of NaOH addition (section 2.3), around 2 mL of the well-stirred solution together with the crystals was sampled by means of a pipette and quickly transferred to a glass petri dish. The morphology of the crystals was characterized using a microscope (Zeiss, Axiovert 200M) with an objective of 63X magnification. The phase identification of the crystals was done by means of Raman microscopy. This method can be used to reliably distinguish between the various polymorphs of calcium carbonate (Nehrke et al., 2012; Tlili et al., 2001). The confocal Raman microscope (WITec®, Ulm, Germany) was equipped with a diode laser (532 nm) and an Olympus® 20X Teflon coated water submersible objective. During the Raman measurements, crystals were maintained in the original solution and placed in a glass petri dish, which was kept cold using an ice-water bath.

5.2.5 Determination of solution supersaturation at onset of precipitation

The logarithm of the ion activity product of Ca^{2+} and CO_3^{2-} (log (IAP)) and the solution supersaturation with respect to ikaite (Ω = IAP/$K_{sp,\ ikaite}$) under different experimental conditions was calculated by using the chemical equilibrium model Visual-Minteq 3.0 (Gustafsson, 2011) which was modified by the implementation of the solubility constant of ikaite ($K_{sp,\ ikaite}$) derived from log $K_{sp,\ ikaite}$ = 0.15981 – 2011.1/T where T (K) is the absolute temperature (Bischoff et al., 1993a).

5.2.6 Quantification of ikaite and PO_4

In order to avoid further precipitation of calcium carbonate after sampling, the samples were diluted with 0.01 M HCl. Before precipitation started, at the pumping time of 10 min, 1 mL solution was withdrawn and diluted with 0.01 M HCl to a final volume of 10 mL (for PO_4 analysis). For calcium analysis, 1 mL diluted solution was further diluted by a factor of 10. After the onset of ikaite precipitation, around 7 mL solutions together with ikaite crystals were sampled every 10 min for 1 h. The samples were collected with a syringe and filtered through a 0.45 µm syringe filter (Thermo Scientific Nalgene); 5 mL filtrate was collected and diluted with 0.01 M HCl to 10 mL. Thereafter, 0.2 mL diluted-solution was further diluted with 0.01 M HCl to a final volume of 10 mL. The first and second diluted solutions were used, respectively, for PO_4 and Ca^{2+} measurements.

Ca^{2+} concentrations were determined using Inductively-Coupled Plasma Optical Emission Spectrometry (IRIS Intrepid Optical Emission Spectrometer Duo HR, Thermo Fisher Scientific). PO_4 concentrations were measured using a Nutrient Autoanalyzer (ALLIANCE). Each sample was measured twice.

The amount of ikaite precipitated at each sampling time was determined by the moles of Ca^{2+} pumped into the reaction vessel minus the moles of Ca^{2+} remaining in solution. The change in solution mass and the loss of Ca^{2+} during sampling were considered. The amount of ikaite precipitated at each sampling time was thus calculated using the equation below:

$$C_{ikaite,\,i} = \frac{\left(\frac{C_0 * m_0 * t_i}{t_0} - C_i * m_i - \sum_{k=0}^{i-1} n_k\right) * M}{m_i}$$

$C_{ikaite,\,i}$: ikaite concentration (g kg^{-1}) in solution at the i^{th} sampling, i = 1 to 5
C_0: Ca^{2+} concentration (mol kg^{-1}) measured at pumping time 10 min
m_0: mass (g) of solution at pumping time 10 min
t_0: pumping time (=10 min)
t_i: pumping time at the i^{th} sampling
C_i: Ca^{2+} concentration (mol kg^{-1}) measured at the i^{th} sampling time after precipitation
m_i: mass (g) of solution at the i^{th} sampling

$\sum_{k=0}^{i-1} n_k$: total moles of Ca^{2+} removed from solution due to samplings

M: ikaite molecular weight (= 208 g mol^{-1})

5.3 Results

5.3.1 The precipitate under different experimental conditions

According to the typical vibration modes seen in the Raman spectra ν_1 (1071 cm^{-1}) and ν_4 (718 cm^{-1}) (Fig. 5.2 a), ikaite was the only calcium carbonate polymorph identified at pH from 8.5 to 10.0, salinities from 0 to 105, temperatures from −4 to 0°C and PO_4 concentrations from 5 to 50 µmol kg^{-1}. The morphology of ikaite crystals precipitated was similar under all conditions, with an average crystal size of approximately 20 µm (Fig. 5.2 b).

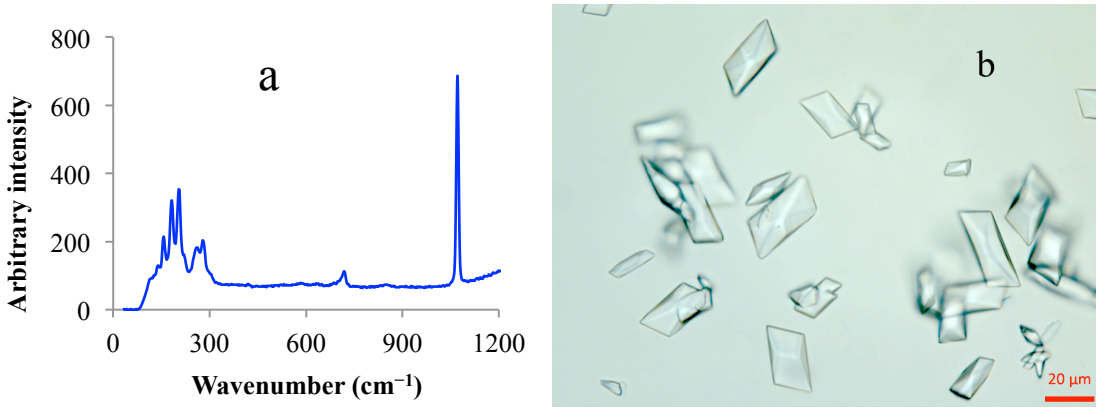

Fig. 5.2 Ikaite Raman spectra (a) and ikaite morphology (b) obtained under the experimental condition of pH = 9.0, S = 70, T = 0°C, [PO_4] = 10 µmol kg^{-1}, and representative for all precipitates in this study.

5.3.2 Removal of PO_4 by ikaite precipitation

Results of the ikaite precipitation experiments conducted at different pH values (8.5 to 10), salinities (0 to 105), temperatures (−4 to 0°C) and initial PO_4 concentrations (5 to 50 µmol kg^{-1}) are shown in Fig. 5.3 to Fig. 5.6. The duplicate experiments (exp. 1 and exp. 2) show a good reproducibility. All experiments show the same pattern for PO_4 removal by ikaite precipitation. The concentration of PO_4 in solution decreases with the amount of ikaite precipitated. The concentration of PO_4 drops steeply during the early stage of ikaite precipitation, followed by a much slower decrease, and then

the PO_4 concentration in solution reaches an equilibrium (within 1 h) even though ikaite crystals continue to grow. The pattern of PO_4 removal by ikaite precipitation under all experimental conditions presented in this study is similar to that observed in studies on PO_4 coprecipitation with calcite and aragonite (House and Donaldson, 1986; Kitano et al., 1978). The total amount of PO_4 in solution being removed by ikaite precipitation is independent of the amount of ikaite being precipitated.

5.3.3 Solution supersaturation at the onset of ikaite precipitation

The solution supersaturation with respect to ikaite (Ω) under different pH values, salinities, temperatures and PO_4 concentrations is shown in Table 5.1. Ω increases with increasing pH from 3.0 to 5.4 at pH from 8.5 to 10. There is no significant difference in Ω at different salinities as well as at different temperatures and PO_4 concentrations.

Table 5.1 Common logarithm of the ion activity product of calcium and carbonate (log (IAP)) and solution supersaturation ($\Omega = IAP/K_{sp,\ ikaite}$) at the onset of ikaite precipitation under different pH, salinity, temperature and phosphate concentration conditions. The standard deviation of log (IAP) is derived from duplicate experiments.

Exp. conditions	Exp. conditions	Log (IAP)	Ω
pH effect:	8.5	-6.73 ± 0.025	3.0
	9.0	-6.67 ± 0.011	3.5
at S 70, T 0°C, PO_4 10 µM	9.5	-6.53 ± 0.005	4.7
	10.0	-6.48 ± 0.020	5.4
S effect:	0	-6.59 ± 0.021	4.2
	35	-6.68 ± 0.051	3.8
at pH 9.0, T 0°C, PO_4 10 µM	70	-6.67 ± 0.011	3.8
	105	-6.61 ± 0.003	4.0
T effect:	0°C	-6.67 ± 0.011	3.5
	-2°C	-6.73 ± 0.023	3.4
at pH 9.0, S 70, PO_4 10 µM	-4°C	-6.74 ± 0.017	3.7
PO_4 concentration effect:	5 µM	-6.71 ± 0.024	3.2
	10 µM	-6.67 ± 0.011	3.5
at pH 9.0, S 70, T 0°C	50 µM	-6.66 ± 0.022	3.5

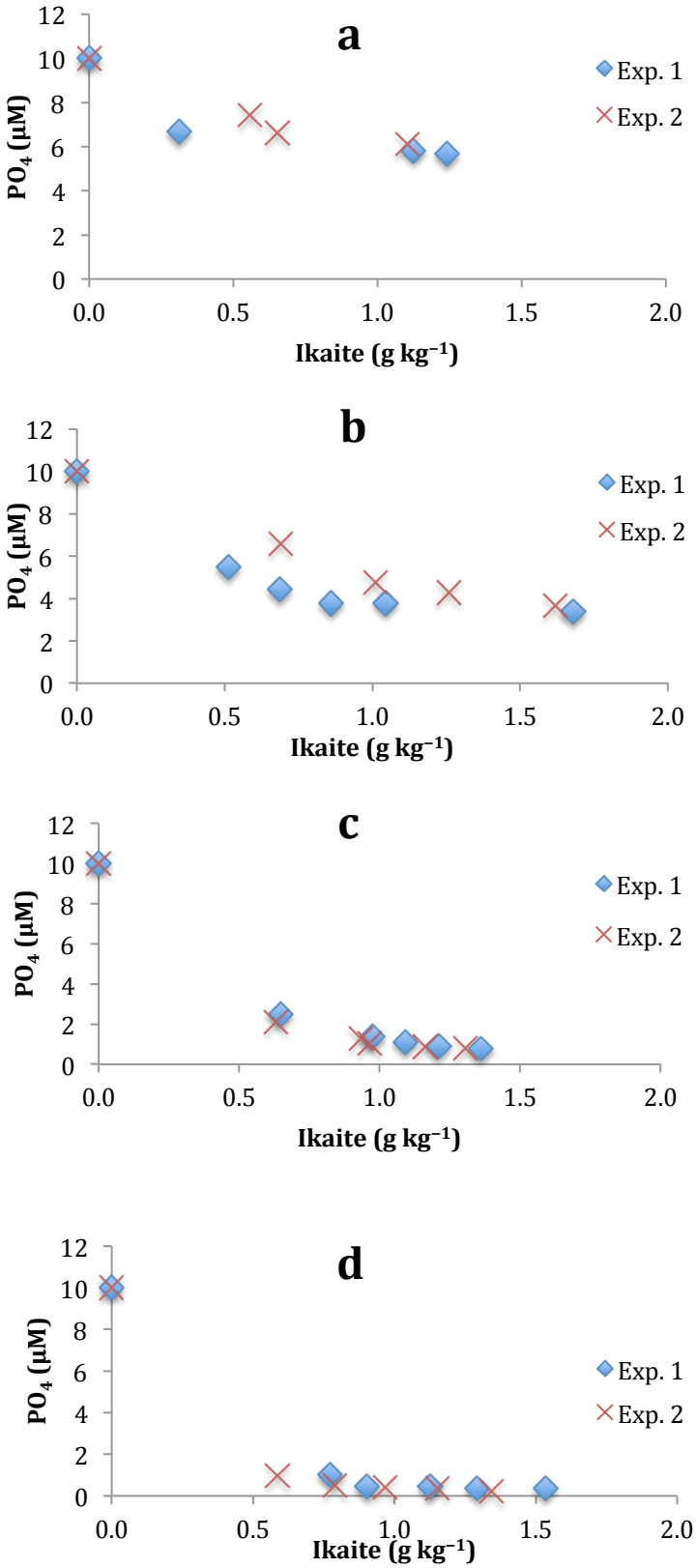

Fig. 5.3 Coprecipitation of PO_4 with ikaite at different pH values and an initial PO_4 concentration of 10 µmol kg^{-1}, S = 70, T = 0°C: (a) pH = 8.5, (b) pH = 9.0, (c) pH = 9.5 and (d) pH = 10.0.

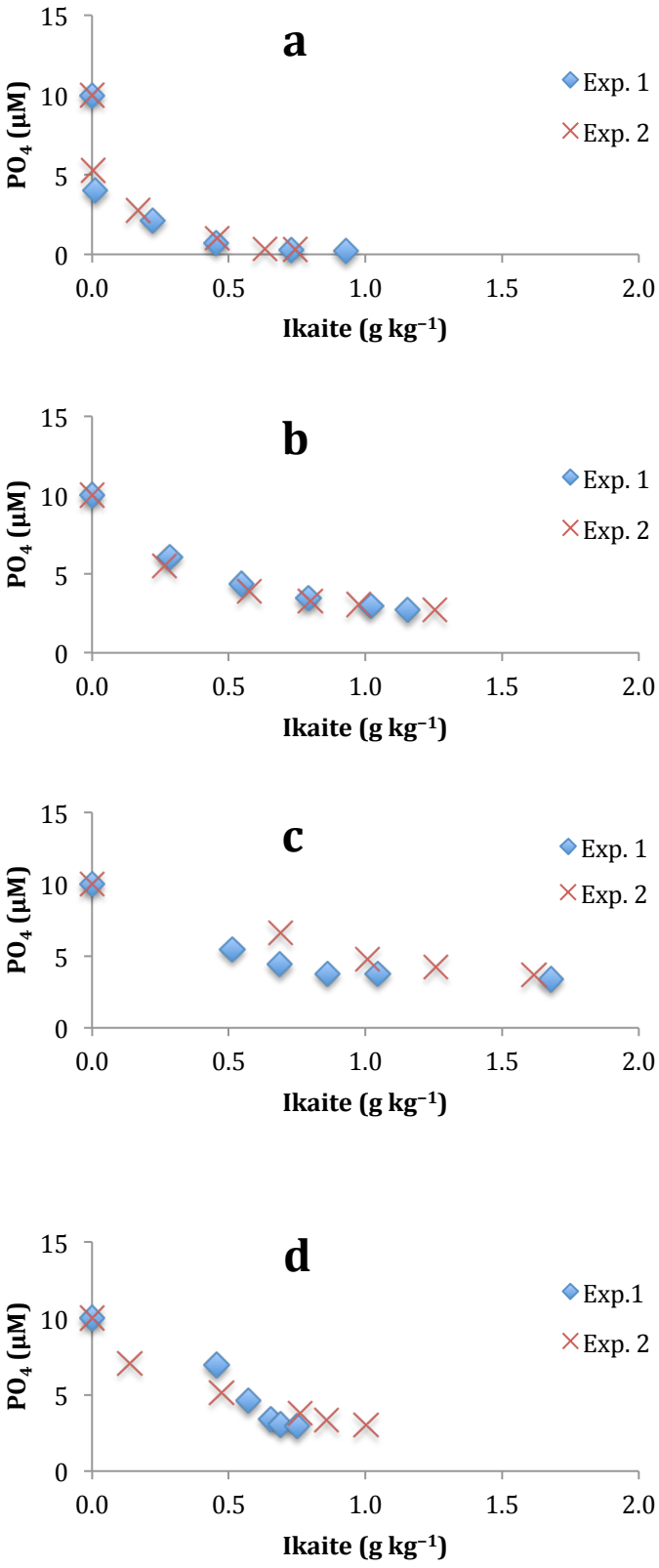

Fig. 5.4 Coprecipitation of PO_4 with ikaite at different salinities and an initial PO_4 concentration of 10 µmol kg^{-1}, pH = 9.0, T = 0°C: (a) S = 0, (b) S = 35, (c) S = 70 and (d) S = 105.

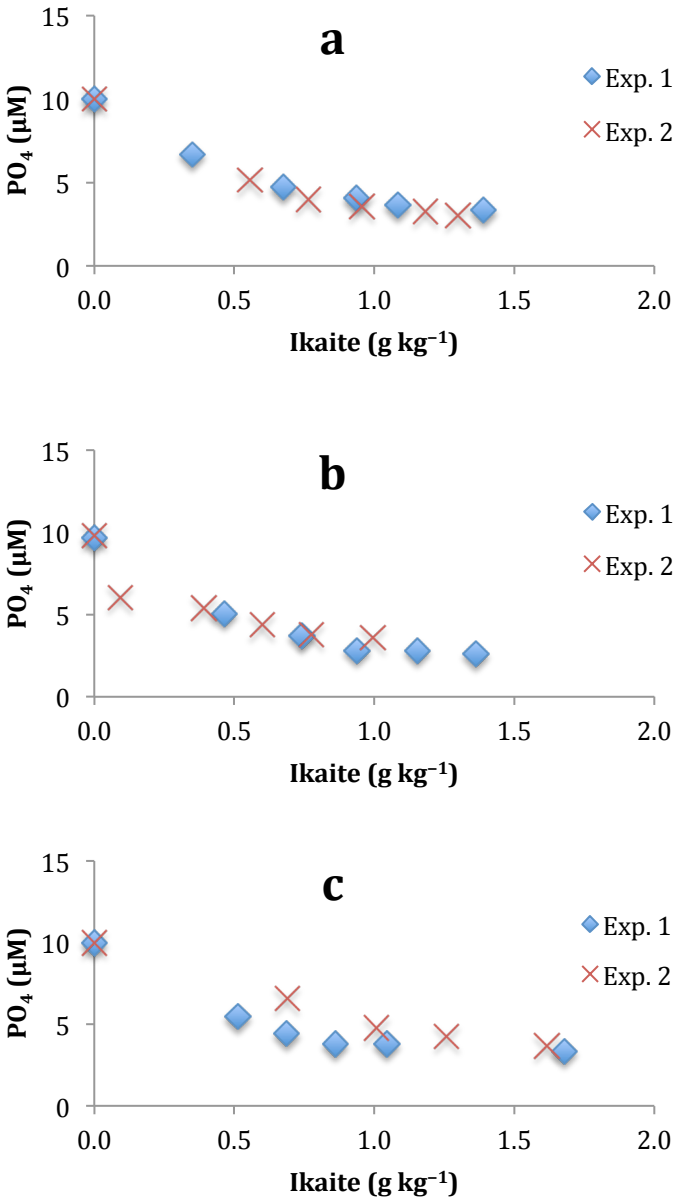

Fig. 5.5 Coprecipitation of PO_4 with ikaite at different temperatures and an initial PO_4 concentration of 10 µmol kg^{-1}, pH = 9.0, S = 70: (a) T = −4°C, (b) T = −2°C and (c) T = 0°C.

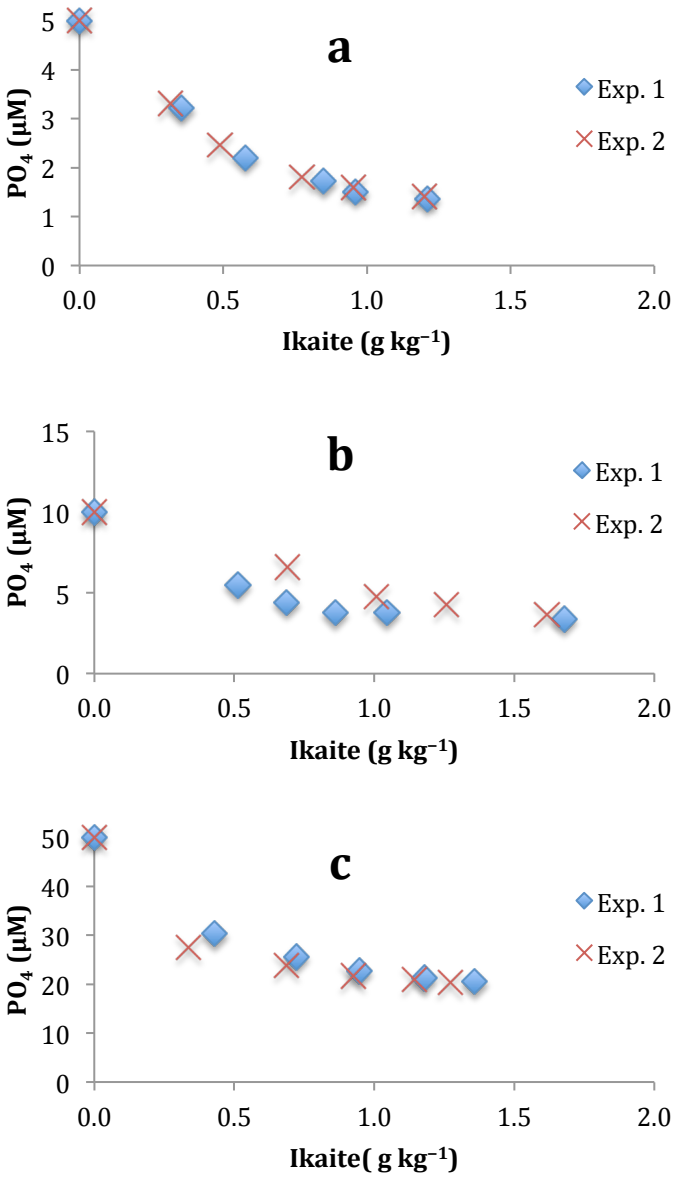

Fig. 5.6 Coprecipitation of PO_4 with ikaite at different initial PO_4 concentrations and pH = 9.0, T = 0°C, S = 70: (a) $[PO_4] = 5$ µmol kg^{-1}, (b) $[PO_4] = 10$ µmol kg^{-1} and (c) $[PO_4] = 50$ µmol kg^{-1}.

5.4 Discussion

5.4.1 General pattern of PO_4 coprecipitation with ikaite

In this study, the concentrations of Ca^{2+} and CO_3^{2-} in solution increase with pumping time until the onset of ikaite precipitation where the solution reaches the highest Ω. After the ikaite precipitation started, Ω decreases until it reaches Ω = 1 (ikaite solubility). As the nucleation rate depends on solution supersaturation (Boistelle and Astier, 1988), a fast nucleation rate will be expected at the initial stage of precipitation. Immediately after the nucleation, the solution saturation level drops rapidly, and so does the nucleation rate while growth of crystals continues (Vekilov, 2010). The removal behavior of PO_4 by ikaite precipitation indicates that coprecipitation of PO_4 with ikaite mainly occurs during ikaite nucleation stage and that the further growth of ikaite crystals has little effect on the removal of PO_4, and thus the PO_4 concentration in solution does not change with the subsequent growth of ikaite. However, the final PO_4 equilibrium concentration differs under different experimental conditions. Next, the effect of each experimental condition on PO_4 coprecipitation with ikaite will be discussed below.

5.4.2 Effect of pH on PO_4 coprecipitation with ikaite

The pH value has a significant effect on PO_4 removal by ikaite precipitation (Fig. 5.7). The coprecipitation of PO_4 with ikaite increases with increasing pH. At pH = 8.5, 42% of PO_4 is removed from solution by ikaite precipitation; above pH = 9.5, more than 90% of PO_4 is coprecipitated with ikaite. This might be due to the fast ikaite nucleation rate resulting from the higher Ω at higher pH (Table 5.1), which leads to more PO_4 being removed as discussed in section 4.1. In sea ice brine, pH can vary from 8 to up to 10 (Gleitz et al., 1995; Papadimitriou et al., 2007). The elevated pH is attributed to photosynthetic activity (Gleitz et al., 1996). It is reasonable to speculate that the initial enrichment of nutrients would enhance photosynthetic activity in sea ice (Gleitz and Thomas, 1993), resulting in an increase of pH in brine. The increase in pH and thus the increase in brine Ω in turn might prompt ikaite precipitation (Hu et al., 2014), which is again likely to limit biological activity due to the removal of PO_4 by ikaite precipitation.

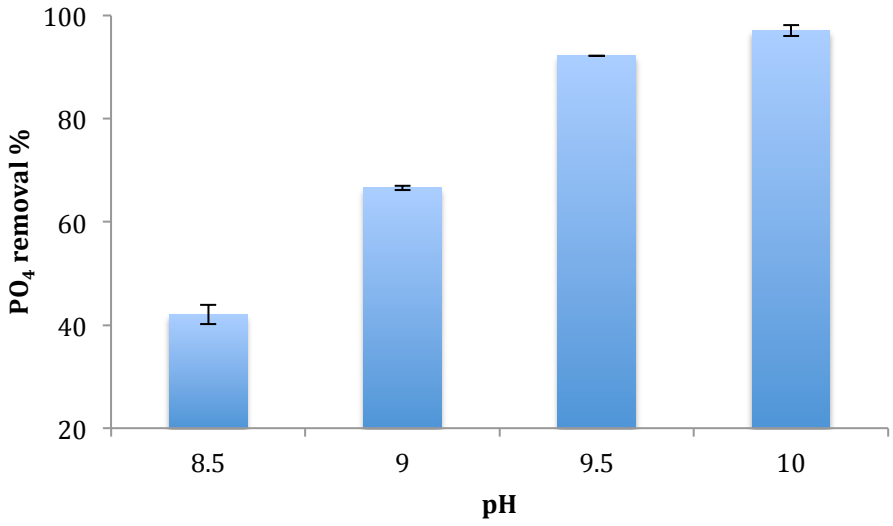

Fig. 5.7 Percentage of PO_4 removal by ikaite precipitation at different pH and an initial PO_4 concentration of 10 µmol kg^{-1}, S = 70, T = 0°C.

5.4.3 Effect of salinity on PO_4 coprecipitation with ikaite

Salinity affects the PO_4 removal by ikaite precipitation (Fig. 5.8). PO_4 is nearly completely coprecipitated with ikaite in freshwater (S = 0). However, at salinity 35 or higher, there is no significant difference in PO_4 removal at varied salinities. As discussed in section 4.1, nucleation rate is driven by the saturation state of the solution. However, the nucleation rate could also be strongly affected by the presence of inhibitor ions, such as Mg^{2+} (Reddy and Wang, 1980). As a result, although the solution Ω at the onset of ikiate precipitation are similar between S = 0 and S ≥ 35 (Table 5.1), the difference in PO_4 removal by ikaite precipitation should be due to the absence/presence of inhibitor ions in solution. The concentrations of inhibitor ions at different salinities do not seem to affect the coprecipitation of PO_4 with ikaite in ASW. It is therefore reasonable to argue that the change in salinity in sea ice brine might not have a significant impact on the amount of PO_4 removed by ikaite precipitation since the brine salinity would not drop to zero.

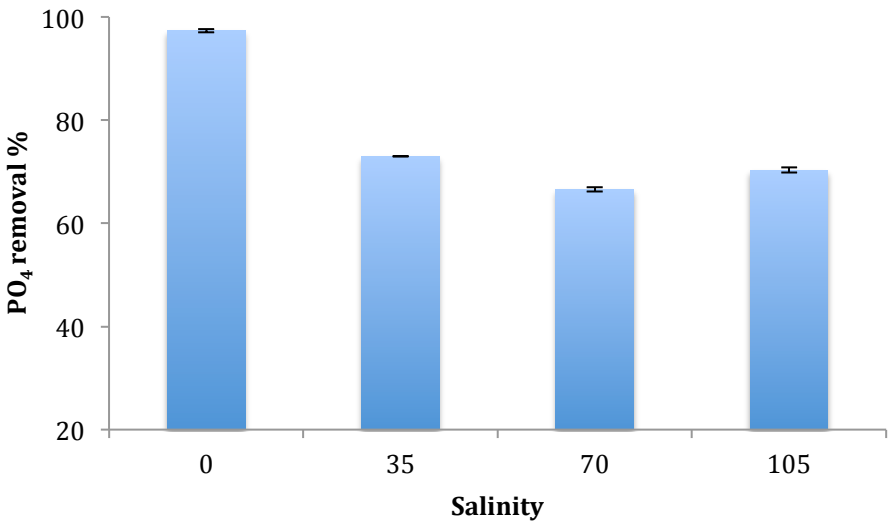

Fig. 5.8 Percentage of PO_4 removal by ikaite precipitation at different salinities and an initial PO_4 concentration of 10 µmol kg^{-1}, pH = 9.0, T = 0°C.

5.4.4 Effect of temperature on PO_4 coprecipitation with ikaite

The change in temperature in the studied range from −4 to 0°C has no effect on the amount of PO_4 coprecipitated with ikaite (Fig. 5.9). The removal of PO_4 by ikaite precipitation is nearly the same in this small temperature range. The temperature range studied here was limited because ASW at S = 70 would have frozen at temperatures below −4°C (Feistel, 2008). Nevertheless, a laboratory study on the coprecipitation of PO_4 with calcite also shows that the amount of PO_4 coprecipitated with calcite is independent of temperature in the temperature range from 12°C to 32°C (Rodriguez et al., 2008). Thus, one might expect that at lower brine temperatures, the removal of PO_4 by ikaite precipitation does not differ substantially from that observed in the temperature range used in this study.

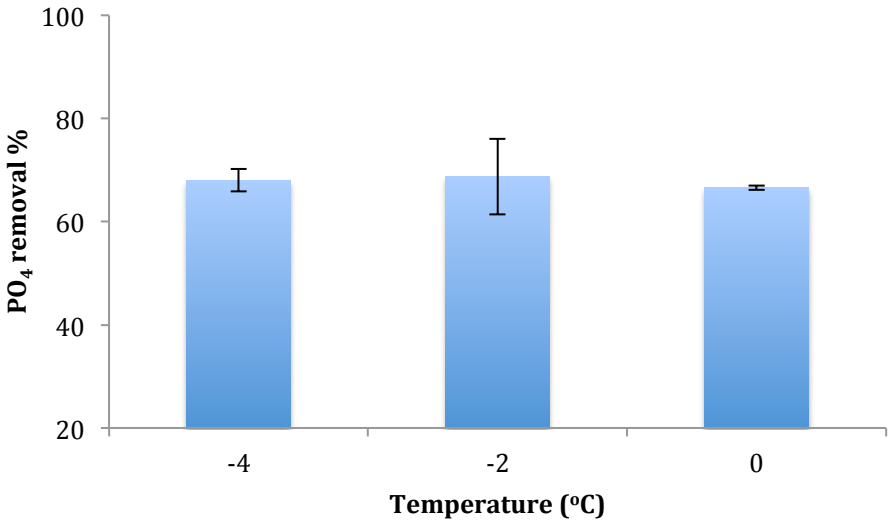

Fig. 5.9 Percentage of PO_4 removal by ikaite precipitation at different temperatures and an initial PO_4 concentration of 10 µmol kg^{-1}, pH = 9.0, S = 70.

5.4.5 Effect of initial PO_4 concentration on PO_4 coprecipitation with ikaite

Initial PO_4 concentration greatly affects the amount of PO_4 coprecipitated with ikaite (Fig. 5.10). The percentage of PO_4 removal by ikaite precipitation decreases slightly with increasing initial PO_4 concentration. This result indicates that the distribution coefficient of PO_4 in solution and PO_4 coprecipitated with ikaite ($k = C_{in\ ikaite}/C_{in\ solution}$) depends on the initial PO_4 concentration; the distribution coefficient k decreases with increasing initial PO_4 concentration. Nevertheless, the absolute amount of PO_4 removed by ikaite precipitation is still larger at higher initial PO_4 concentrations. For example, 3.6 µmol kg^{-1} PO_4 was removed at an initial PO_4 concentration of 5 µmol kg^{-1}; while about 30 µmol kg^{-1} can be removed at an initial PO_4 concentration of 50 µmol kg^{-1}. From this result, we can infer that if the PO_4 concentration in sea ice brine is low, the precipitation of ikaite can remove PO_4 more efficiently while if ikaite precipitation occurs at high PO_4 concentrations, more PO_4 can be removed from sea ice.

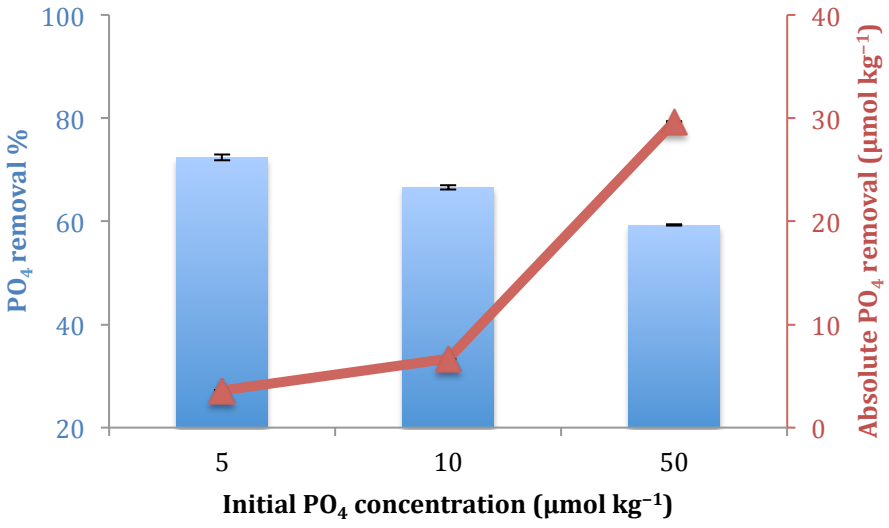

Fig. 5.10 Percentage and absolute amount of PO_4 removal by ikaite precipitation at different initial PO_4 concentrations and pH = 9.0, T = 0°C, S = 70.

5.5 Conclusions

We investigated the effect of ikaite precipitation on phosphate (PO_4) concentration under conditions representative for sea ice brine and show that the concentration of PO_4 in solution is strongly affected by ikaite precipitation. PO_4 can be coprecipitated with ikaite. The coprecipitation of PO_4 with ikaite mainly occurs at the early stage of ikaite formation (nucleation), and PO_4 reaches a constant concentration in solution even when ikaite crystals continue to grow. The highly variable physico-chemical conditions in sea ice are likely to have an impact on PO_4 removal by ikaite precipitation. The amount of PO_4 coprecipitated with ikaite increases with increasing pH and initial PO_4 concentration. Salinity ($S \geq 35$) and temperature have little effect on PO_4 coprecipitation with ikaite in ASW. The fact that PO_4 can be strongly coprecipitated with ikaite indicates that ikaite precipitation could deplete the phosphate concentration in sea ice and thus have an impact on biological activity.

Chapter 6

Summary and perspective

In this thesis, I show that amorphous calcium carbonate (ACC) is not a necessary precursor in ikaite formation. pH as well as phosphate (PO_4) can act as a switch between ikaite and vaterite polymorphs. High pH and/or the presence of PO_4 favor the formation of ikaite in freshwater. However, PO_4 is not, like previously postulated, crucial for ikaite formation in sea ice brine due to the presence of other ions (Mg^{2+} and SO_4^{2-}), which could also favor ikaite formation. According to the study concerning the onset time (defined as the time from the moment when the pumping starts until the moment that crystals are observed), pH is the controlling factor in ikaite precipitation; high pH dramatically shortens the onset time. The change in salinity as well as temperature influences CO_3^{2-} concentrations and activities of Ca^{2+} and CO_3^{2-} in opposite directions; the resulting impact on ikaite precipitation depends on the competition between these two effects. The change in PO_4 concentrations does not affect ikaite precipitation.

The coprecipitation of PO_4 with ikaite was studied for the first time in this thesis. The findings reveal that the precipitation of ikaite can greatly affect PO_4 concentrations in sea ice. The coprecipitation of PO_4 with ikaite only occurs at the early stage of ikaite precipitation and PO_4 reaches an equilibrium concentration even though ikaite continues to grow. The equilibrium concentration of PO_4 is greatly affected by the chemical environments in sea ice brine, especially pH and initial PO_4 concentrations. The fact that PO_4 can be coprecipitated with ikaite indicates that ikaite can act as a stock for PO_4 in sea ice, with possible consequences for the nutrient regime within sea ice.

A question that needs to be addressed in future work is the fate of ikaite after sea ice melts as well as that of the PO_4 coprecipitated with ikaite. When sea ice melts, ikaite might be released to the underlying seawater. As the seawater is undersaturated with respect to ikaite, from the thermodynamic point of view, ikaite is expected to dissolve, which means that the PO_4 will also be released to the seawater, which might enhance algae growth. However, the dissolution of ikaite is also controlled by kinetics, so far the fate of ikaite in sea ice is still not known and the same applies to the coprecipitated PO_4. Thus there is a need for further lab studies on kinetics controlling

ikaite dissolution as well as the PO_4 release mechanism during ikaite dissolution processes. Furthermore, in situ investigation of PO_4 removal by ikaite precipitation in sea ice should be carried out in the future to better understand the biogeochemical processes in sea ice.

Bibliography

Assur, A., 1958. Composition of sea ice and its tensile strength, Arctic Sea Ice. National Academy of Sciences - National Research Council, pp. 106-138.

Behrens, G., Kuhn, L.T., Ubic, R. and Heuer, A.H., 1995. Raman Spectra of Vateritic Calcium Carbonate. Spectrosc. lett., 28(6): 983-995.

Bischoff, J.L., 1968. Kinetics of calcite nucleation: Magnesium ion inhibition and ionic strength catalysis. J. Geophys. Res., 73(10): 3315-3322.

Bischoff, J.L., Fitzpatrick, J.A. and Rosenbauer, R.J., 1993a. The solubility and stabilization of ikaite ($CaCO_3.6H_2O$) from 0° to 25°C: Environmental and paleoclimatic implications for thinolite tufa. J. Geol., 101(1): 21-33.

Bischoff, J.L., Stine, S., Rosenbauer, R.J., Fitzpatrick, J.A. and Stafford, T.W., 1993b. Ikaite Precipitation by Mixing of Shoreline Springs and Lake Water, Mono Lake, California, USA. Geochimica et cosmochimica acta, 57(16): 3855-3865.

Boistelle, R. and Astier, J.P., 1988. Crystallization mechanisms in solution. J. Cryst. Growth, 90(1-3): 14-30.

Bots, P., Benning, L.G., Rodriguez-Blanco, J.-D., Roncal-Herrero, T. and Shaw, S., 2012. Mechanistic Insights into the Crystallization of Amorphous Calcium Carbonate (ACC). Cryst. Growth Des., 12(7): 3806-3814.

Brečević, L. and Nielsen, A.E., 1989. Solubility of amorphous calcium carbonate. J. Cryst. Growth, 98(3): 504-510.

Buchardt, B., Israelson, C., Seaman, P. and Stockmann, G., 2001. Ikaite tufa towers in Ikka Fjord, southwest Greenland: Their formation by mixing of seawater and alkaline spring water. J. Sediment. Res., 71(1): 176-189.

Buchardt, B. et al., 1997. Submarine columns of ikaite tufa. Nature, 390: 129-130.

Burton, E.A. and Walter, L.M., 1990. The role of pH in phosphate inhibition of calcite and aragonite precipitation rates in seawater. Geochim. Cosmochim. Acta, 54(3): 797-808.

Cartwright, J.H.E., Checa, A.G., Gale, J.D., Gebauer, D. and Sainz-Díaz, C.I., 2012. Calcium carbonate polyamorphism and its role in biomineralization: How many amorphous calcium carbonates are there? Angew. Chem. Int. Ed. Engl., 51(48): 11960-11970.

Council, T.C. and Bennett, P.C., 1993. Geochemistry of ikaite formation at Mono Lake, California: Implications for the origin of tufa mounds. Geology, 21(11): 971-974.

Danen-Louwerse, H.J., Lijklema, L. and Coenraats, M., 1995. Coprecipitation of phosphate with calcium carbonate in Lake Veluwe. Wat. Res., 29(7): 1781-1785.

De Lurio, J.L. and Frakes, L.A., 1999. Glendonites as a paleoenvironmental tool: implications for early Cretaceous high latitude climates in Australia. Geochim. Cosmochim. Acta, 63(7–8): 1039-1048.

Delille, B., Jourdain, B., Borges, A.V., Tison, J.L. and Delille, D., 2007. Biogas (CO_2, O_2, dimethylsulfide) dynamics in spring Antarctic fast ice. Limnol. Oceanogr., 52(4): 1367-1379.

Demichelis, R., Raiteri, P., Gale, J.D., Quigley, D. and Gebauer, D., 2011. Stable prenucleation mineral clusters are liquid-like ionic polymers. Nat. Commun., 2: 590.

Di Tommaso, D. and de Leeuw, N.H., 2010. First principles simulations of the structural and dynamical properties of hydrated metal ions Me^{2+} and solvated metal carbonates (Me = Ca, Mg, and Sr). Cryst. Growth Des., 10(10): 4292-4302.

Dickens, B. and Brown, W.E., 1970. Crystal structure of calcium carbonate hexahydrate at ~ -120^{o}. Inorg. Chem., 9(3): 480-486.

Dickson, A.G., 1990. Standard potential of the reaction: AgCl(s) + 1/2 H_2(g) = Ag(s) + HCl(aq), and the standard acidity constant of the ion HSO_4^- in synthetic sea water from 273.15 to 318.15 K. J. Chem. Thermodyn., 22(2): 113-127.

Dickson, A.G. and Millero, F.J., 1987. A comparison of the equilibrium constants for the dissociation of carbonic acid in seawater media. Deep Sea Res. A, 34(10): 1733-1743.

Dieckmann, G.S., Lange, M.A., Ackley, S.F. and Jennings, J.C., Jr., 1991. The nutrient status in sea ice of the Weddell Sea during winter: effects of sea ice texture and algae. Polar Biol., 11(7): 449-456.

Dieckmann, G.S. et al., 2008. Calcium carbonate as ikaite crystals in Antarctic sea ice. Geophys. Res. Lett., 35(8): L08501.

Dieckmann, G.S. et al., 2010. Brief Communication: Ikaite ($CaCO_3.6H_2O$) discovered in Arctic sea ice. The Cryosphere, 4(2): 227-230.

Eicken, H., 2003. From the microscopic, to the macroscopic, to the regional scale: Growth, microstructure and properties of sea ice. In: D.N. Thomas and G.S. Dieckmann (Editors), Sea ice: An introduction to its physics, chemistry, biology and geology. Blackwell Science, Oxford, pp. 22-81.

Feistel, R., 2008. A Gibbs function for seawater thermodynamics for -6 to 80°C and salinity up to 120 g kg^{-1}. Deep Sea Res. Part 1 Oceanogr. Res. Pap., 55(12): 1639-1671.

Fernández-Díaz, L., Fernández-González, Á. and Prieto, M., 2010. The role of sulfate groups in controlling $CaCO_3$ polymorphism. Geochimica Et Cosmochimica Acta, 74(21): 6064-6076.

Fischer, M. et al., 2013. Quantification of ikaite in Antarctic sea ice. Antarctic Science, 25(03): 421-432.

Gebauer, D., Cölfen, H., Verch, A. and Antonietti, M., 2009. The multiple roles of additives in $CaCO_3$ crystallization: A quantitative case study. Adv. Mater. , 21(4): 435-439.

Gebauer, D., Völkel, A. and Cölfen, H., 2008. Stable Prenucleation Calcium Carbonate Clusters. Science, 322(5909): 1819-1822.

Geilfus, N.X. et al., 2013. First estimates of the contribution of $CaCO_3$ precipitation to the release of CO_2 to the atmosphere during young sea ice growth. J. Geophys. Res., 118(1): 244-255.

Geilfus, N.X. et al., 2012. Dynamics of pCO_2 and related air-ice CO_2 fluxes in the Arctic coastal zone (Amundsen Gulf, Beaufort Sea). J. Geophys. Res., 117: C00G10.

Gleitz, M., Kukert, H., Riebesell, U. and Dieckmann, G.S., 1996. Carbon acquisition and growth of Antarctic sea ice diatoms in closed bottle incubations. Mar. Ecol. Prog. Ser., 135: 169-177.

Gleitz, M., Loeff, M.R.v.d., Thomas, D.N., Dieckmann, G.S. and Millero, F.J., 1995. Comparison of summer and winter inorganic carbon, oxygen and nutrient concentrations in Antarctic sea ice brine. Mar. Chem., 51(2): 81-91.

Gleitz, M. and Thomas, D.N., 1993. Variation in phytoplankton standing stock, chemical composition and physiology during sea-ice formation in the southeastern Weddell Sea, Antarctica. J. Exp. Mar. Biol. Ecol., 173(2): 211-230.

Greenwald, I., 1941. The dissociation of calcium and magnesium carbonates and bicarbonates. J. Biol. Chem., 141(3): 789-796.

Günther, S., Gleitz, M. and Dieckmann, G.S., 1999. Biogeochemistry of Antarctic sea ice: a case study on platelet ice layers at Drescher Inlet, Weddell Sea. Mar. Ecol. Prog. Ser., 177: 1-13.

Gustafsson, J.P., 2011. Visual MINTEQ ver. 3.0. KTH, Department of Land and Water Resources Engineering, Stockholm, Sweden. http://www2.lwr.kth.se/English/OurSoftware/vminteq/.

Han, Y.S., Gunawan, H., Masayoshi, F. and Minoru, T., 2006. Crystallization and transformation of vaterite at controlled pH. J. Cryst. Growth, 289(1): 269-274.

Hetherington, N.B.J. et al., 2011. Porous single crystals of calcite from colloidal crystal templates: ACC is not required for Nnanoscale templating. Adv. Funct. Mater., 21(5): 948-954.

House, W.A., 1990. The prediction of phosphate coprecipitation with calcite in freshwaters. Wat. Res., 24(8): 1017-1023.

House, W.A. and Donaldson, L., 1986. Adsorption and coprecipitation of phosphate on calcite. J. Colloid Interf. Sci., 112(2): 309-324.

Hu, Y.-B., Wolf-Gladrow, D.A., Dieckmann, G.S., Völker, C. and Nehrke, G., 2014. A laboratory study of ikaite ($CaCO_3 \cdot 6H_2O$) precipitation as a function of pH, salinity, temperature and phosphate concentration. Mar. Chem., 162(0): 10-18.

Ito, T., 1996. Ikaite from cold spring water at Shiowakka, Hokkaido, Japan. J. Min. Petr. Econ. Geol., 91: 209-219.

Jansen, J.H.F., Woensdregt, C.F., Kooistra, M.J. and van der Gaast, S.J., 1987. Ikaite pseudomorphs in the Zaire deep-sea fan: An intermediate between calcite and porous calcite. Geol. Soc. Am., 15: 245-248.

Kester, D.R. and Pytkowicz, R.M., 1969. Sodium, magnesium, and calcium sulfate ion-pairs in seawater at 25C. Limnol. Oceanogr., 14(5): 686-692.

Kitano, Y., Okumura, M. and Idogaki, M., 1978. Uptake of phosphate ions by calcium carbonate. Geochem. J., 12: 29-37.

Kralj, D. and Brečević, L., 1995. Dissolution kinetics and solubility of calcium carbonate monohydrate. Colloids Surf., A, 96(3): 287-293.

Lam, R.S.K., Charnock, J.M., Lennie, A. and Meldrum, F.C., 2007. Synthesis-dependant structural variations in amorphous calcium carbonate. CrystEngComm, 9(12): 1226-1236.

Loose, B., Miller, L.A., Elliott, S. and Papakyriakou, T., 2011. Sea ice biogeochemistry and material transport across the frozen interface. Oceanogr., 24(3): 202-218.

Lu, Z.L. et al., 2012. An ikaite record of late Holocene climate at the Antarctic Peninsula. Earth Planet. Sci. Lett., 325–326(0): 108-115.

Marland, G., 1975. the stability of $CaCO_3 \cdot 6H_2O$ (ikaite). Geochim. Cosmochim. Acta, 39: 83-91.

McLachlan, I.R., Tsikos, H. and Cairncross, B., 2001. Glendonites (pseudomorphs after ikaite) in late carboniferous Marine Dwyka beds in Southern Africa. South African Journal of Geology, 104(3): 265-272.

Mehrbach, C., Culberson, C.H., Hawley, J.E. and Pytkowicz, R.M., 1973. Measurement of the apparent dissociation constants of carbonic acid in seawater at atmospheric pressure. Limnol. Oceanogr., 18(6): 897-907.

Millero, F., Huang, F., Zhu, X.R., Liu, X.W. and Zhang, J.Z., 2001. Adsorption and desorption of phosphate on calcite and aragonite in seawater. Aquat. Geochem., 7(1): 33-56.

Millero, F. and Pierrot, D., 1998. A chemical equilibrium model for natural waters. Aquat. Geochem., 4(1): 153-199.

Millero, F.J., 2006. Chemical Oceanography. CRC Press, Boca Raton, FL.

Millero, F.J., 2010. Carbonate constants for estuarine waters. Mar. Freshwater Res., 61(2): 139-142.

Morse, J.W., Arvidson, R.S. and Luttge, A., 2007. Calcium carbonate formation and dissolution. Chem. Rev., 107(2): 342-381.

Murphy, T.P., Hall, K.J. and Yesaki, I., 1983. Coprecipitation of phosphate with calcite in a naturally eutrophic lake. Limnol. Oceanogr., 28(1): 58-69.

Nehrke, G., 2007. Calcite precipitation from aqueous solution: transformation from vaterite and role of solution stoichiometry, Utrecht University, 133 pp.

Nehrke, G., Poigner, H., Wilhelms-Dick, D., Brey, T. and Abele, D., 2012. Coexistence of three calcium carbonate polymorphs in the shell of the Antarctic clam Laternula elliptica. Geochem. Geophys. Geosyst., 13(5): Q05014.

Nehrke, G. and Van Cappellen, P., 2006. Framboidal vaterite aggregates and their transformation into calcite: A morphological study. J. Cryst. Growth, 287(2): 528-530.

Notz, D. and Worster, M.G., 2009. Desalination processes of sea ice revisited. J. Geophys. Res., 114(C5): C05006.

Ostwald, W., 1897. Studien über die Bildung und Umwandlung fester körper. zeitschrift für Phzsikalische Chemie, 22: 289-330.

Papadimitriou, S., Kennedy, H., Kennedy, P. and Thomas, D.N., 2013. Ikaite solubility in seawater-derived brines at 1 atm and sub-zero temperatures to 265 K. Geochimica Et Cosmochimica Acta, 109: 241-253.

Papadimitriou, S. et al., 2012. The effect of biological activity, $CaCO_3$ mineral dynamics, and CO_2 degassing in the inorganic carbon cycle in sea ice in late winter-early spring in the Weddell Sea, Antarctica. J. Geophys. Res., 117.

Papadimitriou, S. et al., 2007. Biogeochemical composition of natural sea ice brines from the Weddell Sea during early austral summer. Limnol. Oceanogr., 52(5): 1809-1823.

Pauly, H., 1963. Ikaite, a new mineral from Greenland. Arctic, 16: 263-264.

Pelouze, M.J., 1865. Sur une combinaison nouvelle d'eau et de carbonate de chaux. C. R. Acad. Sci., 60: 429-431.

Pierrot, D., Lewis, E. and Wallace, D.W.R., 2006. MS Excel program developed for CO_2 system calculations. ORNL/CDIAC-105a. Carbon dioxide information analysis center, Oak Ridge National Laboratory, U.S. Department of energy, Oak Ridge, Tennessee.

Plummer, L.N. and Busenberg, E., 1982. The solubilities of calcite, aragonite and vaterite in CO_2-H_2O solutions between 0 and 90 °C, and an evaluation of the aqueous model for the system $CaCO_3$-CO_2-H_2O. Geochim. Cosmochim. Acta, 46(6): 1011-1040.

Pytkowicz, R.M. and Hawley, J.E., 1974. Bicarbonate and carbonate ion-pairs and a model of seawater at 25°C. Limnol. Oceanogr., 19(2): 223-234.

Reddy, M.M., 1977. Crystallization of calcium carbonate in the presence of trace concentrations of phosphorus-containing anions: I. Inhibition by phosphate and glycerophosphate ions at pH 8.8 and 25°C. J. Cryst. Growth, 41(2): 287-295.

Reddy, M.M. and Wang, K.K., 1980. Crystallization of calcium carbonate in the presence of metal ions: I. Inhibition by magnesium ion at pH 8.8 and 25°C. J. Cryst. Growth, 50(2): 470-480.

Redfield, A.C., Ketchum, B.H. and Richards, F.A., 1963. The influence of organisms on the composition of sea-water. In: M.N. Hill (Editor), The Sea. Interscience, New York, pp. 26-77.

Rickaby, R.E.M. et al., 2006. Potential of ikaite to record the evolution of oceanic $\delta^{18}O$. Geol. Soc. Am., 34(6): 497-500.

Rodriguez, I.R., Amrhein, C. and Anderson, M.A., 2008. Laboratory studies on the coprecipitation of phosphate with calcium carbonate in the Salton Sea, California. Hydrobiologia, 604: 45-55.

Rodriguez-Blanco, J.D., Shaw, S. and Benning, L.G., 2011. The kinetics and mechanisms of amorphous calcium carbonate (ACC) crystallization to calcite, via vaterite. Nanoscale, 3(1): 265-271.

Rodríguez-Ruiz, I. et al., 2014. Transient calcium carbonate hexahydrate (ikaite) nucleated and stabilized in confined nano- and picovolumes. Cryst. Growth Des., 14(2): 792-802.

Rysgaard, S. et al., 2012. Ikaite crystals in melting sea ice - implications for pCO_2 and pH levels in Arctic surface waters. The Cryosphere, 6(4): 901-908.

Rysgaard, S., Glud, R.N., Sejr, M.K., Bendtsen, J. and Christensen, P.B., 2007. Inorganic carbon transport during sea ice growth and decay: A carbon pump in polar seas. J. Geophys. Res., 112(C03016).

Rysgaard, S. et al., 2013. Ikaite crystal distribution in winter sea ice and implications for CO_2 system dynamics. The Cryosphere, 7: 707-718.

Sander, R., Burrows, J. and Kaleschke, L., 2006. Carbonate precipitation in brine - a potential trigger for tropospheric ozone depletion events. Atmos. Chem. Phys., 6(12): 4653-4658.

Sander, R. and Morin, S., 2009. Introducing the bromide/alkalinity ratio for a follow-up discussion on "Precipitation of salts in freezing seawater and ozone depletion events: a status report". Atmos. Chem. Phys., 9: 20765-20773.

Sawada, K., Yoshida, S. and Suzuki, T., 1992. Adsorption of phosphate on vaterite. J. Chem. Soc., Faraday Trans., 88(15): 2227-2231.

Selleck, B., Carr, P.F. and Jones, B.G., 2007. A review and synthesis of glendonites (pseudomorphs after ikaite) with new data: assessing applicability as recorders of ancient coldwater conditions. J. Sediment. Res., 77 980-991.

Song, R.-Q. and Colfen, H., 2011. Additive controlled crystallization. CrystEngComm, 13(5): 1249-1276.

Suess, E. et al., 1982. Calcium carbonate hexahydrate from organic-rich sediments of the Antarctic Shelf: Precursors of glendonites. Science, 216: 1128-1131.

Sugiura, Y., Onuma, K., Kimura, Y., Tsukamoto, K. and Yamazaki, A., 2013. Acceleration and inhibition effects of phosphate on phase transformation of amorphous calcium carbonate into vaterite. Am. Mineral., 98(1): 262-270.

Swainson, I.P. and Hammond, R.P., 2003. Hydrogen bonding in ikaite, $CaCO_3.6H_2O$. Mineral. Mag., 67(3): 555-562.

Thomas, D., N. and Dieckmann, G.S., 2010. Sea ice. Wiley Blackwell Publishing, Oxford.

Tlili, M.M. et al., 2001. Characterization of $CaCO_3$ hydrates by micro-Raman spectroscopy. J. Raman Spectrosc., 33: 10-16.

Uppström, L.R., 1974. Boron/chlorinity ratio of deep-sea water from Pacific Ocean. Deep Sea Res., 21(2): 161-162.

Vekilov, P.G., 2010. Nucleation. Cryst. growth des., 10(12): 5007-5019.

Washington, W.M. and Parkinson, C.L., 1986. An introduction to three-dimensional climate modeling. University Science Books, 422 pp.

Weeks, W.F., 2010. On sea ice. University of Alaska Press, Fairbanks, Alaska.

Yagi, S. and Fukushi, K., 2011. Phosphate sorption on monohydrocalcite. J. Miner. Petrol. Sci., 106(2): 109-113.

Zhang, Y. and Dawe, R.A., 2000. Influence of Mg^{2+} on the kinetics of calcite precipitation and calcite crystal morphology. Chem. Geol. , 163(1–4): 129-138.

List of figures

List of tables

Appendix

Publication: Characterization of ikaite ($CaCO_3 \cdot 6H_2O$) crystals in first-year Arctic sea ice north of Svalbard

Characterization of ikaite ($CaCO_3 \cdot 6H_2O$) crystals in first-year Arctic sea ice north of Svalbard

Daiki NOMURA,[1,2,3] Philipp ASSMY,[1] Gernot NEHRKE,[4] Mats A. GRANSKOG,[1] Michael FISCHER,[4] Gerhard S. DIECKMANN,[4] Agneta FRANSSON,[1] Yubin HU,[4] Bernhard SCHNETGER[5]

[1]*Norwegian Polar Institute, Fram Centre, Tromsø, Norway*
E-mail: daiki.nomura@npolar.no
[2]*Japan Society for the Promotion of Science, Chiyoda, Tokyo, Japan*
[3]*Institute of Low Temperature Science, Hokkaido University, Sapporo, Japan*
[4]*Alfred Wegener Institute for Polar and Marine Research, Bremerhaven, Germany*
[5]*Institute for Chemistry and Biology of the Marine Environment, Oldenburg, Germany*

ABSTRACT. We identified ikaite crystals ($CaCO_3 \cdot 6H_2O$) and examined their shape and size distribution in first-year Arctic pack ice, overlying snow and slush layers during the spring melt onset north of Svalbard. Additional measurements of total alkalinity (TA) were made for melted snow and sea-ice samples. Ikaite crystals were mainly found in the bottom of the snowpack, in slush and the surface layers of the sea ice where the temperature was generally lower and salinity higher than in the ice below. Image analysis showed that ikaite crystals were characterized by a roughly elliptical shape and a maximum caliper diameter of 201.0 ± 115.9 μm (n = 918). Since the ice-melting season had already started, ikaite crystals may already have begun to dissolve, which might explain the lack of a relationship between ikaite crystal size and sea-ice parameters (temperature, salinity, and thickness of snow and ice). Comparisons of salinity and TA profiles for melted ice samples suggest that the precipitation/dissolution of ikaite crystals occurred at the top of the sea ice and the bottom of the snowpack during ice formation/melting processes.

INTRODUCTION

Ikaite ($CaCO_3 \cdot 6H_2O$) is a hydrated calcium carbonate polymorph that is generally found in cold and saline conditions (e.g. Pauly, 1963). The precipitation of calcium carbonate during the formation of polar sea ice was a controversial subject for decades and has only recently been shown to really occur (Dieckmann and others, 2008, and references therein). Dieckmann and co-workers were the first to report the occurrence of ikaite in Antarctic sea ice (Dieckmann and others, 2008) and shortly after in Arctic sea ice (Dieckmann and others, 2010). Low-temperature and high-salinity conditions during sea-water freezing and brine formation in sea ice lead to supersaturation for ikaite and subsequent precipitation of ikaite crystals in sea-ice brine.

So far little is known about the fate of ikaite if the sea ice starts to melt. Two scenarios are possible: (1) during the sea-ice melt season, an increase in ice temperature and decrease in brine salinity could induce dissolution of ikaite crystals; or (2) ikaite crystals could be rejected from the melting ice to the underlying water column, which could affect the carbonate chemistry in underlying sea water (Fransson and others, 2011). The precipitation/dissolution of ikaite crystals in sea ice could be an important contributor to the atmosphere–sea-ice–ocean carbon cycle in polar seas throughout sea-ice formation/melting processes (Rysgaard and others, 2007).

Thus far the quantification of ikaite in sea ice has been examined by measuring the weight of the ikaite crystals (Dieckmann and others, 2008), by measuring the calcium concentration after dissolution of ikaite crystals (Fischer and others, 2012) and by analyzing the carbonate system in melted ice/brine samples (Rysgaard and others, 2007; Fransson and others, 2011; Geilfus and others, 2012). Dieckmann and others (2008, 2010) described the typical morphology of ikaite crystals and based part of the phase identification on morphological grounds. However, to date, a detailed morphometric characterization of ikaite crystals found in polar sea ice is lacking.

In this study, we examine the shape and size distribution of ikaite crystals in Arctic first-year sea ice based on image analysis. A detailed characterization of crystal shape and size will provide important information to identify the environmental conditions and history leading to the formation/dissolution of ikaite crystals in polar sea ice. Additionally, total alkalinity (TA) was used as a simple indicator to quantify precipitation/dissolution.

MATERIALS AND METHODS

Sea-ice field observations were carried out at eight sea-ice stations on first-year Arctic pack ice at the spring melt onset north of Svalbard from 27 April to 11 May 2011 (Fig. 1; Table 1) during the Norwegian Polar Institute's Centre for Ice, Climate and Ecosystems (ICE) cruise on R/V *Lance*.

Snow and slush samples were collected using a clean polycarbonate shovel and transferred into polyethylene zip-lock bags. Snow and slush temperature was measured using a needle-type temperature sensor (Testo 110 NTC, Brandt Instruments, Inc., USA).

Sea-ice samples were collected using an ice corer with an inner diameter of 9 cm (Mark II coring system, KOVACS Enterprises, Inc., USA). Immediately after sea-ice collection, ice temperature was measured by inserting a needle-type temperature sensor into holes drilled at 5–10 cm intervals into the core. Thereafter, a second ice core for ikaite crystals

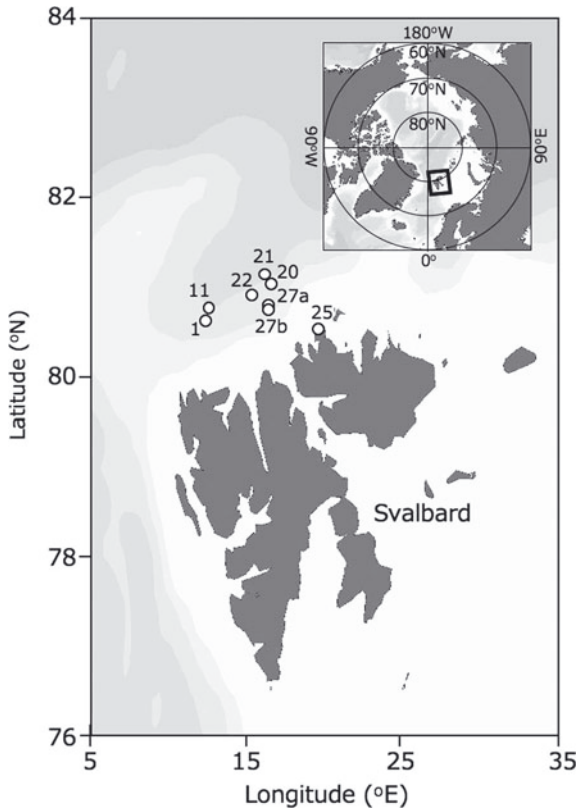

Fig. 1. Location map of the sampling area north of Svalbard.

was collected within 10 cm of the temperature core and cut into 5–10 cm thick sections with a stainless-steel saw. The ice sections were placed in polyethylene zip-lock bags. At station 21, a third core for measurements of ice algal pigments and phosphate concentrations was collected within 10 cm of the ikaite core and cut into 3–20 cm thick sections, which were transferred into polyethylene zip-lock bags and stored in the dark in a large cooler box.

Brine samples from sea ice were obtained at station 21 using the sack hole method (e.g. Gleitz and others, 1995). Sack holes were made using an ice corer as described above for ice coring. A 25–50 cm deep hole in the sea ice was covered with a 5 cm thick urethane lid to reduce heat and gas transfer across the brine–atmosphere interface. After the brine accumulated at the bottom of the hole over a period of ~10–15 min, the brine was sampled with a diaphragm pump (EWP-01, As One Corporation, Japan) and collected into a 100 mL polypropylene bottle (I-Boy, As One Corporation, Japan) for measurement of salinity and a 120 mL amber glass vial (Maruemu Co. Ltd, Japan) for measurement of TA. Brine temperature was measured in situ after the sampling of brine by the same sensor as described above for ice cores.

A detailed account of ikaite sample treatment is provided by Dieckmann and others (2008). Briefly, once back on board, snow, slush and sea-ice samples were immediately transferred into a refrigerator (+4°C) for melting. The melting process was checked regularly. During the final melt phase, samples were swirled until the last pieces of ice had melted. This ensured that the sample remained at a temperature of ~0°C throughout the melting process of 2–3 days. The melted ice samples were transferred from polyethylene zip-lock bags into 1000 mL Nalgene polycarbonate containers (Thermo Fisher Scientific, USA). In order to examine the presence/absence of ikaite crystals in the samples, the meltwater was stirred in the container to induce a vortex. Ikaite crystals, if present, accumulated in the centre of the container and could be detected by eye. When present, the ikaite crystals were sampled with a pipette and filtered over 0.4 μm polycarbonate filters (Millipore, USA) under low vacuum, not exceeding 200 mbar. The filter was placed in a 2 mL Nalgene cryovial (Thermo Fisher Scientific, USA) with 75% cold ethanol and stored at –80°C. Photographs of ikaite crystals were taken with a stereomicroscope (Model M205C, Leica Microsystems, Germany) prior to filtration.

For TA measurements, the supernatant of the remaining melted snow, slush and sea-ice samples was transferred to a 120 mL amber glass vial.

Once on board, sea-ice samples for ice algal pigment and phosphate were transferred into light-proof ice-core boxes and thawed at +4°C. After thawing, meltwater was filtered onto Whatman GF/F glass-fiber filters under low vacuum. For ice algal pigment, filters were placed in a 2 mL Nalgene cryovial (Thermo Fisher Scientific, USA), shock-frozen in liquid nitrogen and stored at –80°C. For phosphate measurements, the filtered water was transferred into a double-rinsed 50 mL polypropylene tube (VWR, Germany) and stored at –20°C until analysis.

The salinities of the brine and melted snow, slush and sea ice were measured with a conductivity sensor (Cond 315i, WTW, Germany). The TAs of the brine and melted snow and sea ice were measured with a titration system (TitroLine alpha plus, SI Analytics GmbH, Germany). The TA measurements were calibrated using an in-house standard (North Sea water collected offshore of Helgoland) traceable to the Certified Reference Material (Batch 111) (Scripps Institution

Table 1. Sampling date, time, location, air temperature, snow and slush depths and ice thickness at sampling stations

Station	Date in 2011	Time UTC	Location	Air temperature °C	Snow depth cm	Slush depth cm	Ice thickness cm
1	27 April	14.23	80°38′49′ N, 12°16′27′ E	–3.5	33.5	No slush	>500
11	29 April	09.00	80°47′38′ N, 12°26′05′ E	–0.7	5.0	No slush	88.0
20	2 May	10.30	81°03′09′ N, 16°27′00′ E	+0.3	19.6	7.0	58.0
21	3 May	11.00	81°09′43′ N, 16°02′41′ E	–6.5	25.0	No slush	125.0
22	6 May	10.00	80°55′47′ N, 15°16′44′ E	–0.9	30.0	No slush	119.0
25	8 May	08.30	80°32′46′ N, 19°27′07′ E	–1.9	3.3	No slush	85.0
27a	10 May	14.00	80°49′04′ N, 16°17′36′ E	–12.8	39.0	3.0	124.0
27b	11 May	09.00	80°48′01′ N, 16°17′27′ E	–10.5	1.0	10.0	31.0

of Oceanography, USA). Ice algal and phytoplankton photosynthetic pigments (chlorophyll *a*) were measured according to Hoffmann and others (2006) by high-performance liquid chromatography (HPLC) with a Waters 600 controller (Waters Corporation, USA).

Phosphate concentrations were determined with an autoanalyzer system (Quaatro, SEAL Analytical, Ltd, UK, method Q-031-04 Rev.2) according to the Joint Global Ocean Flux Study (JGOFS) spectrophotometric method (JGOFS, 1996). The analyzer was calibrated from 0 to 3 µmol L^{-1} with standard reference materials for nutrient analysis (CertiPUR, Merck, Germany) and checked with spiked low-nutrient sea water (LNSW) provided by OSIL, UK.

Phase identification for the ikaite crystals was undertaken using a WITec alpha 300 R (WITec GmbH, Germany) confocal Raman microscope. Ikaite crystals stored in a freezer (–20°C) were transferred to a glass Petri dish in the cold room (+4°C) and immediately set to the microscope to keep cool during the investigation (within 2–3 min). Photographs of the ikaite crystals were also taken under the stereomicroscope (SteREO Discovery V12, Carl Zeiss Microscopy Co. Ltd, Germany).

The image-analysis program ImageJ (software version 1.45s, Wayne Rasband, National Institutes of Health, USA; http://rsb.info.nih.gov/ij) was used to investigate the shape and size of the ikaite crystals from micrographs (Fig. 2). The surface area (S), perimeter (P) and maximum/minimum caliper diameters (d_{max}/d_{min}) were determined for each crystal. The diameter of a circle that has the same area, $d_S = (4S/\pi)^{1/2}$, and the same perimeter, $d_P = P/\pi$, as the crystal was calculated. Relationships between d_S and d_P are measures of deformation of the crystals and have been used previously in a sea-ice floe study (e.g. Toyota and others, 2006).

RESULTS

Air temperature ranged from –12.8°C to +0.3°C during the sampling time (Table 1). Air temperatures measured continuously at 30 s intervals during the study period (27 April–11 May) over R/V *Lance* indicated that the mean air temperature was –5.3 ± 4.4°C.

A slush layer had developed at the snow–sea-ice interface at stations 20, 27a and 27b (Table 1). Snow accumulation over sea ice leads to the formation of a slush layer below sea level (Haas and others, 2001). In this study, slush was generally observed at stations with high snow depth/low ice thickness (Table 1).

Snow and slush depth ranged from 1.0 to 39.0 cm for all stations and 3.0 to 10.0 cm for stations 20, 27a and 27b, respectively (Table 1). Ice thickness ranged from 31.0 to 125.0 cm, with the notable exception of >500.0 cm at station 1 (multi-year or rafted ice). Generally, slush was observed at stations with high snow depth/low ice thickness (Table 1).

Mean temperature ranged from –5.3°C to –0.4°C for snow, –2.8°C to –1.5°C for slush (–3.9°C for brine) and –4.2°C to –0.8°C for sea ice (Table 2). For sea ice, temperatures at the top of the core were generally lower than those at the middle and bottom of the core.

Mean salinity ranged from 0.0 to 6.0 for snow, 20.2 to 23.4 for slush layers and 0.0 to 7.1 for sea ice (Table 2). In general, slush salinity was higher than snow and sea-ice salinity. Extremely high salinity (78.3) was measured for the brine samples at station 21 (Table 2).

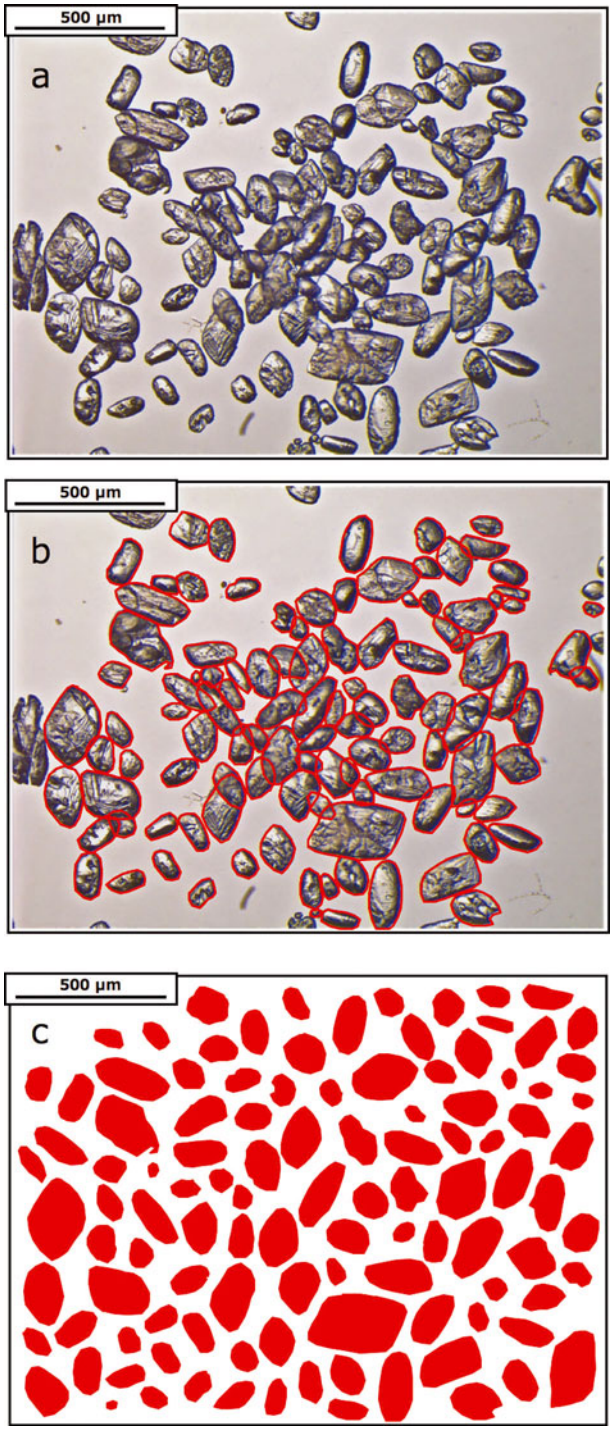

Fig. 2. (a) Photographic image of ikaite crystals in slush. Owing to the overlap of ikaite crystals (a), ImageJ software could not extract each crystal. Therefore, each crystal was outlined by visually drawing a red line around its perimeter (b) and moved to eliminate the overlap between crystals (c). Each crystal was then colored red and extracted according to its brightness using ImageJ. Note that crystals touching the edge of the image were excluded from the analysis.

Phase identification of collected crystals with a confocal Raman microscope confirmed that the crystals found during the cruise were indeed ikaite. The general appearance of ikaite crystals is shown for the slush sample collected at station 20 (Fig. 2a). Similar images of ikaite crystals were obtained from other stations.

During the study period, a total of 96 samples of melted snow ($n = 13$), slush ($n = 5$) and sea ice ($n = 78$) were checked

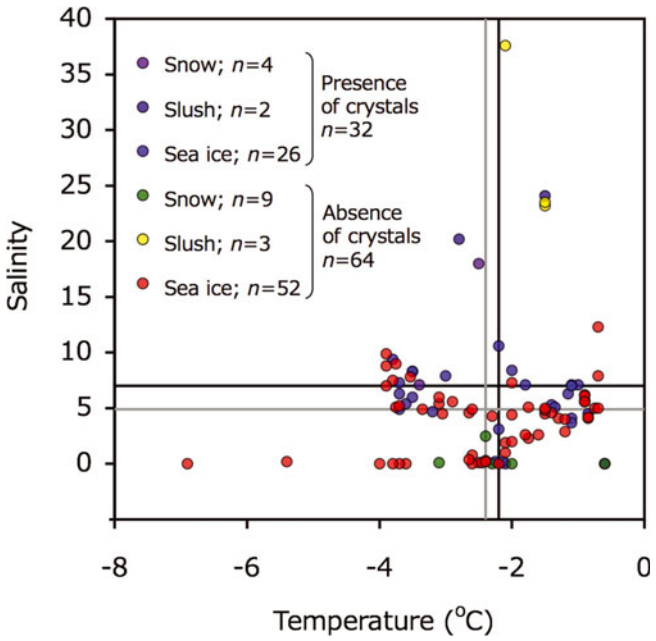

Fig. 3. Relationships between temperature and salinity for melted snow, slush and sea-ice samples. Symbols are shown for presence and absence of ikaite crystals. Black and gray lines indicate the mean value for presence and absence of ikaite crystals, respectively.

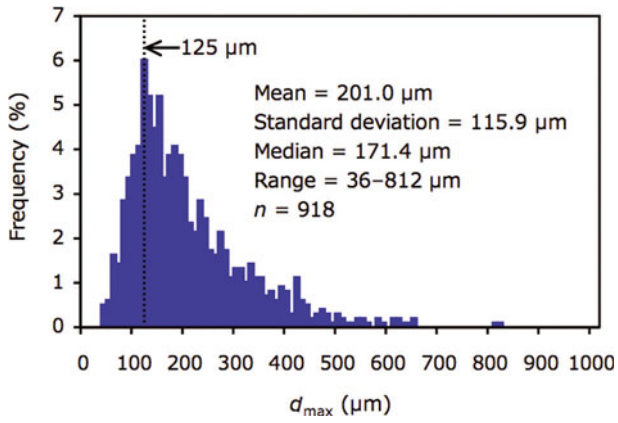

Fig. 4. Size distribution of d_{max} for all ikaite crystals ($n = 918$) examined in this study.

for the presence of ikaite crystals. We found ikaite crystals in 32 samples (one-third of all samples). Ikaite was more often found in sea-ice samples ($n = 26$) than snow ($n = 4$) and slush ($n = 2$) samples. The highest numbers of crystals were found in samples from the bottom of snow, slush layers at the ice–snow interface (e.g. Fig. 2a) and the topmost part of sea ice, while only small amounts were discovered in the remaining samples, especially in the down-core samples where crystals were virtually absent.

Temperature and salinity deviated widely and there was no clear relationship between the two for presence/absence of ikaite crystals (Fig. 3). The average temperatures of samples containing ikaite crystals and those lacking crystals were very similar: -2.2 ± 1.1°C and -2.4 ± 1.2°C, respectively (Fig. 3). The average salinity was 7.0 ± 5.3 for samples with crystals and 4.9 ± 6.1 for samples without.

Mean and median of d_{max} ranged from 112.4 to 375.7 µm and 108.3 to 381.0 µm between stations (Table 3). For all crystals ($n = 918$), mean and median of d_{max} were 201.0 and 171.4 µm, respectively (Table 3; Fig. 4). The mode of the size distribution for d_{max} was 125.0 µm (Fig. 4). No relationships were found between d_{max} (mean) and parameters ($r = 0.5$, $p = 0.3$ for ice temperature; $r = 0.4$, $p = 0.5$ for air temperature; $r = 0.3$, $p = 0.6$ for salinity; $r = 0$, $p = 0.9$ for ice thickness; $r = 0$, $p = 0.8$ for snow thickness).

The slope of the relationship between d_S and d_P and d_{min} and d_{max} for all crystals ($n = 918$), of 1.14 and 1.65 respectively (Fig. 5), represents the deformation ratio in the former and the aspect ratio in the latter.

Bulk ice/snow TA tended to decrease with depth, from 1238.9 µmol L^{-1} at the bottom of the snow to 305.7 µmol L^{-1} at the bottom of the sea ice (Fig. 6). For the upper parts of the snow, bulk TA was almost zero (12.8 µmol L^{-1}). Bulk ice/snow salinity also tended to decrease with depth, from 18.0 at the bottom of the snow to 4.0 at the bottom of the sea ice. For the upper parts of the snow, salinity was zero. Bulk ice/snow TA and salinity profiles showed very similar trends except for the bottom of snow and the top 25 cm of sea ice (Fig. 6).

Bulk ice/snow TA was normalized to a salinity of 5.4, the mean value of bulk ice/snow salinity. The normalized TA (n-TA) was constant (410.3 ± 10.0 µmol L^{-1}) for the middle and the bottom parts of the sea ice, while it deviated more than 39 µmol L^{-1} from the mean values (410.3 µmol L^{-1}) for the bottom of snow and the top 25 cm of sea ice.

Table 2. Mean (range) temperature and salinity for sampled snow, slush (brine) and sea ice

Station	Temperature			Salinity		
	Snow	Slush	Sea ice	Snow	Slush	Sea ice
	°C	°C	°C			
1	–3.0 (–5.1 to –1.7)	No slush	–4.2 (–4.7 to –3.6)	0.0 (0.0–0.0)	No slush	0.0 (0.0–0.0)*
11	–1.2 (–2.5 to +0.1)	No slush	–2.3 (–3.5 to –1.0)	0.0 (0.0–0.0)	No slush	6.5 (5.2–8.3)
20	–0.5 (–1.5 to ±0.0)	–2.8 (–2.8 to –2.8)	–1.6 (–2.0 to –0.9)	1.3 (0.0–2.5)	20.2†	7.1 (4.1–10.6)
21	–2.2 (–3.2 to –1.9)	–3.9 (–3.9 to –3.8) ‡	–2.9 (–4.1 to –1.1)	6.0 (0.0–18.0)	78.3 (77.6–79.6)‡	5.3 (3.1–9.0)
22	–2.4 (–3.4 to –0.1)	No slush	–2.9 (–3.9 to –1.5)	2.4 (0.0–7.1)	No slush	5.8 (4.3–8.8)
25	–0.4 (–0.6 to –0.1)	No slush	–1.0 (–1.5 to –0.7)	0.0*	No slush	6.4 (3.7–12.3)
27a	–5.3 (–8.9 to –2.4)	–2.1†	–2.1 (–2.7 to –1.2)	0.1 (0.0–0.2)	37.6†	1.4 (0.1–2.9)
27b	–3.3†	–1.5 (–1.5 to –1.5)	–0.8 (–0.9 to –0.6)	No data	23.4 (23.2–23.5)	5.3 (4.1–7.0)

*Only top 15 cm of sea ice. †Only one datum. ‡Brine (no slush).

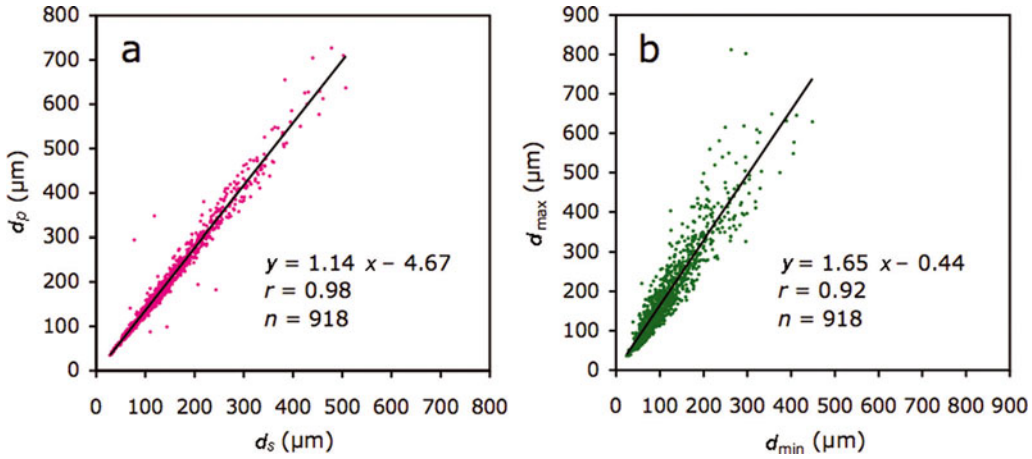

Fig. 5. Relationships between (a) d_S and d_P and (b) d_{max} and d_{min}. d_S and d_P indicate the diameters based on the area and perimeter, respectively. d_{max} and d_{min} indicate maximum and minimum caliper diameters, respectively.

Chlorophyll-*a* concentrations at station 21 were $<0.3\,\mu g\,L^{-1}$ throughout the core, except for the bottom 3 cm ($5.8\,\mu g\,L^{-1}$). Phosphate concentrations were $<0.12\,mol\,L^{-1}$ throughout the core.

For the middle and the bottom parts of the sea ice and upper parts of the snow, bulk ice/snow TA and salinity were highly correlated ($r=0.99$, $p<0.0001$; Fig. 7a). Data points for the bottom of the snow and the top of the sea ice deviated from this regression line (Fig. 7a). Brine TA was considerably higher ($4440.3 \pm 132.5\,\mu mol\,L^{-1}$) and located below the regression line (Fig. 7b).

DISCUSSION AND CONCLUSION

Comparison of the images taken of the ikaite crystals in this study with those from previous studies in Antarctic sea ice (Dieckmann and others, 2008; Fischer and others, 2012) and Arctic sea ice (Dieckmann and others, 2010) indicates that they share a similar morphology.

Generally, cold and saline conditions favor the precipitation of ikaite crystals in the natural environment (e.g. Omelon and others, 2001). The lowest temperatures are generally measured at the top of the sea-ice cover, closest to the cold atmosphere, leading to the formation of the highest brine salinity through the sea ice. Therefore, ikaite crystals were most frequently found at the top of sea ice (Dieckmann and others, 2008, 2010; Fischer and others, 2012). Additionally, the slush layer formation observed during the study period supplied sea water to the top of the sea ice and likely enabled ikaite precipitation in the slush, snow and sea ice when the temperature decreased. On the other hand, for the warm sea ice, sea-water supply to the top of sea ice leads to the undersaturation for ikaite due to a dilution effect. Therefore, ikaite crystals tend to dissolve.

Temperature and salinity relationships showed no significant difference between samples with and without ikaite crystals. During the sampling period, snow and sea-ice temperatures were relatively high and it is reasonable to assume that ikaite crystals tend to dissolve during the spring melt onset. Therefore, relationships between temperature and salinity measured during the study period did not reflect the physico-chemical conditions that prevailed when the precipitation of ikaite occurred. This is one reason why we did not detect significant differences in temperature and salinity conditions for samples with and without ikaite crystals (Fig. 3). Our results suggest that knowledge of the sea-ice growth history, particularly low temperatures during the freezing season, will be important in elucidating the conditions for ikaite formation because brine salinity is strongly driven by brine temperature (e.g., Eicken, 2003), which in turn will determine precipitation.

Most ikaite crystals were roughly elliptical to elongate in shape (Figs 2 and 5). Dieckmann and others (2008) reported that the shape of ikaite crystals varied from almost idiomorphic to xenomorphic and some were apparently constrained by the dimensions of the brine channel network. The size range for the ikaite crystals obtained in this study (36–812 µm) is consistent with that for Antarctic sea ice

Table 3. Mean, standard deviation (SD) and median for d_{max} (μm) of ikaite crystals

Sample name	Station	Sample type	Sample position	Number of crystals	d_{max}		
					Mean	SD	Median
#03	20	Sea ice	Top 7 cm	168	200.7	86.4	181.2
#09	20	Slush	–	111	150.9	56.4	143.5
#10	20	Sea ice	Top 10 cm	132	213.6	130.0	122.6
#16	21	Snow	Bottom 9 cm	76	375.7	153.7	381.0
#17	21	Sea ice	Top 10 cm	177	112.4	44.1	108.3
#29	22	Snow	Bottom 10 cm	210	218.0	94.5	199.2
#35	27b	Sea ice	Top 5 cm	44	265.0	80.8	263.5
All crystals	–	–	–	918	201.0	115.9	171.4

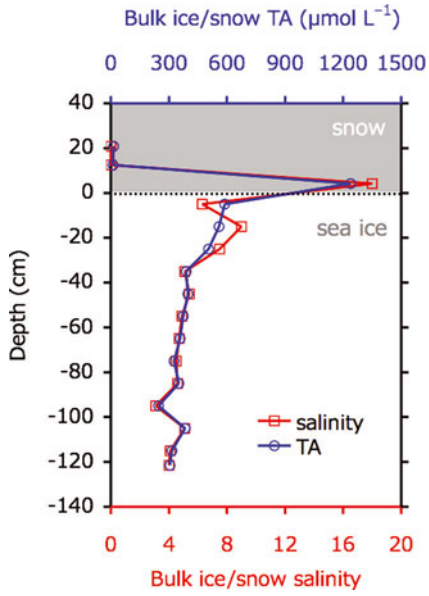

Fig. 6. Depth profiles for the bulk ice/snow TA (blue) and salinity (red) in snow and sea ice at station 21.

(<5–600 μm; Dieckmann and others, 2008). Although crystal size was not quoted, light micrographs of ikaite crystals in Arctic sea ice (fig. 2 in Dieckmann and others, 2010) showed a similar size range to that obtained in this study. At the saline spring discharge, much larger sizes of ikaite crystals (up to 5000 μm) were observed (Omelon and others, 2001) although the water quality and environmental conditions were much different from those of sea ice. Therefore, like the shape of the ikaite crystals (e.g. Dieckmann and others, 2008), the size of the crystals in sea-ice systems might also be restricted by the size of the brine channel and pockets.

Comparison of TA and salinity profiles suggests that precipitation/dissolution of ikaite crystals occurred at the bottom of snow and in the top parts of the sea ice and brine, where ikaite crystals were found. Additionally, deviations of n-TA, for the bottom of snow and the top parts of the sea ice, from the mean values for the middle and bottom parts of the sea ice also suggest precipitation/dissolution of the ikaite crystals at the bottom of snow and in the top parts of the sea ice. During calcium carbonate precipitation, TA decreases (Zeebe and Wolf-Gladrow, 2001). Therefore, TA and salinity relationships can be useful indicators for the precipitation/dissolution of ikaite crystals: the precipitation of ikaite crystals leads to a decrease in the TA:salinity ratio (n-TA) (data points would be below the regression line given in Fig. 7). Although the dissolution of ikaite crystals leads to an increase in n-TA, the dissolution of all ikaite crystals previously formed in a given depth of sea ice would compensate changes in alkalinity (data points would stay on the regression line given in Fig. 7). However, one data point above the regression line (Fig. 7a) suggests excess dissolution of ikaite crystals transferred from adjacent parts of the sea ice. The well-developed brine channel network during the spring melt onset could facilitate ikaite transport.

In addition to the precipitation/dissolution of calcium carbonate, biological activity also alters TA (Zeebe and Wolf-Gladrow, 2001). The largest deviations in TA and salinity were observed at low chlorophyll-*a* concentrations at the surface of sea ice, while TA and salinity were not deviated at high chlorophyll-*a* concentrations measured in the bottom 3 cm of the core. These results suggest that the effect of biological activity on TA was minor for the sea-ice system in this study.

Relationships between TA and salinity were used to quantify ikaite concentrations in sea ice and snow. Deviation of TA from the regression line was used as a measure for the amount of ikaite crystals in sea ice and snow. We have calculated ikaite concentrations at the bottom of snow and the top of sea ice, except for the one data point from the top of sea ice where the plot was above the regression line. Ikaite concentrations (expressed as mg ikaite L^{-1} of melted samples) ranged between 5.6 and 11.3 mg L^{-1}. Our values fall within the range reported by previous studies on Antarctic sea ice (0–19.4 mg L^{-1}: Dieckmann and others, 2008; 0.01–126 mg L^{-1}: Fischer and others, 2012). Previous maximum values were higher than those reported in this study.

The variation in ikaite concentrations reported so far for polar sea ice can be explained by different scenarios. Since the ice-melting season had already started when this study was conducted, ikaite crystals may already have begun to dissolve, which might explain the lack of a relationship between ikaite crystal size and sea-ice parameters (temperature, salinity, and thickness of snow and ice). It is also possible that differences in ikaite concentration are related to differences in the sea-water (brine) composition. It has been reported that high concentrations of phosphate favor

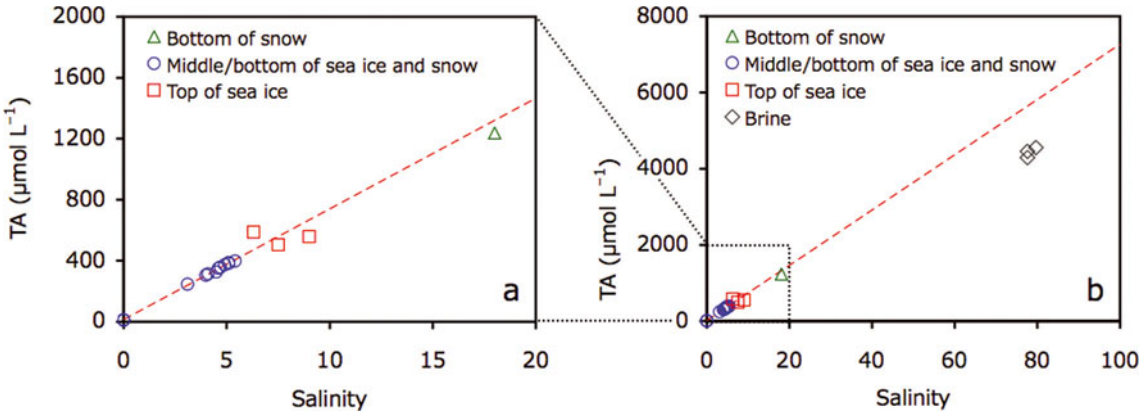

Fig. 7. Plots of (a) TA and salinity for snow and sea ice at station 21 and (b) addition of brine data to (a). Dotted red line represents the regression of data points from the middle and the bottom of the sea ice and the top of the snow (blue circles).

the precipitation of ikaite (Bischoff and others, 1993). In this study, phosphate concentrations were almost zero ($<0.1\ \mu mol\ L^{-1}$) in the top parts of the sea ice. However, sea-ice growth history, especially ice temperature, can be expected to be the most important driving force behind ikaite precipitation (dissolution) in sea ice. Without knowing this parameter exactly over time, it is difficult to determine why ikaite concentrations reported so far (this study; Dieckmann and others, 2008; Fischer and others, 2012) differ. A solid quantification of ikaite formation in polar sea ice requires investigations in which the temperature and other physico-chemical parameters are determined from the beginning of ice formation until the time of sampling.

ACKNOWLEDGEMENTS

We thank the crew of R/V *Lance,* N. Koc, H. Hop, A. Sundfjord, M. Lenau and all the members of the ICE11-3 cruise for support in conducting the fieldwork. We thank J. Hölscher for support in the TA analyses. This work was supported by the Centre for Ice, Climate and Ecosystems (ICE) at the Norwegian Polar Institute and the Fram Centre. G.N. and G.D. were supported by the Deutsche Forschungsgemeinschaft by grant NE 1564/1-1 (SPP 1158).

REFERENCES

Bischoff JL, Fitzpatrick JA and Rosenbauer RJ (1993) The solubility and stabilization of ikaite ($CaCO_3{\cdot}6H_2O$) from 0°C to 25°C: environmental and paleoclimatic implications for thinolite tufa. *J. Geol.*, **101**(1), 21–33

Dieckmann GS and 7 others (2008) Calcium carbonate as ikaite crystals in Antarctic sea ice. *Geophys. Res. Lett.*, **35**(8), L08501 (doi: 10.1029/2008GL033540)

Dieckmann GS and 6 others (2010) Brief communication: ikaite ($CaCO_3{\cdot}6H_2O$) discovered in Arctic sea ice. *Cryosphere*, **4**(2), 227–230 (doi: 10.5194/tc-4-227-2010)

Eicken H (2003) From the microscopic, to the macroscopic, to the regional scale: growth, microstructure and properties of sea ice. In Thomas DN and Dieckmann GS eds. *Sea ice: an introduction to its physics, chemistry, biology and geology*. Blackwell Publishing, Oxford, 22–81

Fischer M and 7 others (2012) Quantification of ikaite in Antarctic sea ice. *Cryos. Discuss.*, **6**(1), 505–530 (doi: 10.5194/tcd-6-505-2012)

Fransson A, Chierici M, Yager PL and Smith WO Jr (2011) Antarctic sea ice carbon dioxide system and controls. *J. Geophys. Res.*, **116**(C12), C12035 (doi: 10.1029/2010JC006844)

Geilfus NX and 7 others (2012) pCO_2 dynamics and related air–ice CO_2 fluxes in the Arctic coastal zone (Amundsen Gulf, Beaufort Sea). *J. Geophys. Res.*, **117**, C00G10 (doi: 10.1029/2011JC007118)

Gleitz M, Van der Loeff MMR, Thomas DN, Dieckmann GS and Millero FJ (1995) Comparison of summer and winter inorganic carbon, oxygen and nutrient concentrations in Antarctic sea ice brine. *Mar. Chem.,* **51**(2), 81–91 (doi: hdl:10013/epic.11568)

Haas C, Thomas DN and Bareiss J (2001) Surface properties and processes of perennial Antarctic sea ice in summer. *J. Glaciol.,* **47**(159), 613–625 (doi: 10.3189/172756501781831864)

Hoffmann L, Peeken I, Lochte K, Assmy P and Veldhuis M (2006) Different reactions of Southern Ocean phytoplankton size classes to iron fertilization. *Limnol. Oceanogr.*, **51**(3), 1217–1229

Joint Global Ocean Flux Study (JGOFS) (1996) *Protocols for the Joint Global Ocean Flux Study core measurements* (JGOFS Report 19). Centre for Studies of Environment and Resources. JGOFS Core Project Office, Bergen

Omelon CR, Pollard WH and Marion GM (2001) Seasonal formation of ikaite ($CaCO_3{\cdot}6H_2O$) in saline spring discharge at Expedition Fiord, Canadian High Arctic: assessing conditional constraints for natural crystal growth. *Geochim. Cosmochim. Acta*, **65**(9), 1429–1437

Pauly H (1963) 'Ikaite', a new mineral from Greenland. *Arctic,* **16**, 263–264

Rysgaard S, Glud RN, Sejr MK, Bendtsen J and Christensen PB (2007) Inorganic carbon transport during sea ice growth and decay: a carbon pump in polar seas. *J. Geophys. Res.*, **112**(C3), C03016 (doi: 10.1029/2006JC003572)

Toyota T, Takatsuji S and Nakayama M (2006) Characteristic of sea ice floe size distribution in the seasonal ice zone. *Geophys. Res. Lett.*, **33**(2), L02616 (doi: 10.1029/2005GL024556)

Zeebe RE and Wolf-Gladrow D (2001) *CO_2 in seawater: equilibrium, kinetics, isotopes* (Elsevier Oceanography Series 65). Elsevier, Amsterdam